MINERALOGY, ALTERATION AND FLUID INCLUSION STUDY OF THE LORDSBURG MINING DISTRICT HIDALGO COUNTY, NEW MEXICO

by
Francis L. Agezo

INDEPENDENT STUDY
Submitted in Partial Fulfillment of
the Requirements for the degree of
Master of Science

New Mexico Institute of Mining and Technology
Socorro, New Mexico
December, 1995

Dedicated To The Memory of My Mother

Charlotte Akuyo Ahepe

ACKNOWLEDGEMENT

This study benefitted from grants from the New Mexico State Mineral Research Institute, the Roswell Geological Society, the New Mexico Geological Society, the Clay Minerals Society, and a Barclay Wycoff scholarship award. Cluff Mining Ghana granted me study leave and provided a continuous financial support throughout my graduate program in the United States. I gratefully acknowledge the support of all my sponsors.

This thesis benefitted immensely from the guidance of Dr. David I. Norman, my academic advisor, who proposed this project and steered it to its successful end. I gratefully acknowledge the great efforts he made to make it possible for me to come to New Mexico Institute of Mining and Technology for this graduate program. Dr. William X. Chavez, Dr. George Austin and Dr. Andrew Campbell, my thesis committee members, are all gratefully acknowledged for their involvement in this study. The stimulating discussions with and the many suggestions offered by Dr. William Chavez on ore mineralogy and Dr. George Austin on clay minerals is very much appreciated.

Mr. Patrick Freeman, president of Goldfield Hidalgo Inc., and Mr. John White, project manager of Lordsburg Mining Company provided all the logistic support for my fieldwork at Lordsburg. The helpful discussions and suggestions as well as the guidance they provided me, can never be fully acknowledged. Mr. Joey Edwards and Mr. Dayton Norvill at the Lordsburg mine are also acknowledged for their companionship and support during my four months stay at the mine. I have also enjoyed those sundown ride around the district and the vivid chats about life in general with Mr. Patrick Freeman and Dr. Robert Shantz of Duncan, Arizona.

I would like to thank Mr. Chris McKee of the New Mexico Bureau of Mines and Mineral Resources for the assistance in the use of the X-ray facilities at the Bureau. I am grateful to John Hall and Tanya Baker, both students of Dr. George Austin, from whom I had fantastic support while working on clay minerals. The assistance of fellow graduate students, John Groff and Maduhka Gundemeda in my fluid inclusion study is highly appreciated. Zana G. Wolf is gratefully acknowledged for her assistance in typing this work.

Special thanks to Dr. George Cunningham, my landlord, for the excellent companionship and support he provided me during my stay in his house in Socorro. Many thanks to Abdel-Aziz Kaina and Erasmus Shivolo for their true friendship. I have enjoyed their companionship and support and benefitted from their counselling and encouragement.

I would like to thank Dr. David B. Johnson, chairman, and Dr. John Shlue, ex-chairman, of the Geoscience Department as well as the office staff; Pat, Nancy, and Connie for their wonderful support while studying at Tech. The great assistance of Dr. Alan Smoake, the Dean of Graduate School, and his secretary, Mrs. Mary Finley can never be fully acknowledged.

Finally, I wish to express my warmest appreciation and gratitude to my wife, Roseline, who kept our `home' running in my absence and my children whose love and patience urged me on to the successful completion of my study.

ABSTRACT

The Lordsburg district has been a major producer of copper, gold and silver and to a lesser extent lead. Production from the district is reported at 300,000 oz. gold, 7.2 million oz. silver, 230 million lbs. copper and 7 million lbs. lead. Mineralization in the district occurs as silicified veins filling faults and fractures that trend northeast and east-west. Mineralization is characterized by repeated episodes of hydrothermal brecciation.

Hypogene mineralization can be divided into six paragenetic stages within the district. Based on dominant vein fill, there are four vein types which correspond roughly to the mineralogic zones and which, listed from the district center outwards, are (1) chalcopyrite veins, (2) pyritic veins, (3) galena-sphalerite veins, and (4) gangue dominant veins. The volume of each paragenetic stage varies over the district; veins closest to the center of the district contain relatively greater proportion of the earlier paragenetic stage assemblages.

Vein mineralization is accompanied by illitic (sericitic), intermediate argillic, and propylitic alteration. Based on diagnostic mineral assemblages and textures, four principal alteration zones are distinguished based on the clay mineralogy. From the vein margin these zones are illitic, chloritic, chlorite-smectite mixed-layer and chlorite-albite-calcite. The wallrock alteration around mineralized veins in the Leitendorf subdistrict suggests that it was overprinted by post-mineralization, low-temperature hot-spring activity. Effects include the retrograde alteration of original hydrothermal illite (sericite) to mixed-layer illite-

smectite and the presence of corrensite as the dominant chlorite-smectite mixed-layer mineral in succeeding alteration zones.

Fluid inclusions within quartz, calcite, and fluorite are dominated by two-phase liquid-dominant and single-phase liquid types. Two-phase vapor-dominant and single-phase vapor types are common in quartz of stage 2. Fluid inclusion data on 21 samples indicate that ore mineralization occurred at temperatures between 128° and > 350°C from fluids with salinities between 3.2 and 7 equiv. wt % NaCl. Stage 2 inclusions have homogenization temperatures (T_h) between 154° and 402°C and calculated salinities of 6 to 7 equiv. wt % NaCl. Stage 3 inclusions indicate T_h range of 150°-270°C and calculated salinities of 3.4 to 5.1 equiv. wt % NaCl. Lower T_h (128°-160°C) and salinities (3.2-4.5 equiv. wt % NaCl) are indicated for stages 4 and 5. Stage 6 inclusions have T_h between 150° and 230°C and salinities between ranges 3.7 and 5.7 equiv. wt % NaCl. Evidence of boiling indicates pressure of $\leq$ 150 bars during the early part of stage 2 mineralization. In the waning portion of stage 2 and subsequent stages of mineralization, high-salinity fluids gave way to progressively cooler, more dilute fluids.

Fluid inclusion volatiles obtained by thermal decrepitation of 18 samples indicate the presence of H_2O, CO_2, CO, CH_4, C_nH_n, H_2, H_2S, and SO_2 in decreasing order of abundance. Minor amounts of He ($\leq$ 0.00005 mol %) and Ar ($\leq$ 0.003 mol %) are present. Fluid inclusion and mineralogical data indicate that stages 2 and 3 ore fluids had the following chemical composition

(calculated for 350°-200°C temp. range): Log fS_2 (-6.4 to -12.2), Log fO_2 (-33.8 to -40.0), Log mΣs (-2.5 to ~0), and pH (4.56 to 5.64). A ternary plot of ratios of H_2, He, and Ar indicate mixing from at least two sources-magmatic and meteoric. Interpretation based on the presence of significant amount of organic species, believed to be sourced from the underlying clastic-carbonate sequence and the ternary plot indicate interaction between deep circulating meteoric waters and magmatic fluid.

Mineral paragenesis and assemblages, mineral zonation and alteration and fluid inclusion data suggest that mineralization in Lordsburg occurred in pulses accompanied by decreasing sulfidation and oxidation states, decreasing temperature and increasing pH through time and in space. Equilibrium thermodynamic interpretation of mineral paragenesis and assemblages and fluid inclusion data indicates that metal precipitation occurred as a result of a progressively decreasing temperature due to boiling and mixing and changes in chemical conditions (fS_2, fO_2, pH, etc.). Base-metals and silver could have been transported as chloride complexes. Gold was probably transported as a chloride complex in the initial fluids and later as a bisulfide complex. Base-metals precipitation occurred mainly as a result of cooling accompanied by changes in the geochemical environment. Gold precipitated in response to boiling and sulfidation.

TABLE OF CONTENTS

LIST OF FIGURES

LIST OF TABLES

INTRODUCTION

The ore deposits at Lordsburg are base-and precious-metal vein systems that occur in a Laramide andesite and granodorite stock. Mineralization occurs as silicified veins filling faults and fractures trending northeast and east-west.

Previous work on the Lordsburg district has been on copper-bearing veins in the northern part of the district and the predominantly silver-bearing veins in the southern part. These studies by Lasky (1938), Flege (1959) and Clark (1962, 1964, 1970) were mostly descriptive and neither detailed alteration studies or fluid inclusion studies have been carried out. The newly opened veins in the northern part of the district (Fig. 3) have no production history and have not been studied. This study was designed to:

I. Characterize the mineralogy of the newly opened veins newly operated and to determine possible district zonation of minerals.

II. Document the alteration associated with the major mineralized veins.

III. Geochemically assess the ore-forming environment of these veins and thus generate ideas applicable to continued exploration in the district and in similar systems elsewhere.

Location and Description

The Lordsburg mining district lies about 3.5 km south-southwest of the city of Lordsburg, Hidalgo County, New Mexico, and covers an area of about 125 km^2 (Fig. 1). The district encompasses the northern end of the Pyramid Mountains which occurs on the eastern margin of the Basin and Range

province. The district is located at the intersection of the northeast-trending Santa Rita lineament that passes southwesterly through the Tyrone, Santa Rita, Bisbee, and Cananea copper porphyry deposits and a northwest-trending lineament that passes through the Safford and Christmas copper porphyry deposits.

Lingren and Graton (1910) and Lasky (1938) divided Lordsburg into two subdistricts, Virginia and Pyramid (Leitendorf), based on the principal type of mineralization. The subdistricts are shown in Figs. 2 and 3. The Virginia subdistrict occupies the northern part of the district and comprises chalcopyrite, bornite, galena, and gold vein deposits. The Leitendorf subdistrict occupies the southern part, and consists of chalcopyrite, bornite, cerargyrite, argentite, and galena-bearing veins. This subdivision is maintained by the writer in this study.

History

The history and production data of the district discussed in this work were obtained mostly from Lasky (1938) and Flege (1959). Information on recent activities were derived from reports made available by the mine office of the Lordsburg Mining Company.

Virginia Subdistrict

The mineral potential of the Virginia subdistrict received attention when in April 1870 the first claim was recorded in the Lordsburg area. Some early attempts were made to ship silver ore but mining activity increased when in 1880 the area was opened up by the construction of the Southern Pacific Railroad through Lordsburg.

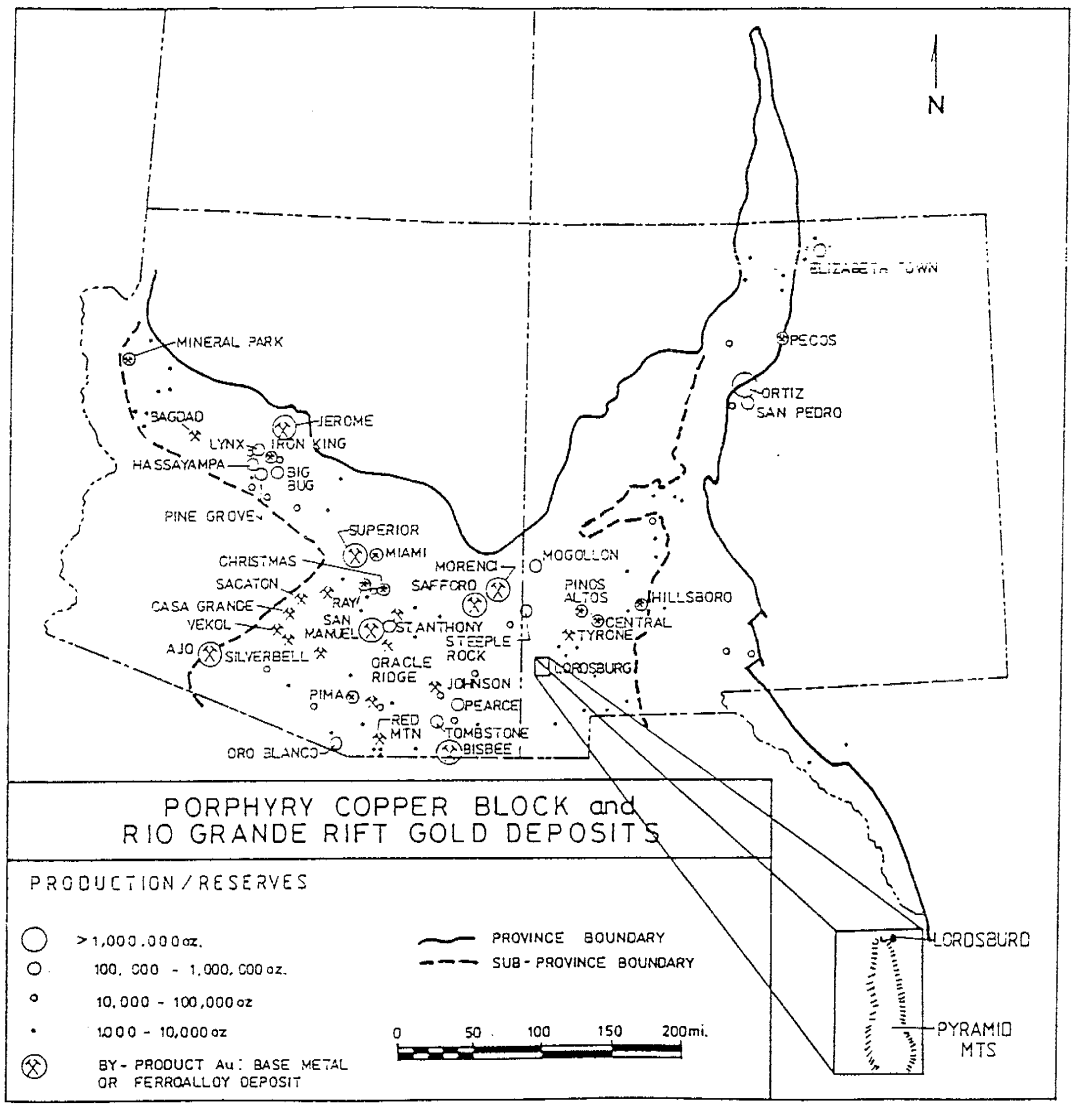

Fig. 1. Location Map of the Lordsburg District. Modified from Wilkins, Jr. (1984)

Silver mining, however, remained the principal interest until the price of silver plummeted to $0.78 per ounce in 1893. Mining activity waned until 1899 when the subdistrict witnessed a rebirth as a copper camp when the price of copper steadily rose to $0.17 per pound.

Most of the subdistrict's production had come from two major vein systems, the Emerald and Bonney (Fig. 3). The Eighty-five group of claims, the biggest producer in the Lordsburg district until 1932, was bought in 1913 by the Eighty-five company. This saw the creation of Valedon township and the construction of a railroad spur from Lordsburg. A 200 ton smelter was constructed and operated between 1918 and 1919. In 1920, the property of the Eighty-five mining company was acquired by Calumet and Arizona mining company. Calumet and Arizona Mining Company, between 1920 and 1931 had shipped about 850,000 tons of ore as siliceous flux to its copper smelter in Douglas, Arizona (Youtz, 1931). Phelps Dodge acquired the property in 1931 and closed down the mine in 1932 when the price of copper plunged to $0.16 per pound.

The second largest producer in the subdistrict prior to 1935 was the Bonney mine, situated on the Bonney vein (Fig. 3). Banner mining company acquired the property in 1935. A flotation plant was constructed and milling commenced in 1936. The Little Annie, Last Chance, Oro and West Oro veins were found and developed in addition to the Bonney and Miser's Chest veins. Federal Resources Corporation purchased the Banner Mining Company property in 1967 and leased the Eighty-five mine which had been operated by Diversified Mines in 1968. Production prior to the Federal Resources

Corporation operation from all six veins has totalled 2,325,005 tons having mill feed assay of 0.6 g/t Au, 25.5 g/t Ag and 2.524 % Cu. Prior to the Banner acquisition of the property there was sporadic production from the Bonney, Miser's chest and Last Chance veins. This production came from small companies and leasing operations and production data is lacking (Federal Resources Annual Report, 1972)..

In addition to these two principal producers in the subdistrict, there are several claims and group claims including Atwood, Henry Clay, Waldo, Anita, and Ruth that had small and sporadic production (Fig. 3). The Atwood mine, between 1943 to 1949 had produced 60,579 tons averaging 2 g/t Au, 193.4 g/t Ag, 2.29% Cu and 1.12% Pb.

Mining and drilling continued in the subdistrict until 1975 with sporadic exploration interest. A detailed assessment of the North Atwood vein for use as smelter flux was carried out between 1983 and 1984 by Phelps Dodge Corporation. A total of 3,499 m in forty-seven holes was drilled. Westar Corporation in 1985 further investigated the vein and carried out a brief mining operation on the vein between 1985 and 1986.

In 1990, the Lordsburg Mining Company, a joint venture between Goldfield Hidalgo and Federal Resources Corporation, initiated an underground development from the North Atwood vein to produce direct shipping siliceous flux ore. Production in the Virginia subdistrict through 1992 is summarized in tables 1a and 1b.

Leitendorf Subdistrict

The Leitendorf subdistrict was discovered in 1880 and by 1881, the subdistrict had become the most active with production from four mines namely Venus, Last Chance, Robert E. Lee, and Nellie Bly (Fig. 3). The Venus mine was the largest producer in the subdistrict. A 20-stamp pan amalgamator mill was constructed at the mine in 1883. Its operation and success was spasmodic until 1893 when the price of silver plummeted. Underground operations continued and ore was shipped directly to smelters until 1923. Smelter records of ore from the mine show average grades of 411 g/tAg, 1 g/t Au, 0.75% Cu, and 2.0% Pb (Lasky, 1938).

The Last Chance mine was worked from 1882 to 1890. It then remained idle for several years until 1918 when it was re-opened and operated till 1923. A flotation plant was constructed and operated in 1919 and 1920. A 50-ton concentration plant was also constructed in 1921.

The Nellie Bly and Robert E. Lee mines were owned by the Pyramid Peak Consolidated Mining Company. The mines produced chiefly copper-silver ore, from 1894 to 1898 and were worked at intervals from 1905 to 1931. The silver-copper ratio of ores in these mines were reported to be similar to the average supergene ore mined at Eighty-five and Bonney mines in the Virginia subdistrict (Lasky, 1938). The subdistrict has been inactive since 1931.

Previous Work

The geology of the district is discussed in detail by Lindgren et al. (1910), Lasky (1938), Flege (1959), and Thorman and Drewes (1978). Belt (1960) described some aspects of wallrock alteration. Belt observed that the

metal content (Cu + Pb) and alteration (total wt % of alteration minerals) showed a diffusion gradient from the fluid channels (mineralized veins). He postulated that the distribution of copper and zinc are related to alteration, and all veins in the district were precipitated from the same ore fluids.

The mineralogy of the district is discussed in detail by Lasky (1938), Huntington (1947), and Clark (1962, 1964, 1970). Lasky (1938) identified 6 stages of accompanying mineralization on the Emerald vein and presented it as a model for the distract. Lasky's paragenetic sequence for the district is summarized in Fig. 11. Clark (1962, 1964, 1970) discussed hypogene zoning and temperatures of formation within the district. Clark recognized four zones of hypogene mineralization. A core zone, which centers on the northeastern extremity of the Lordsburg granodiorite stock, hosts the assemblage specularite-pyrite-chalcopyrite. This zone is surrounded in succession by a central zone of chalcopyrite-pyrite-specularite, an intermediate zone of galena-sphalerite, and a peripheral zone of fluorite-calcite-barite. Clark also estimated maximum temperature of formation of 550°-580°C based on sphalerite geothermometry. Elston (1965) studied the orogenesis and periods of mineralization in southwestern New Mexico with particular attention to the mining districts in Hidalgo county. Jones (1904,1907), Wells (1909), Hill (1924), and Darton (1933) documented early mining activities in the district. Mining operation at 85 mines were described by Youtz (1931) and at Atwood group by Huttington (1947) and Storms (1949).

Methods

Fieldwork consisted of four months of mapping surface alteration, collecting surface and underground samples for fluid inclusion, alteration and paragenesis study. Samples were collected from the North Atwood mine down to the 4th level, and drill core from the mine areas was examined and sampled.

Laboratory studies consisted of transmitted light microscopy on 40 thin sections, reflected light microscopy on 30 polished sections, X-ray diffraction analysis on 100 hundred samples to determine alteration clay mineralogy (Appendices II, III). A microthermometry study and quadrapole mass spectrometry analysis of fluid inclusions and fluid inclusion gas on 21 and 18 samples, respectively, were undertaken to determine physico-chemical characteristics of the ore-forming fluids.

Table 1a. Production of Gold, Silver and Copper in the Virginia Subdistrict

Year	Description	Tons	% Cu	g/t Ag	g/t Au
1870- 1903	Early Work	Unknown	Unknown	Unknown	Unknown
1904-1931	Douglas Flux	1,674,100	2.38	84.0	3.9
1936-1976	Bonney Mill	2,500,000	2.50	51.4	1.2
1985-1986	Webster Pit	45,000	0.18	30.5	1.65
Totals		4,219,000	1.69	55.3	2.25

Table 1b.

Year	Tons	% Cu	g/t Ag	g/t Au	
1990	18,183	0.38	35.0	1.75	
1991	50,182	0.58	49.7	2.95	
1992	35,052	0.68	72.3	3.05	

Production data obtained from Lasky (1938), Flege (1959), and Federal Resources Corp. Annual Reports (1967-1976), recent and current production records in the North Atwood mine area.

GENERAL GEOLOGY

The sequence of the rock types and their chronological relation to mineralization in the Lordsburg district can be summarized as:

Pleistocene - Holocene:

Stream gravel and valley fill

Uncomformity

Miocene:

Flows, volcanic necks and dikes (quartz latite)

Breccia and tuff

Unconformity

Early Tertiary:

Quartz latite dikes with faint mineralization

Quartz latite dikes and plugs, felsite dikes

Mineralized veins (economic mineralization)

Aplite and granodiorite prophyry dikes

Granodiorite stock

Upper Cretaceous

Intrusive rhyolite

Intrusive breccia

Andesite (basaltic flow, tuffs, etc.)

Lower Cretaceous

Sandstones

Pennsylvanian - Mississipian

Limestone, dolomite with minor shales

Precambrian

Granite, greiss, schist

Regional Setting

The Lordsburg district lies within a Late Cretaceous-Early Tertiary porphyry copper province which encompasses southwestern New Mexico, southeastern Arizona, and northern Mexico (Fig. 1). Continental sedimentation characterizes the Triassic and the Jurassic periods, but there are areas of non-deposition and erosion in southern Arizona and southern New Mexico (Turner, 1962). In the early Cretaceous, a basin developed in southeastern Arizona and southwestern New Mexico resulting in the accumulation of thick overall section of sedimentary rocks in this area. The Cretaceous to early Tertiary Laramide Orogeny and its accompanying igneous activity and mineralization followed.

The tectonic style in this area is characterized by differential vertical uplift along northeast trending faults. This resulted in both northeast and southwest directed transport from block edges (Davis, 1975). Some workers (Schmitt, 1966; Lacy, 1959) have suggested that there also was transcurrent movement along northwest trending faults.

In southwestern New Mexico, Laramide deformation was accompanied by andesitic and basaltic volcanism and intrusion of stocks of intermediate composition. Later, in the Oligocene, large scale volcanism resulted in formation of several major ash-flow tuff cauldrons (Figs. 2, 3).

Geology

Local Basement

The Precambrian basement consists of granite, gneiss, schist and greenstone. Exposures are present about 60 to 80 km north of the district.

The oldest rocks in the district are Lower Cretaceous clastic sedimentary rocks exposed 1.6 km northwest of the Leitendorf mines. Lithologies include fine-grained to gritty quartzose sandstone, siltstone, shale, and some quartzite lenses. The rocks are well indurated due to thermal metamorphism and commonly banded on outcrop surfaces (Thorman and Drewes, 1978). Thorman and Drewes (1978) reported the occurrence of fossils that resemble those in the Lower Cretaceous sandstone in the Brockman Hills 35 km to the southeast (Thorman, 1978) and of the Lower Cretaceous Mojado Formation in the Big Hatchet Mountains 65 km to the south-southeast (Zeller, 1965).

The nature of the Cretaceous and Paleozoic stratigraphy in the Lordsburg area is not well understood. About 32 km to the northeast are the Burro Mountains with only a thin Cretaceous clastic sequence resting on Precambrian rocks. Twenty-four kilometers to the west are the Peloncillo Mountains that have 700 metres of Cretaceous Bisbee group rocks overlying about 220 metres of Paleozoic rocks. Between 48 and 80 km to the southeast are the Big and Little Hatchet Mountains which contain about 3050 metres of Bisbee group rocks and 3050 metres of Paleozoic rocks.

In both the Hatchet and Peloncillo mountain ranges, the Bisbee group comprises an upper clastic sequence with little or no limestone and a lower predominantly limestone sequence.

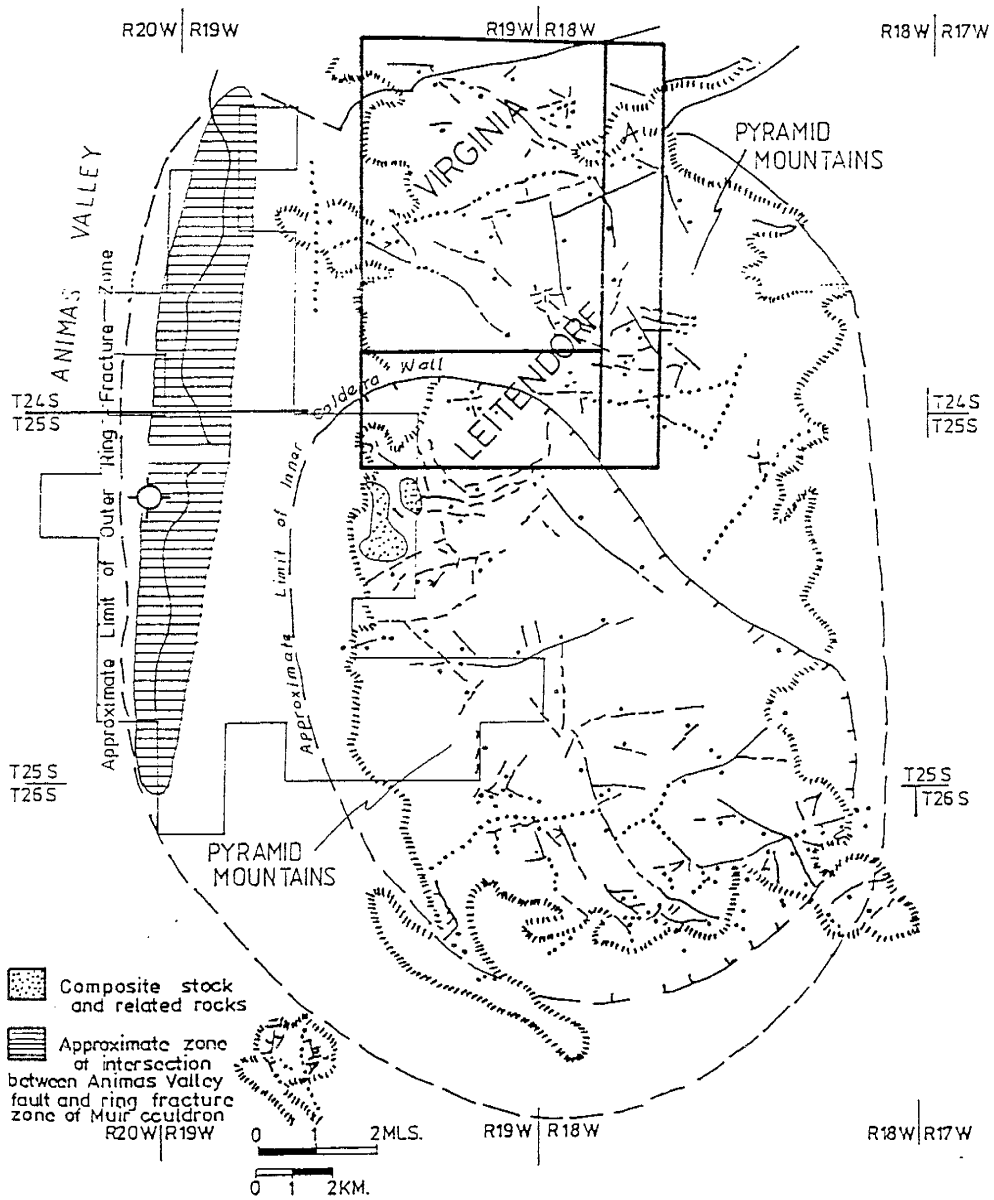

Fig. 2. Tectonic sketch map of the Lordsburg district and adjacent areas. Note the locations and boundaries of the Muir Cauldron and the Lightning Dock Known Geothermal Resources Area. Inset is the Lordsburg mining district. Modified from Elston et al. (1979).

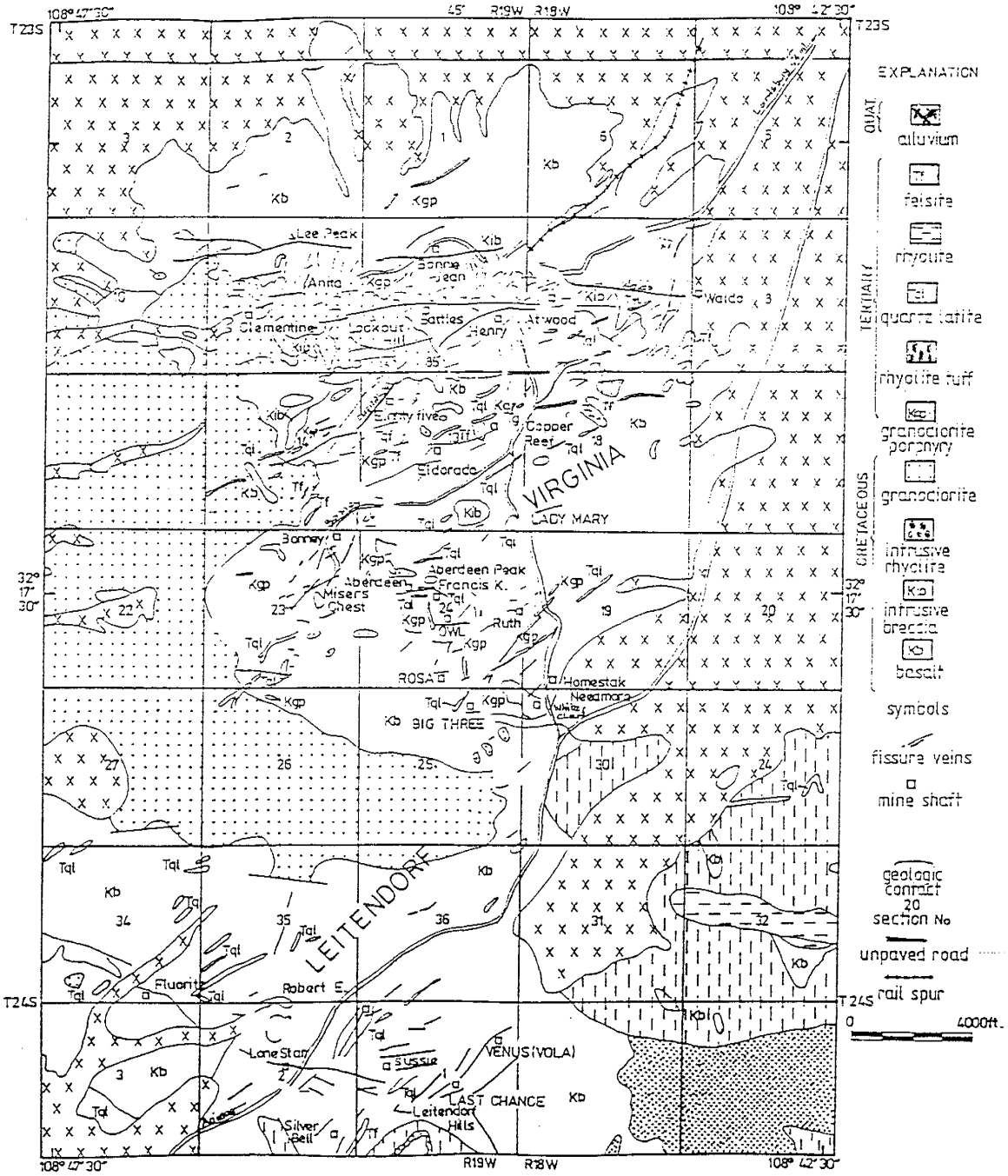

Fig. 3. General geologic map of Lordsburg. Modified from Clark (1970).

The upper clastic sequence is mostly an interbedded sequence of sandstone and shale. Calcareous fossiliferous marine beds of silty and sandy limestone are present in the sequence. The lower limestone formation consist of beds of bioclastic limestone alternating with thin beds of shales and sandy calcarenite (Zeller, 1965; Gillerman, 1958)

Underlying the lower Cretaceous sequence in these areas is a Paleozoic section of limestone. This section consists of thick beds of limestone and dolomite interbedded with thin beds and lenses of shale, claystone, siltstone and sandstone.

Andesite

The most extensive rock unit in the district is the Upper Cretaceous andesite of Shakespeare. It includes andesite flows, tuff breccias, flow breccias, epiclastic beds and scattered small intrusive masses (Thorman and Drewes, 1978). The andesite is the main host rock to subsequent igneous activity and accompanying mineralization. The andesite is at least 600-670 metres thick as determined from the top of the Cretaceous section below the surface in the vicinity of Bonney mine.

The rocks are generally medium to dark grey, brownish grey or dark greenish gray. The flow rocks are generally fine-grained. Flow thickness up to between 30 to 50 metres have been reported by previous workers. At the contact zone with the granodiorite stock, the andesite exhibits varying degrees of alteration. A hybrid rock is what is observed in the contact zone. The andesite looks more of a granodiorite with a characteristic pale green color.

Intrusive Breccia

The Cretaceous andesite is intruded at several places in the district by small plugs of intrusive breccia. The Atwood hill is one of such plugs and the most prominent, extending over a strike length of about 1.6 km with a width of about 300 metres. Small plugs intrude the andesite and rhyolites southwest of the 85 Hill. The Atwood hill plug contain included masses of basalt up to about 60m in length.

The breccia consist of fragments of gray to green basalt in finely granular basaltic matrix. At several places the fragments are of white to light colored rhyolite and locally felsite.

Intrusive Rhyolite

The intrusive rhyolite occur as large masses, plugs and dikes that intrude the andesite and intrusive breccia. It has a light-gray to greenish-gray or chalky-white appearance and is fine-to medium-grained.

Thorman and Drewes (1978) postulated that the intrusive rhyolite is younger than the granodiorite. Field observations indicate that the intrusive rhyolite is older. It either occurs separately, or found associated with intrusive breccia and is intruded at several places by small bodies of granodiorite. Lasky (1938) and Flege (1959) stated that the intrusive rhyolite are remnants of volcanic necks.

Granodiorite

The Lordsburg granodiorite is the major intrusive unit in the district. Richter et al (1983) and Richter and Lawrence (1983) report an age of 59-56

+Ma (K-Ar dating). The reported age of the Lordsburg granodiorite falls within the Laramide orogeny and mineralization epoch recorded for the southwestern United States and northern Mexico. The stock consists of light-gray to light brownish-gray, fine to medium grained porphyritic granodiorite and minor quartz monzonite. The granodiorite stock intrudes andesite and rhyolite units.

Aplite and Granodiorite Porphyry Dikes

Small intrusive bodies of aplite occur within or near the granodiorite stock. They are typically pinkish orange-gray and fine-grained. The andesite and granodiorite are cut by dikes of granodiorite porphyry believed to be related to the granodiorite stock.

Post Granodiorite Tertiary Rocks

Volcanism resumed during the Upper Paleocene to Oligocene after a period of erosion. This resulted in the formation of andesite flows and breccias in the northeast and northwest and rhyolite tuff-breccias, rhyolite flows and tuffs to the southeast (Flege, 1959; Elston et al, 1979). The rocks greatly constitute the Leitendorf hills in the southeastern part of the district.

Quartz Latite Dikes and Plugs

Eocene latite porphyry dikes intrude earlier andesite and granodiorite in the district (Flege, 1959). This rock type contains abundant pyrite. These dikes are generally long and narrow and may extend for nearly 1.5 km.

North Pyramid Rhyolite

Rhyolite flows of Oligocene (Lasky, 1938; Flege, 1959) spread from the volcanic neck of the North Pyramid Peak. They are found in the southeastern end of the district.

Felsite

Late Tertiary rhyolite dikes and plugs which mark the last phase of igneous activity in the district and intrude all other rocks. This rock unit is white, dense, homogeneous, and commonly silicified.

Quaternary Deposits

Stream gravel and valley fill are found in the desert basins surrounding the Pyramid Mountain. Flege (1959) stated that the alluvial contact at the flank of the Pyramid Mountain ranges in elevation from 1341 to 1433 metres.

Structure

Regional strike-slip faults controlled the localization of stocks, dikes and veins at Lordsburg. The Lordsburg veins are principally contained in three major sets of steeply dipping faults and fractures.

The first group of fissure veins are a northeasterly trending group comprising economically-important vein systems, including the Emerald, Bonney, and Miser's Chest at Virginia and Robert E. Lee and Nellie Bly veins at Leitendorf. These veins are poorly defined at the surface. However, they extend over 1.5 km en echelon. The second set of historically and currently economically-significant fissure veins are currently being mined and trend east-west. The North and South Atwood veins, Anita, Bonnie Jean, Dacotah Pearl, Owl, and Susie veins are among this vein set. These veins have prominent siliceous outcrops in the northern part of the district. However, in the southern part of the district the outcrops are less prominent. The mineralogy of this group of fissure veins is very similar to that of the northeasterly trending group.

The third set of veins is northwest trending. These veins are less than

2 m wide and are gangue-dominant. The other minor vein sets trend east-northeast and north-south. The El Dorado vein is the only prominent east-northeast trending veining that carries sulfides. The north-south veins are gangue-dominant and sulfides are minor.

The veins were believed (Lasky, 1938, Flege, 1959) to have been brecciated by repeated movements after emplacement of the granodiorite stock and before the late Paleocene andesitic volcanism. Post-ore faulting is evidenced in few faults that are filled with minor amounts of late gangue minerals and are barren or cut ore-bearing structures. Post-ore faulting is relatively minor.

MINERALIZATION

General Vein Characteristics

Mineralization in the Lordsburg district consists of over 100 veins, about 40 of which have witnessed some kind of development.

The Lordsburg veins tend to have extensive lateral and vertical continuity with several splits and offshoots, cymoid structures, and pinch and swell structures. In general, veins branch and rejoin and at times split into several members. At many places the vein filling lies in overlapping simple fissures or cross along a link from one fissure to a parallel one, the main fissure continuing as tight or gouge-filled, nearly barren stringers. Commonly, these gouge-filled stringers merge to form a wide quartz vein. Ore shoots occur in highly vuggy and drusy mass of quartz and calcite gangue. Vein structures are generally very irregular with several planes of movement. Most structures have en-echelon pattern and exhibit several stages of brecciation and cementation.

Veins are quite persistent; the Emerald vein has been traced on the surface for approximately 1525 metres with a minable width of 0.6 metres to 3 metres, averaging 1.5 metres. The combined Bonney and Oro veins reach 915 metres attaining a width of about 6 metres. North Atwood had been traced for 1000 metres, attaining width of 6 metres. Ore grade mineralization is present throughout the entire Emerald vein, and no bottom to mineralization has been found.

In the Leitendorf subdistrict, veins have no prominent outcrops. The vein systems in this part consist of several parallel short veins. Widths range from 1 to 4 m and strike lengths are typically less than 100 m.

Vein Types

The veins in the Lordsburg district can be divided into four types, namely, chalcopyrite, pyrite-gold, galena-sphalerite, and gangue-dominant veins (Tables 2 and 3; Fig. 4).

Chalcopyrite Veins

The chalcopyrite veins occupy an approximately central position. Chalcopyrite is the chief ore mineral occurring as blebs and stringers in fissure fillings in the veins. Galena and sphalerite occur locally but are not of economic importance. There are minor and local occurrences of bornite and covellite. Specularite is abundant with other gangue being chiefly quartz, some calcite, tourmaline and minor barite.

The principal chalcopyrite veins are the Emerald and Bonney vein systems. The chalcopyrite veins may reach up to 5 m in width, but typical widths range from 1 to 3 m. The contact between the veins and the wallrocks is sharp and is moderately to strongly fractured. Chalcopyrite and pyrite are characteristically present in the quartz seamed wallrock as stringers and scattered grains. These veins are generally massive.

Pyrite-Gold Veins

Pyrite-gold veins are defined as veins in which pyrite is the most abundant sulfide and gold grades are generally greater than 2 g/t (Table 2). Chalcopyrite is less abundant than pyrite while galena and sphalerite become more significant locally, exceeding chalcopyrite and pyrite in abundance. Non-sulfide gangue is quartz, some calcite and limited amounts of rhodochrosite.

Vein Type	g/t Au	g/t Ag	% Cu	% Pb	% Zn
Chalcopyrite Vein	3.9	84	2.4	—	—
Pyrite-gold Vein	3.0	54	0.6	0.3	0.3
Galena-Sphalerite Veins	1.0	215	1.2	2.6	< 0.5
Gangue-dominant Veins	—	—	—	—	—

Assays from old mine records (1903-1975), recent drill core data of Webster (1984), Phelps Dodge (1984), and Lordsburg Mining Co. (1990) and present production and exploration data (1990-1993). Values represent mean values.

Table 2. Metal content of the principal vein types at Lordsburg.

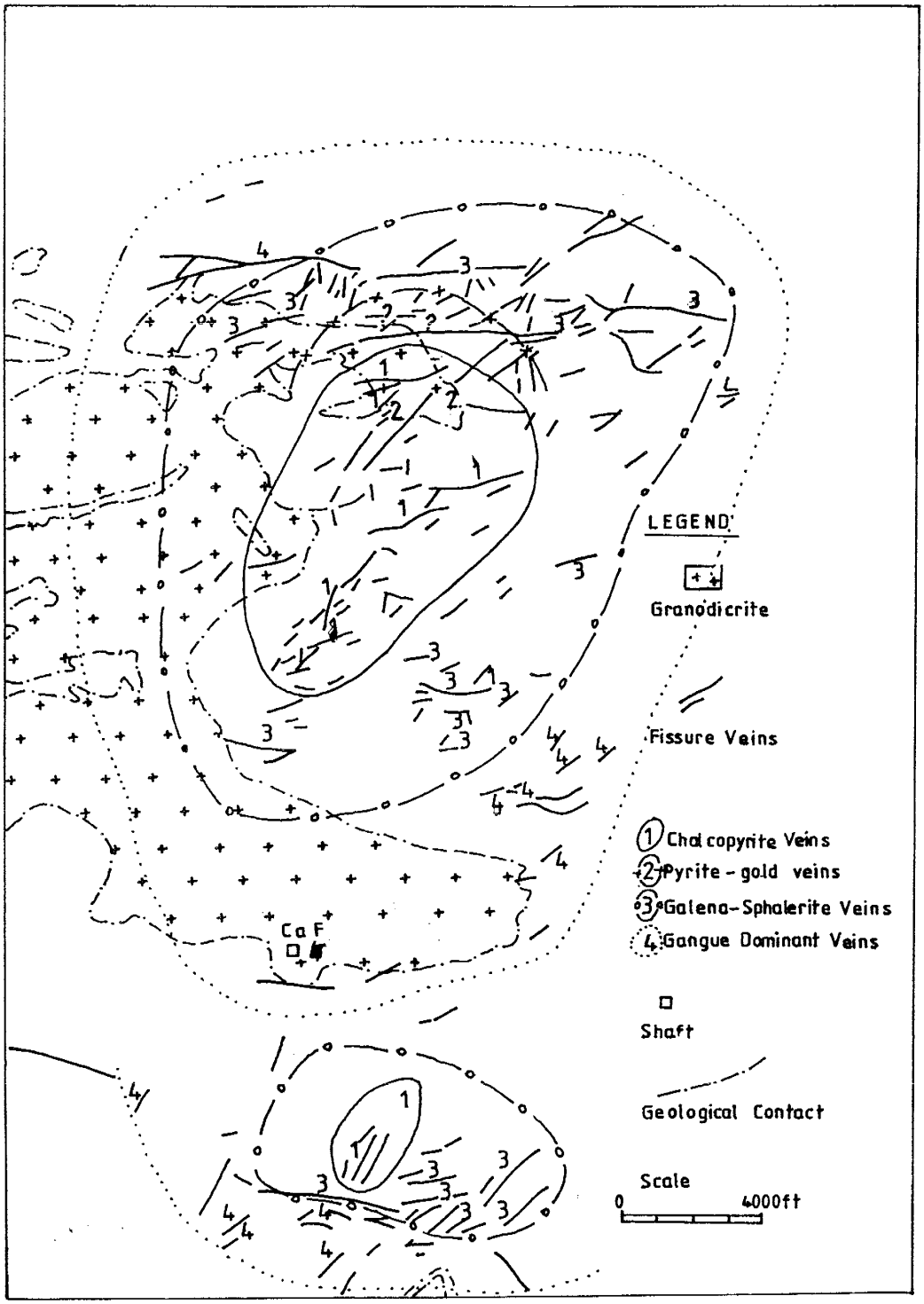

Fig. 4. Map of Lordsburg showing vein types. (See text for details.)

These veins have variable width, from a few tens of cm up to about 15 m. Wallrock and vein fragments incorporated within these structures indicate that brecciation was continuous during the formation of these veins. The contact of these veins with the wallrock is sharp, although minor quartz veinlets in the wallrock can result in locally anomalous gold values. Most sulfides, other than pyrite are intertitial quartz, locally, filling interstitial voids between quartz crystals as anhedral grains. The main pyrite-gold structures are the North Atwood and Comstock vein systems (Fig. 4).

Galena-Sphalerite Veins

These veins are defined as veins in which the volume of galena and sphalerite are equal to or exceed the volume of chalcopyrite. These veins are well expressed on the surface as silicified outcrops that attain widths up to about 40 m. The principal galena-sphalerite veins in the Virginia subdistrict are South Atwood, Atwood, Anita, and Waldo veins. Others include the veins of the Owl, Francis Kay, Ruth, Gamco, and Poly Anna mines (Figs. 3 and 4). In the Leitendorf subdistrict, the Last Chance, Suzzie, and Venus veins are the principal galena-sphalerite veins (Figs. 3 and 4). Locally, sphalerite may become dominant over galena. Mangano-calcite, rhodochrosite, quartz, and calcite are common gangue minerals.

Gangue-Dominant Veins

Gangue-dominant veins are defined as veins in which the sulfides are virtually absent. The types of gangue-dominant veins are: quartz, calcite, fluorite, quartz-calcite, quartz-fluorite, and calcite-fluorite veins.

The calcite-fluorite veins attain maximum width of 0.5 m. The quartz-fluorite veins attain a width of about 2 m. Barren quartz-dominant veins with minor amounts of calcite and manganosiderite are the most common.

Mineralogy and Paragenesis

Introduction

The Paragenesis and vein mineralogy study covered the whole district with focus on the veins exposed in the North Atwood mine. The North Atwood vein mineralogy was then related to the generalized mineralogy and paragenetic sequence presented by Lasky (1938) and Clark (1962, 1970). A general description of mineral phases and textures based on detailed observations from several locations within the district are also discussed. Mine dumps, exposures in over 50 mine workings, recent open cuts, and surface exposures were examined.

The sulfide mineralogy of Lordsburg consists of pyrite, chalcopyrite, sphalerite, and galena with minor amounts of bornite, covellite, digenite, and chalcocite. These minor phases may occur as hypogene and/or supergene minerals. Pyrargyrite is the only primary mineral phase of silver observed in the polished ore sections. Gangue minerals are quartz, calcite, fluorite, barite, manganoan-calcite, rhodochrosite, and manganosiderite. Chalcedonic and cherty quartz found locally in the Virginia subdistrict are the dominant variety of quartz in the Leitendorf subdistrict.

Mineralogy of North Atwood Mine

Detailed visual examination in the field supported by ore microscopy (15 polished sections) on underground and surface samples provided details on vein mineralogy in the North Atwood mine area.

Pyrite

Pyrite occurs as subhedral to anhedral crystals between grains of quartz (Fig. 5), perched on quartz crystals and within druzy vugs. Size of grains range from less than 10 mm to over 1.5 mm in diameter. In areas of moderate to intense leaching and oxidation, 15% to 40% of the surface areas of the pyrite grains are pitted, resulting in a spongy appearance. These pyrite grains are commonly rimmed by hematite (Fig. 5). Pyrite is the most abundant sulfide in the samples examined.

Chalcopyrite

Chalcopyrite is less abundant than pyrite. It occurs as anhedral to subhedral grains ranging from 50 to 300 mm in interstitial voids between quartz crystals. Chalcopyrite rarely occurs in contact with pyrite grains and is confined to the grey quartz masses. Chalcopyrite grains locally show rims of supergene covellite, chalcocite, and hematite (Fig. 6). Grains coated by hematite are also present.

Sphalerite

Sphalerite occurs as anhedral to subhedral grains interstitial to quartz crystals. The grains range from 0.05 to 1.0 mm in diameter. Most of the sphalerite grains exhibit minute blebs of chalcopyrite, `chalcopyrite disease'

(Fig. 7). The blebs are typically less than 0.01 mm in diameter. Sphalertie grains are rimmed by covellite and hematite.

Galena

Galena occurs as disseminated subhedral to anhedral grains and as massive blebs. Disseminated grains, which are interstitial to quartz, have sizes less than 0.8 mm. The galena grains are typically inclusion free but are rimmed by covellite. Massive blebs show fractures.

Minor Sulfide Minerals

Covellite typically occurs with minor amounts of intergrown bornite, and rims chalcopyrite, sphalerite, pyrite, and galena. Chalcocite is common in the severely leached and partially disaggregated massive chalcopyrite. It forms thin rims on pyrite, sphalerite, and chalcopyrite. Digenite is rare but typically occurs as rims on chalcopyrite.

Precious Metal Phases

Microscopic examination of 15 ore sections studied revealed minute grains of gold. The grains are dispersed and are interstitial to stage 2 quartz and stage 3 gray druzy quartz. The gold grains are associated with masses of hematite that appear to be pseudomorphs after pyrite grains.

Rhodochrosite

Rhodochrosite occurs in minor amounts typically as coatings and small crystals. It is intimately associated with chalcopyrite in stage 3 clear quartz.

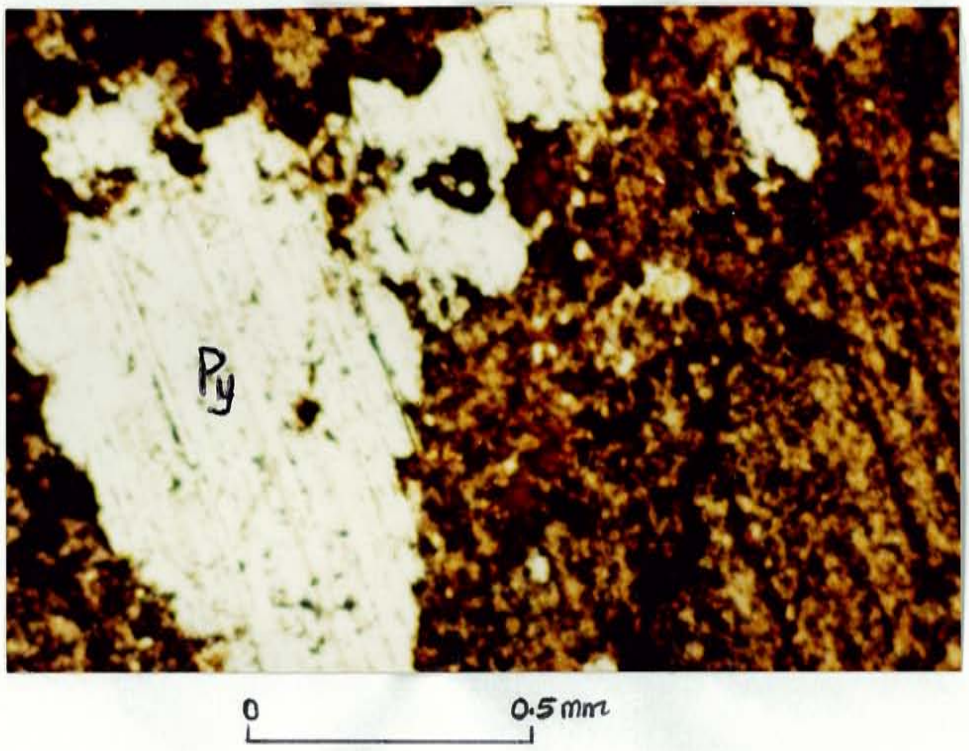

Fig. 5. Reflected-light photomicrograph of pyrite. Pyrite is interstitial to quartz. Note the hematite rims on the pyrite grains. Pyrite grains are also pitted.

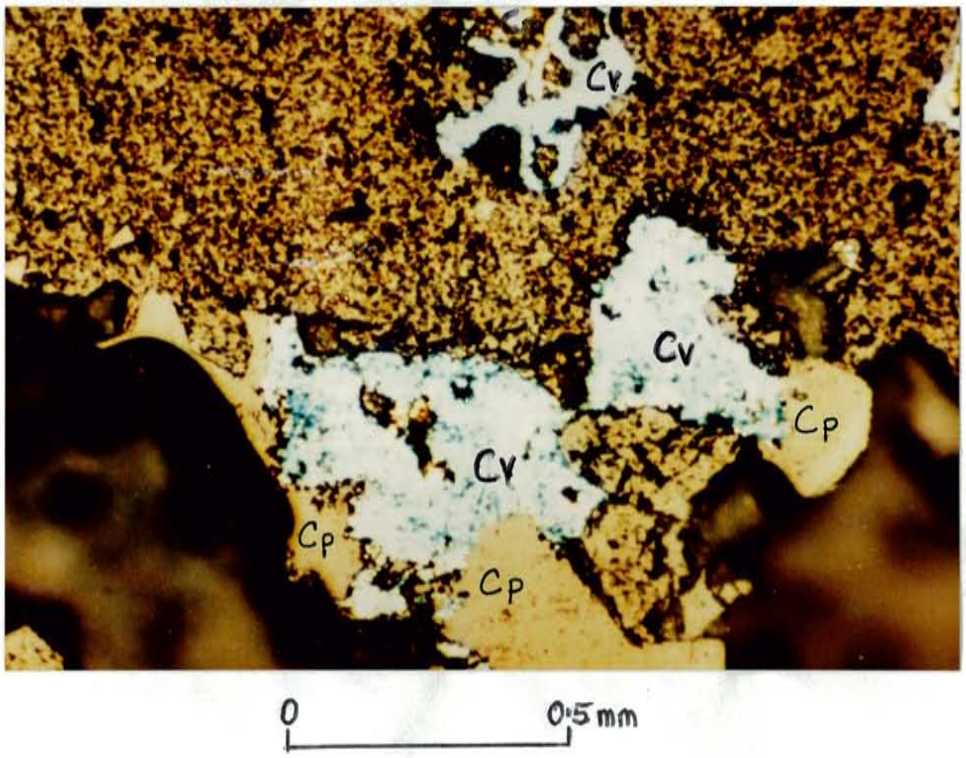

Fig. 6. Reflected-light photomicrograph of chalcopyrite rimmed and completely replaced by covellite. Cp = Chalcopyrite. Cv = Covellite.

Specularite

Two varieties of specularite occurs in the North Atwood mine. One variety occurs as fracture fillings, breccia fragment coatings, and as veinlets in wallrocks. The specularite grains typically exceed 0.5 mm in diameter.

Oxide-Zone Minerals

Oxide-zone minerals comprises volumetrically dominant "ocher" geothite and black iron and manganese oxides. The oxides phases of iron are hematite and goethite that form massive porous aggregates, annular to colloform crust or masses and coatings; the concentrations of these minerals are quite variable vein along strike. Oxides typically fill fractures and vugs although hematite locally occurs as pseudomorphs after pyrite and chalcopyrite.

Mn-oxides, jarosite, and goethite occurs as coatings on quartz crystals in vugs. Locally, goethite pseudomorphs after minute rhodochrosite occupy drusy vugs. Azurite, malachite, brochanthite, and chrysocolla are also present in voids and vugs.

Paragenesis of North Atwood Mine

Paragenetic sequence in the North Atwood mine was derived from the study of 15 polished sections, thorough examination of exposures in underground workings and handspecimens. Vug sequences, replacement and cross-cutting relationships, cleavage-veining, and overgrowth rims formed basis of the paragenetic study. Vein formation in the North Atwood mine area is separated into four distinct stages on the basis of consistent replacement

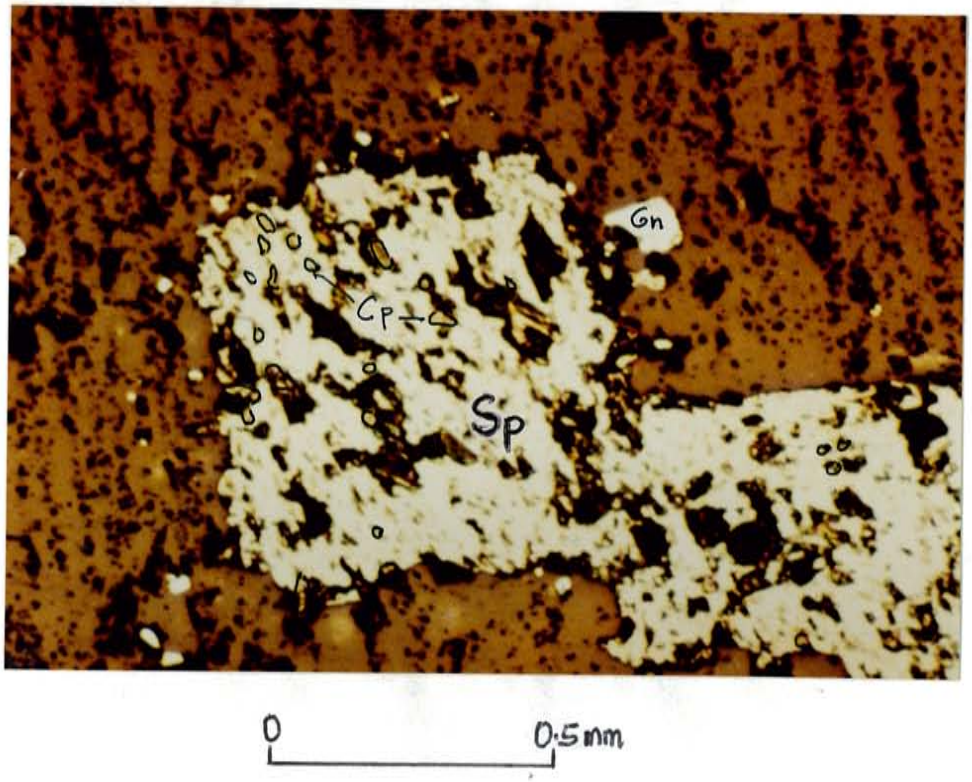

Fig. 7. Reflected-light photomicrograph of sphalerite showing blebs of chalcopyrite (chalcopyrite disease). Sp = Sphalerite, Cp = Chalcopyrite, Gn = Galena.

textures and brecciation events recognized in both polished sections and exposures (Fig. 8).

Stage 1 mineralization is typified by hydrothermal alteration of wallrock and the deposition of specularite in wallrock and vein openings. Wallrock hydrothermal minerals are sericite (illite), chlorite, and calcite. This stage is observed in products of later brecciation events. The transition between stage 1 and stage 2 mineralization is marked by a brecciation event.

Stage 2 mineralization is marked by breccia fragments within silicified vein material. Silicified fragments and vein materials are reddish-brown to light orange as a result of the presence of inclusions of specularite of the preceding stage. Open-space mineralization consist of fine grained to microcrystalline quartz; pyrite; lesser amounts of fine grained chalcopyrite; and considerable amounts of gangue sericite, chlorite, and calcite. Minor amounts of sphalerite and galena were also deposited. Trace amounts of bornite and covellite occur. Textural relationships with other sulfides suggest that pyrite was the earliest formed vein mineral. This pyrite is corroded and coated with hematite. Dark gray, gray and red dense varieties of quartz are present as streaks and patches within the veins. Transition to stage 3 mineralization is marked by a brecciation event.

Stage 3 mineralization is characterized by abundant white to colorless quartz and significant amounts of sulfides. The quartz forms druses on surfaces and vugs, lightly intergrown compact masses, cement and impregnates breccia fragments. Initial quartz deposition was followed by pyrite and later minor chalcopyrite and moderate amounts of sphalerite and galena.

Minor bornite and trace hypogene covellite were also deposited. Sphalerite and galena are equal in amount and locally volumetrically exceed chalcopyrite. Pyrite is the major sulfide mineral. Sphalerite exhibits blebs and minute inclusions of chalcopyrite, as `chalcopyrite disease.' Grain contacts, cross-cutting and replacement relationships indicate that sphalerite and galena are in part contemporaneous but typically galena is later than sphalerite and chalcopyrite. Chlorite and calcite were also deposited. The transition of stages 3 and 4 mineralization is again marked by a brecciation event.

Stage 4 vein-fill is minor, localized and occurs sporadically. It consists of white, monocrystalline quartz veinlets with disseminated pyrite grains and minor amounts of galena and sphalerite grains. Calcite occurs in significant amounts as veinlets and fills vugs and cavities. This stage of mineralization locally crosscuts stage 3, however, typically it fills fractures and vugs distal to the main vein structure and is a minor component of the total vein volume.

Vein Mineralogy and Paragenetic Sequence in Other Mines

Samples were obtained from mine dumps, outcrops, and over 50 mine workings throughout the district. Field examination of exposures was augmented by ore microscopy on 15 polished sections (85 mine-3, Bonney-Miser's Chest mines-4, Atwood mine-2, Anita mine-1, Ruth Mine-2, and Robert Lee-Nellie Bly-3).

Chalcopyrite in the mines listed above occurs as either massive blebs and coarse grains intergrown with quartz or as anhedral grains interstitial to quartz.

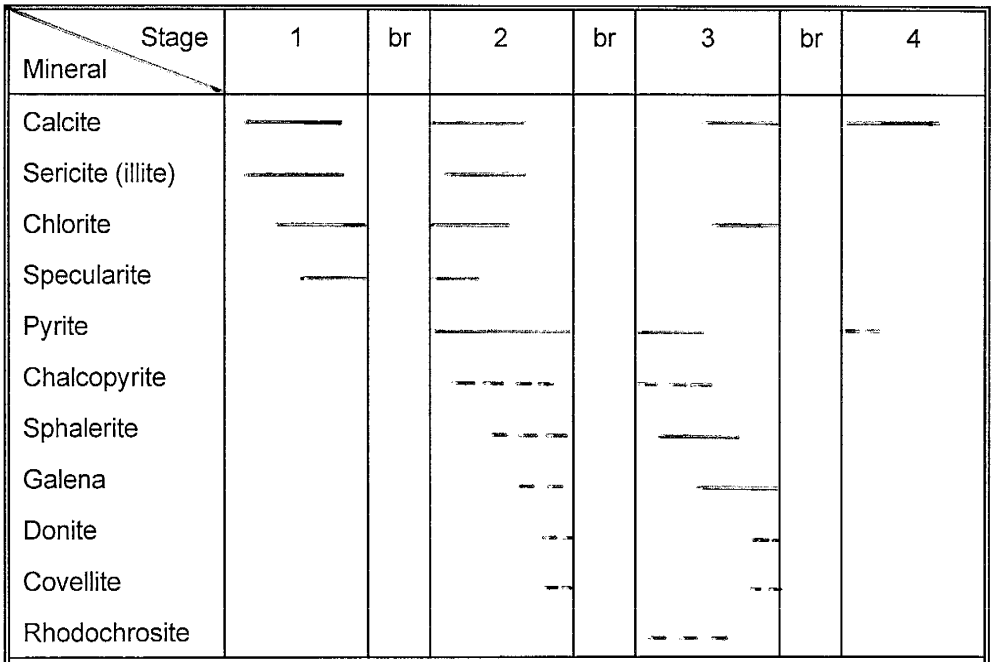

Fig. 8. Paragenetic sequence of hypogene minerals in the North Atwood Vein System. Solid lines represent major phases. Minor-trace phases are represented by dashed lines. br, brecciation event.

Chalcopyrite blebs in the 85 and Bonney mines reach 3.8 cm in diameter. Chalcopyrite grains interstitial to quartz are typically less than 50 mm in diameter. Chalcopyrite grains show rims of supergene covellite and chalcocite (Fig. 6). In the Robert Lee and Nellie Bly mines, chalcopyrite grains contain inclusions of galena and sphalerite. Replacement by galena is common in these mines.

Sphalerite grains observed in samples from the 85 and Bonney mines exhibit no `chalcopyrite disease.' In the Anita mine, the sulfide fraction is dominated by sphalerite and galena. Galena is the most abundant sulfide in the Ruth mine, where massive blebs reach up to about 3 cm in diameter. Galena in this mine is interstitial to white, colorless or milky quartz and locally intergrown with quartz. Galena inclusions in chalcopyrite are common. Galena are typically rimmed by covellite (Fig. 9). Pyrite in the 85 and Bonney mines occur as grains, and as clusters in quartz and wallrock. Massive blebs and veinlets of pyrite in the wallrock are not uncommon.

Bornite, digenite, and chalcocite occur in significant amounts in the Robert Lee and Nellie Bly mines. These sulfides occur typically as irregular patches and euhedral blades and are interstitial to quartz. The textural features of these sulfides are suggestive of hypogene origin. At least three periods of brecciation and quartz and calcite mineralization followed that of bornite, digenite, and chalcocite, suggesting these minerals are hypogene. A polished section of a specimen from the 85 mine contains pyrargyrite. It occurs as an inclusion in a chalcopyrite grain. Specularite is absent in the veins of Leitendorf subdistrict.

Common gangue minerals observed in the veins examined include quartz, barite, rhodochrosite, fluorite, calcite, sericite, chlorite, and tourmaline. Calcite is the only gangue mineral of stages 4 and 5 mineralization, and occurs as scalenohedrons and prisms that fill vugs and cavities. Barite occurs in significant amounts as white platy crystals in the 85, Robert Lee, and Nellie Bly mines. It is intergrown with galena and sphalerite and is closely associated with chalcopyrite in vuggy quartz. Rhodochrosite occurs in minor amounts in the Robert Lee and Nellie Bly mines where it is intimately associated with barite and chalcopyrite. Fluorite has been identified as an ore-stage (stage 2) gangue and as late stage veins in the 85, Bonney, Robert Lee, and Nellie Bly mines. Calcite, quartz,and fluorite occur in approximately equal amounts in the gangue-dominant veins.

The veins in the district display similarities in mineralogy and paragenesis. In detail, minor differences sometimes occur between individual veins. In general terms, the mineralogy of the deposits can be seen to reflect the 6 paragenetic stages (Fig. 10) described by Lasky (1938). The succession of ore and gangue minerals in each of the mines fits Lasky's paragenetic sequence, however, all 6 stages may not occur in each mine.

Vein Types and Paragenesis

The vein designations in this study not only indicate characteristic mineralogy but reflect a general district-wide paragenetic sequence that is consistent with a time sequence of mineralizing episodes. The time sequence is depicted by the crosscutting relations of these vein types and the associated

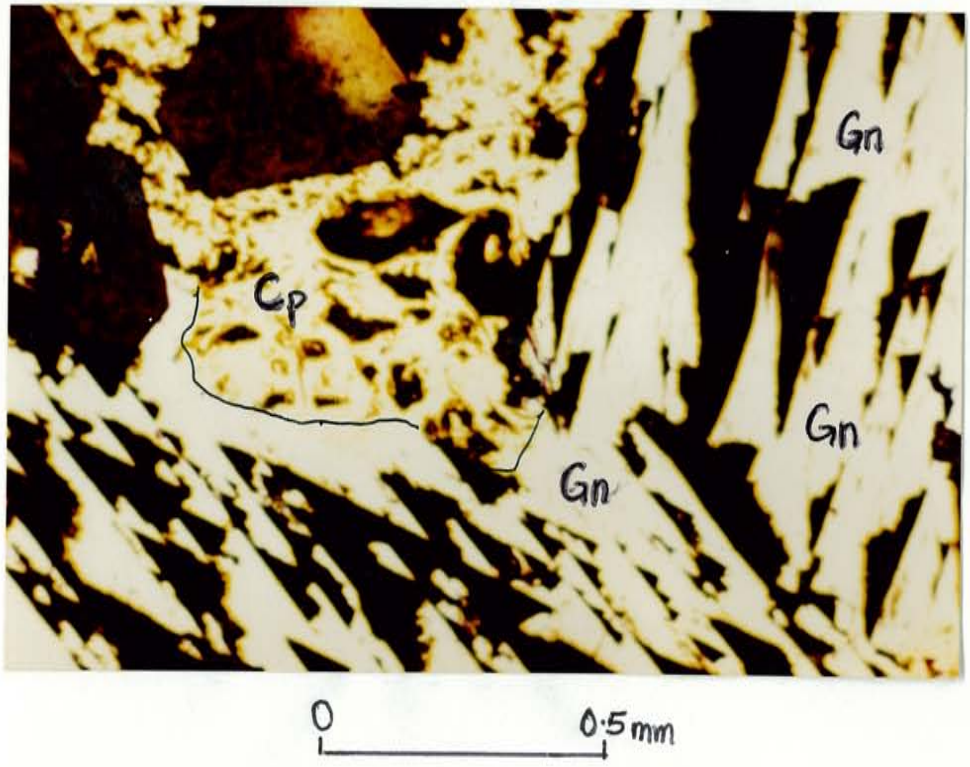

Fig. 9. Reflected-light photomicrograph of galena replacing chalcopyrite. Gn = Galena, Cp = Chalcopyrite.

veinlets. On the 85-hill,a pyrite gold vein, the Comstock, cuts the chalcopyrite-rich Emerald vein. The Cobre Negro vein, another pyrite-gold vein, intersects the Emerald vein at its southern extremity (Figs. 3 and 4). At the 6th levels in 85 and Henry Clay mines and the 4th level in the Atwood Mine, the chalcopyrite-rich Emerald vein splits to the chalcopyrite-galena-sphalerite-rich South Atwood vein (Federal Resources Corp Mine records).

At levels 2 and 3 in the North Atwood mine, the main vein splits into a north (predominantly pyritic) vein and a south (galena-sphalerite) vein. The south vein may be seen cutting the north veins at its ends. At two other locations on the surface (Oakley-North Atwood ridge), the veins merge. It can be inferred from these observations that the galena-sphallerite-rich south vein postdate the pyritic vein. The galena-rich Florence vein (Waldo mine) on the surface either cuts or merges with several splits of the South Atwood veins. In an open cut in the Anita-Clementine mines area, gangue-dominant carbonate-quartz veins cut galena-sphalerite-rich veins. The observed field relations of these vein types reflected a time sequence of vein fill deposition in the district.

Crosscutting relations between veinlets were observed in the North Atwood mine and dump samples (wallrock and vein material) from the Banner mines. A time sequence of (from oldest to youngest): chalcopyrite ± pyrite + specularite, pyrite ± specularite ± chalcopyrite, galena ± sphalerite ± pyrite, and calcite ± quartz ± fluorite is discerned. The field relations displayed by the major veins and the observed veinlets formation sequence suggest a time sequence of early chalcopyrite veins followed by, pyrite-gold veins, galena-sphalerite veins, and latest gangue-dominant veins. This time sequence is in

good agreement with the paragenetic sequence of vein minerals documented for the district. (Lasky, 1938; Flege, 1959).

The paragenetic sequence observed at the North Atwood mine (Fig.8) corresponds well with stages 1 to 4 to Lasky's generalized paragenetic sequence for the district (Fig.10). Similarities in terms of mineralogy of individual stages and mineralizing events (brecciation and fracturing) that seperate the stages of mineralization are striking. This further suggests that mineralization occurred in various pulses district-wide.

Zonal Distribution of Minerals

The Lordsburg district is an example of metal and mineral zoning. Three concentric zones asymmetrically arranged around the granodiorite stock were delineated based on vein mineral distribution.

Mineral zoning in the district is best seen laterally along the 3.5 km length from the Emerald vein system at the 85 Mine, along the North and South Atwood vein systems in the North Atwood and Atwood mines, respectively, and the east-west trending Florence veins at the Waldo mine. Vein mineralogy changes from chalcopyrite-pyrite at the 85 mine through a transitional halo of pyrite-gold to galena-sphalerite-chalcopyrite in the Atwood mine and finally to galena-silver in the Waldo mine.

Four mineral zones (Fig. 12), based on the distribution of the vein types (Fig. 4), were delineated in the Lordsburg district. A central zone, occupying an area around the granodiorite stock has chalcopyrite as the principal ore mineral,

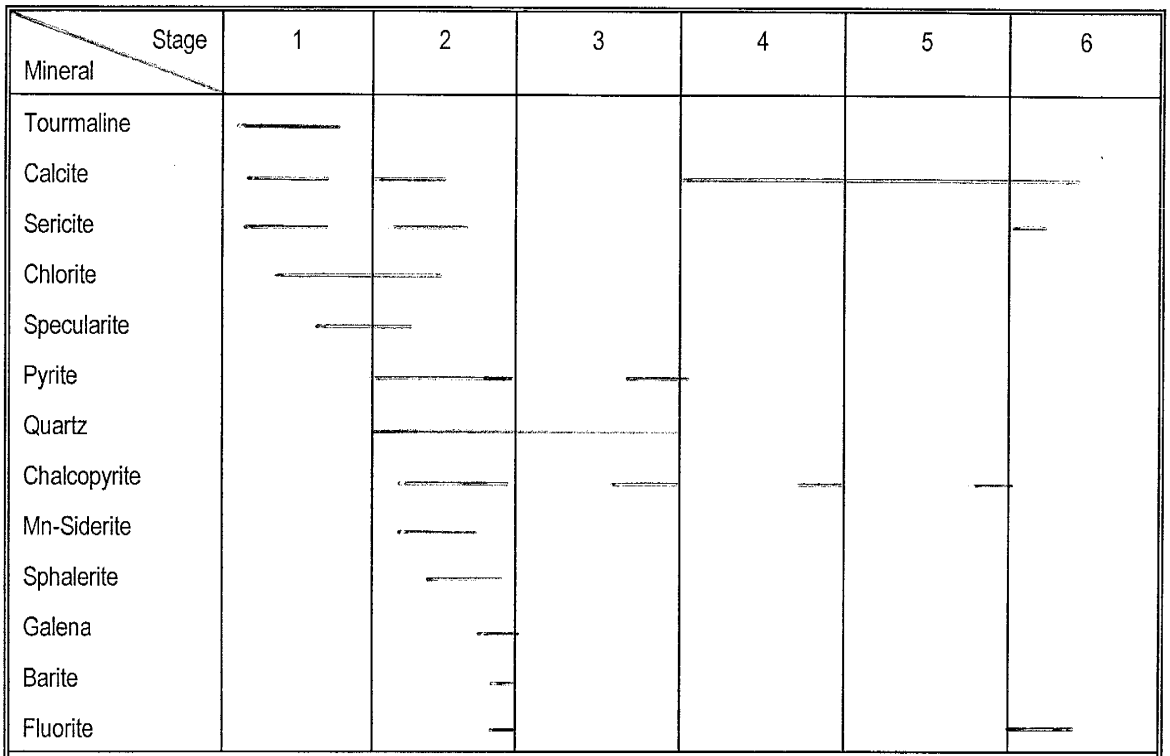

Figure 10.Generalized paragenetic sequence of hypogene vein minerals in the Virginia subdistrict (after Lasky, 1938)

with minor bornite, and subordinate sphalerite and galena. Gangue minerals include specularite and tourmaline.

A gold-rich transition zone in which pyrite is the dominant sulfide mineral surrounds the central zone. The pyrite content of this zone is much higher than the pyrite contents of the preceding and succeeding zones, and galena and sphalerite become more volumetrically significant ore minerals. Copper ($\leq$ 1.5%) is by far exceeded in value by the precious metals (Au $\leq$ 6 ppm; Ag $\leq$ 100 ppm) in this zone. Specularite occurs but tourmaline is absent. Carbonates are found in small quantities throughout the zone.

The transition zone is succeeded by the intermediate zone which is further subdivided into two subzones. In the inner subzone, galena, sphalerite, and chalcopyrite occur in economic quantities. Lead and zinc values are equal and may locally exceed copper values. Locally, galena may be more abundant than sphalerite and vise versa. Tourmaline and specularite also occur as gangue minerals. Carbonate becomes a major ore-associated gangue. In the outer subzone of the intermediate zone, galena is the major sulfide mineral. Gold values rarely exceed 1 ppm and are generallysubeconomic. Silver values are most economically important here.

The intermediate zone is succeeded by a peripheral zone, in which chalcopyrite, galena, sphalerite, gold, and silver do not occur in commercial quantities.

Table 3. Definition of Mineralogic Zones and Vein Types

Zone	Characteristic Definition	Vein Types
Central	Chalcopyrite is principal mineral	• Chalcopyrite - • Pyrite - minor • Gangue dominant
Transition	Pyrite is the dominant sulfide; galena and sphalerite become more abundant	• Pyrite - dominant • Gangue dominant
Intermediate	Galena and sphalerite occur in economic quantities	• Chalcopyrite - minor •Galena/sphalerite - dominant
Peripheral	Presence of abundant gangue minerals ; fluorite + calcite + quartz	• Gangue - dominant

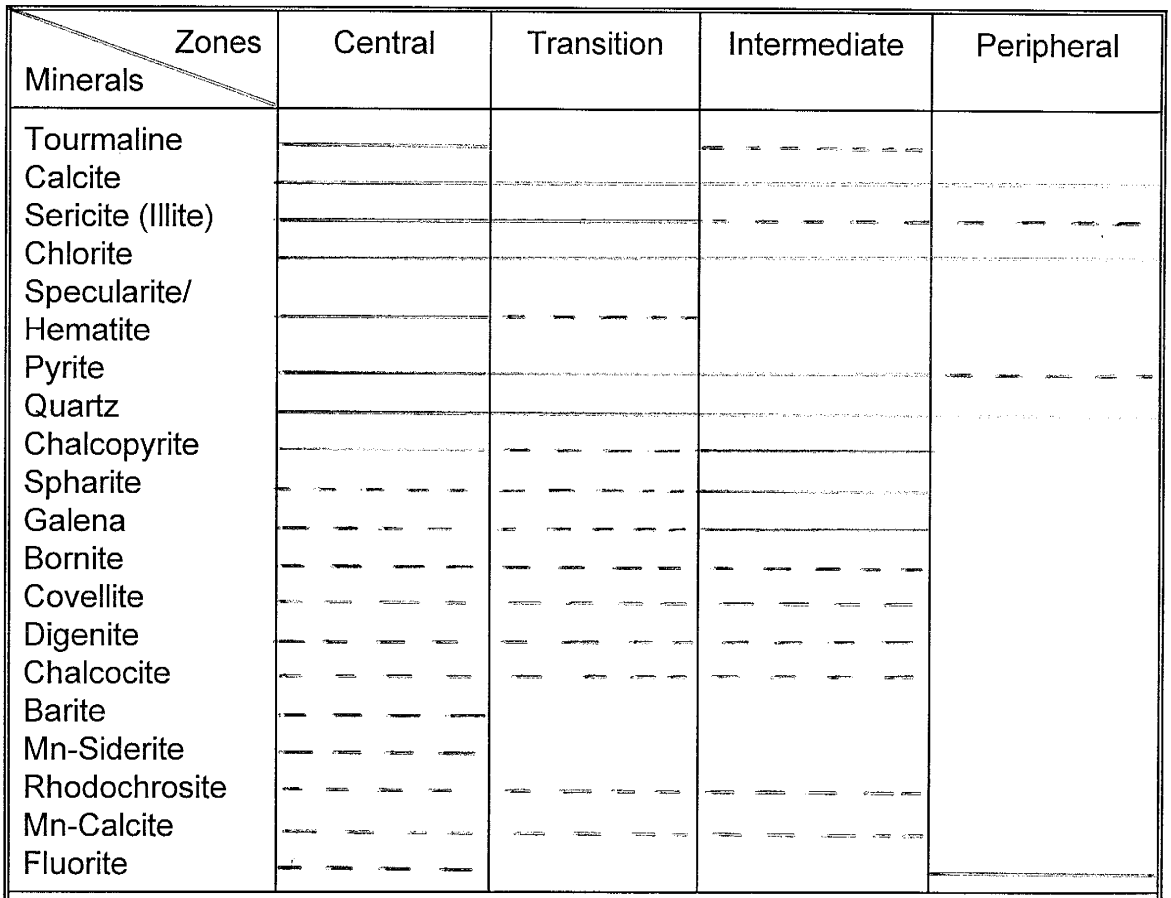

Figure 11. Zonal distribution of vein-fill minerals in Lordsburg; solid lines represent major phases; minor-trace phases are represented by dashed lines.

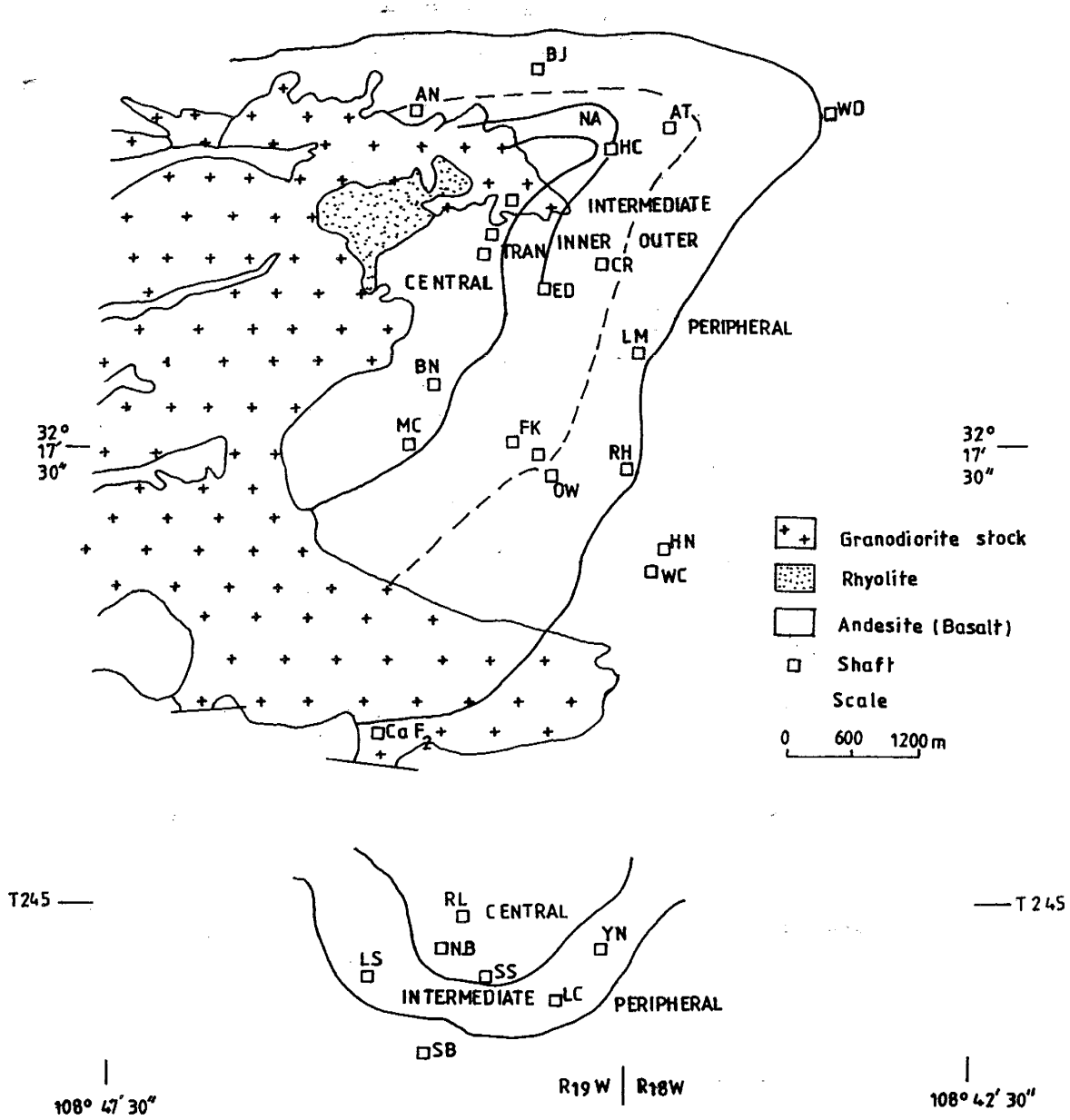

Fig. 12. District-wide mineral zonation in Lordsburg. Mines abbreviated: AN = Anita, AT = Atwood, BJ = Bonnie Jean, BN = Bonney, CR = Copper Reef, ED = El Dorado, FK = Francis K, HN = Homestake Needmore, HC = Henry Clay, LC = Last Chance; LM = Lady Mary, LS = Lone Star, MC = Miser's Chest, NB = Nellie Bly, OW = Owl, RH = Ruth, RL = Robert E. Lee, SB = Silver Bell, SS = Sussie, WC = White Cloud, WD = Waldo, 85 mine, and CaF_2 = Fluorite Mine. Solid lines represent boundaries of major mineralogic zones and dashed lines subdivide major zones. See text for details.

ALTERATION

Introduction

Hydrothermally altered rocks around the mineralized veins in the district host a characteristic sequence of mineralogic and textural alteration types. These alteration products were studied and defined megascopically in the field and were examined and characterized by petrographic and X-ray diffraction methods. The distribution and temporal relations between stages of hydrothermal alteration around veins and on a district-scale was also examined.

Sets of samples were taken along sample lines perpendicular to selected major veins (Appendix I). Samples were collected from both sides of the veins when accessible. Seventeen traverses across major veins in the district were mapped and sampled. Drill core samples of two drill holes in the North Atwood mine area were also selected for analysis. Clay minerals were studied by X-ray diffraction on 96 clay separate samples (separations were done using the techniques described in Moore and Reynolds (1989). Petrographic examination was carried out on 40 thin sections.

The North Atwood mine area was the focal point for detailed alteration study. Detailed mapping supported by petrological (15 thin sections) and X-ray (34 diffractograms) data on 34 outcrop, underground, and drill core samples provided detail about the surface and subsurface alteration in the mine area. In order to recognize any differences or similarities in alteration patterns around other vein types, traverses across Emerald, Bonney, Miser's Chest, Atwood-Waldo, Robert Lee-Nellie Bly veins were also studied.

Alteration Types

Three distinct types of alteration, based on major mineral assemblages and textures, are discernible. Each alteration type grades over several metres into that adjacent, making it impossible for sharp alteration boundaries to be drawn. From the vein margins, these alterations types are illitic, intermediate argillic, and propylitic.

The alteration types are segregated into four alteration zones. These zones are classified according to diagnostic mineral assemblages and textures, and all zones are distinct on the basis of clay mineralogy. The definitive alteration mineral assemblages for each zone in the Lordsburg district are given in Table 4. From the vein margins the zones are illitic, chloritic, chlorite-smectite mixed-layer, and chlorite-albite-calcite. The terms illite and sericite are considered synonymous in this study. The alteration zones surrounding major veins, namely Emerald, North Atwood, Robert Lee-Nellie Bly, and Bonney-Miser's Chest veins, are shown in Figs.13, 14, and 15.

Alteration Zones

Illitic Zone

This zone occurs directly adjacent to veins. Andesite and granodiorite have been bleached white, red to reddish-brown when specularite is present and dark green when tourmaline is present. X-ray diffractograms of 25 clay separate samples and 12 thin sections of samples from this zone were studied.

Quartz, illite, and chlorite occur as volumetrically-important alteration minerals. Quartz is abundant, occurring as magmatic phenocrysts in groundmass, as veinlets, and as alteration product of plagioclase phenocrysts.

Table 4. Characteristic Mineral Assemblages of Alteration Zones

Zones	Clay Minerals	Other Minerals
Illitic	Illite*, chlorite*, kaolinite I/S ML (R≥3)	Albite, calcite, epidote K-feldspar, quartz*, pyrite
Chloritic	Illite*, chlorite*, smectite, kaolinite, I/S ML (R≥3), C/S ML (ROC+/S)	Albite*, calcite*, epidote, K-feldspars*, pyrite, (Ca-plagioclase, Fe-Ti oxides), quartz
Chlorite-smectite mixed-layer Minerals	Corrensite*, ROC/S+*, ROC+/S, chlorite, smectite, kaolinite, illite, tosudite, K/S ML, I/S ML (R≥1)	Albite*, calcite, K-feldspars*, epidote, analcime, phlogopite, (Ca-plagioclase, pyroxenes amphiboles, Fe-Ti oxides)
Chlorite-albite-calcite	Chlorite*, smectite, illite	Albite*, calcite*, epidote, K-feldspars, (Ca-plagioclase, pyroxenes amphiboles, Fe-Ti oxides)

* Mineral that is always present in the given zone.
\+ Predominant mineral in the mixed-layer (〉80%).
Corrensite - regular trioctahedral C-S ML.
Tosudite - regular dioctahedral C-S ML.
ROC/S - random C-S ML.
R - Reichweite
ML - mixed-layer
C-S- Chlorite-Smectite

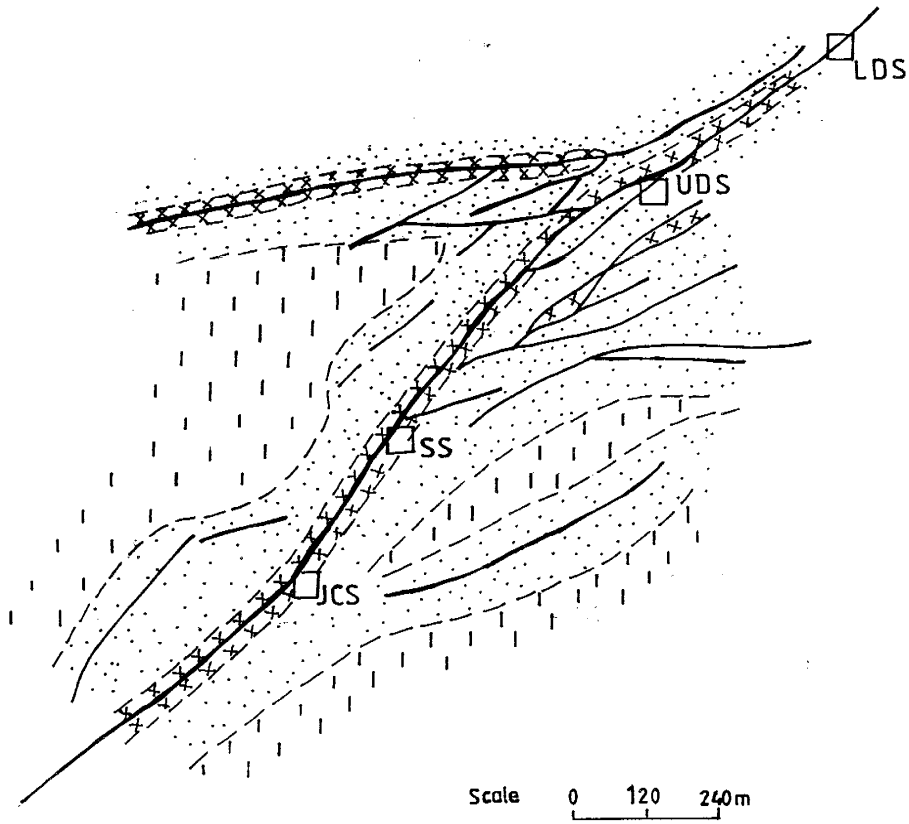

LEGEND	
	Illitic
	Chloritic
	chl-smec ML
	vein
	alteration zone boundary
	shaft
	Fresh rock

Fig. 13. Surface expression of the Emerald vein system and associated overlapping alteration haloes in the 85 hill area. JCS = Jim Crow Shaft, SS = Superior Shaft, UDS = Upper Dundee Shaft, LDS = Lower Dundee Shaft.

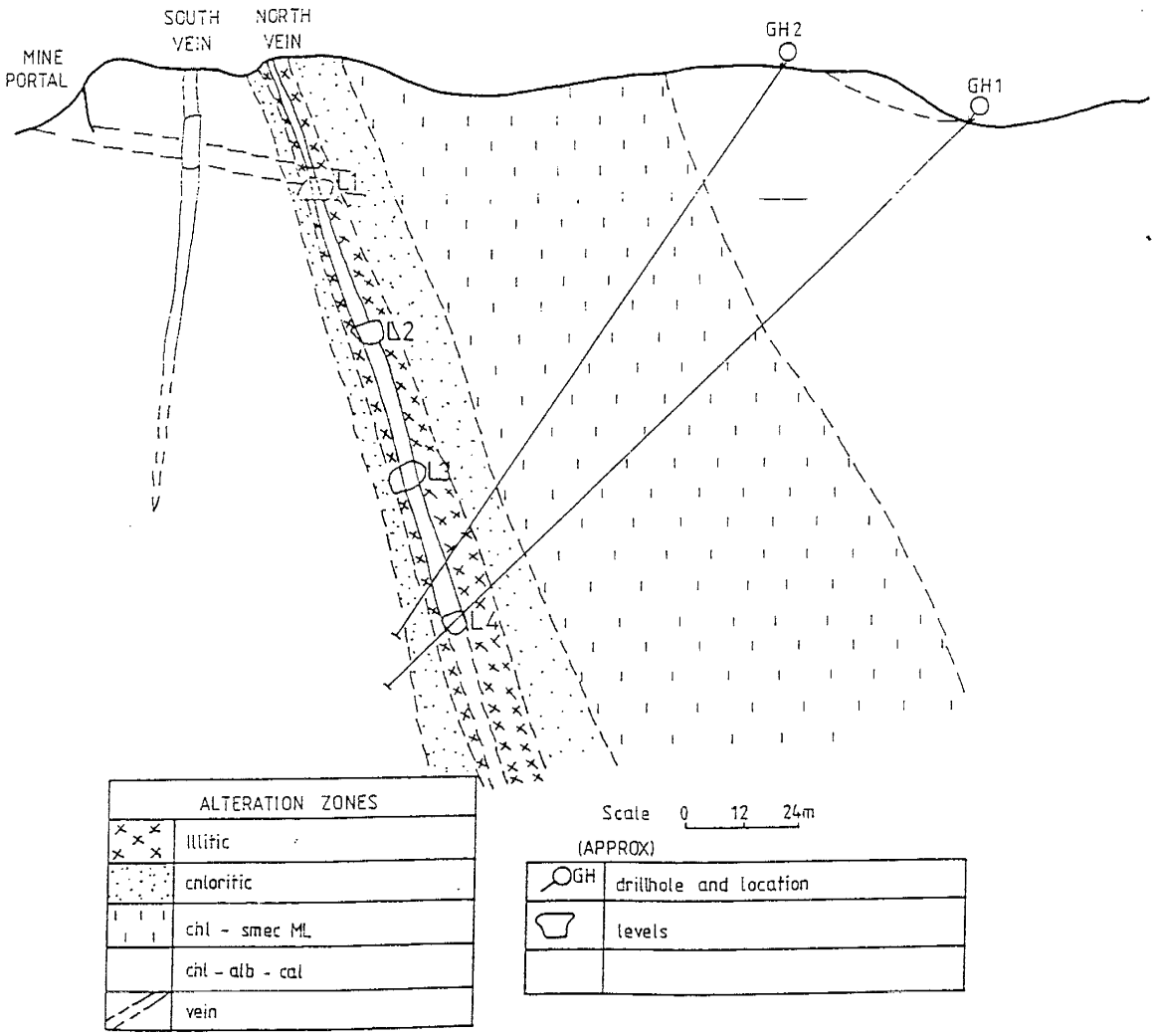

Fig. 14. North Atwood vein system and associated alteration zones. Alteration study is based on drill core samples from drillholes GH1 and GH2 and surface outcrop samples.

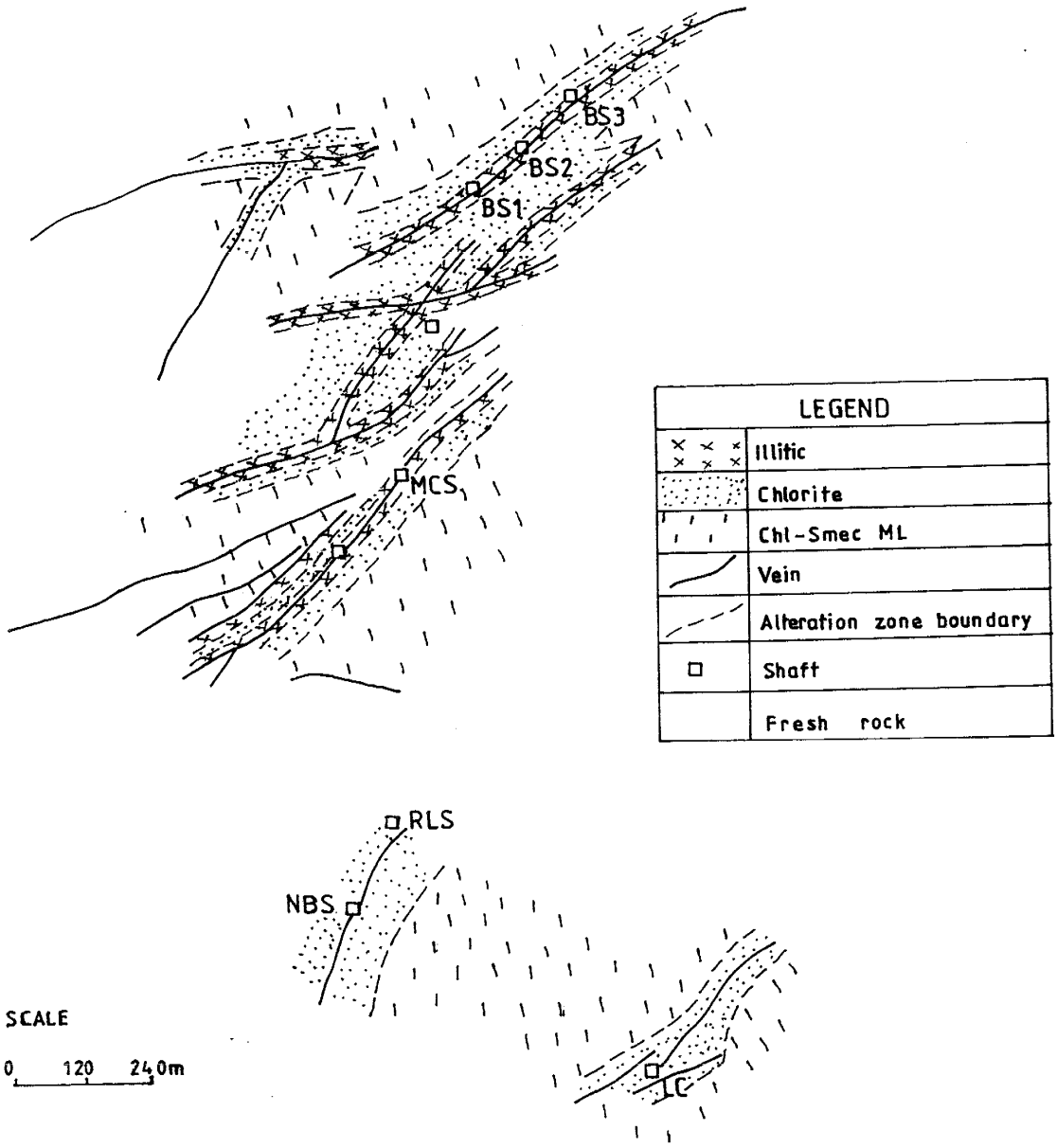

Fig. 15. Surface expressions of the Bonney-Miser's Chest vein systems (above). Robert Lee-Nellie Bly-Last Chance vein systems (below) and associated overlapping alteration haloes. BS = Bonney Shaft (1, 2, 3 represent shaft numbers), MCS = Miser's Chest Shaft, RLS = Robert Lee Shaft, NBS = Nellie Bly Shaft, LCS = Last Chance Shaft.

Illite occupies dissolution cavities in magmatic feldspars and occurs as inclusions in quartz (Fig. 18). Significant amounts of illite formed as a vein mineral, occuring in vugs and fractures, and in groundmass (Fig. 16). Illite is highly crystalline, as indicated by its birefringence and sharp X-ray diffraction peaks (Appendix II). The polytypes of illite from XRD analysis are $2M_1$ and 1M (Appendices II and III).

Chlorite occurs with illite in vein fillings, vesicles, vugs, and fractures. This chlorite, introduced during alteration, is the dioctahedral type (Fig 17). Ferromagnesium minerals are wholly replaced by chlorite. Silicification is largely restricted to intensely fractured or brecciated zones directly adjacent to veins. Calcite occurs as veinlets and fills cavities and vugs. The characteristic assemblage in this zone in the North Atwood mine is quartz-illite-chlorite-pyrite, with variable quantities of I/S, Kaolinite calcite, epidote, albite and K-feldspar.

Chloritic Zone

This zone is defined on information obtained from the study of 10 thin sections and X-ray diffractograms of 24 clay separates, and is characterised by the relative decrease in magmatic groundmass quartz and the absence of quartz veinlets. Quartz, illite, and pyrite occur in significant quantities although, andesite and granodiorite display relict propylitic chlorite and the formation of hydrothermal vein-related chlorite. Chlorite replaces biotite and other ferromagnesian minerals (Fig. 18). It occurs as a patchy replacement of phenocrysts and groundmass, occupying dissolution cavities in plagioclase and ferromagnesian minerals. Typically, this chlorite is green slightly pleochroic, weakly birefringent, and has variable crystallinity.

Fig. 16. Transmitted-light photomicrograph of diffused illite veinlets and quartz. I = illite, and Q = Quartz.

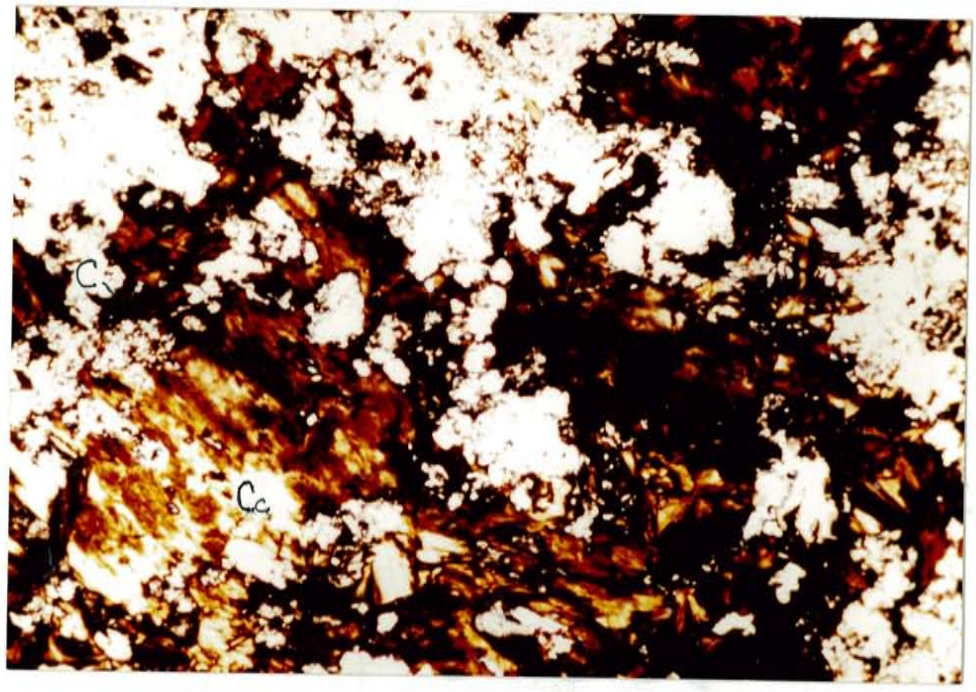

Fig. 17. Transmitted-light photomicrograph of chlorite and calcite after feldspars and ferromagnesian minerals. C = Chlorite, and Cc = Calcite.

The X-ray diffractograms of these chlorites indicate obvious structural and compositional differences (Appendix II). These chlorites are identified as trioctahedral and dioctahedral types with compositions falling between end-members clinochlore (Mg_5 Al_2 Si_3 O_{10} $(OH)_8$) and chamosite (Fe_3 Al_2 Si_3 O_{10} $(OH)_8$). The diffractograms of oriented-clay samples indicate that they are iron-rich (Moore and Reynolds, 1989).

The illite in this zone is a mixture of $2M_1$ and 1M polymorphs with 1M dominant. The illite-smectite is mainly R=3 I/S with expandability of 10% to 15%. The characteristic assemblage in this zone in the North Atwood mine is chlorite + illite, ± quartz, ± pyrite, ± I/S, ± kaolinite, ± calcite, ± epidote, ± albite, and ± K-feldspar.

Chlorite-Smectite Mixed-Layer Zone

X-ray diffractograms of clay separates and 10 thin sections of samples from this zone were studied. Quartz occurs in small amounts in groundmass. Plagioclase is partly or wholly altered to albite and to various C/S minerals, with or without discrete chlorite and/or smectite (Fig. 19). In the inner parts of this zone, alteration of plagioclase is complete, discrete chlorite is more abundant than chlorite-smectite mixed-layer minerals. In the outer part of the zone, smectite-rich random C/S, corrensite and albite are the dominant alteration minerals. K-feldspar locally replaces plagioclase and co-exists with albite within the same phenocryst. Calcite occurs as patchy replacements of plagioclase phenocrysts and/or in the groundmass as grains (Fig. 18).

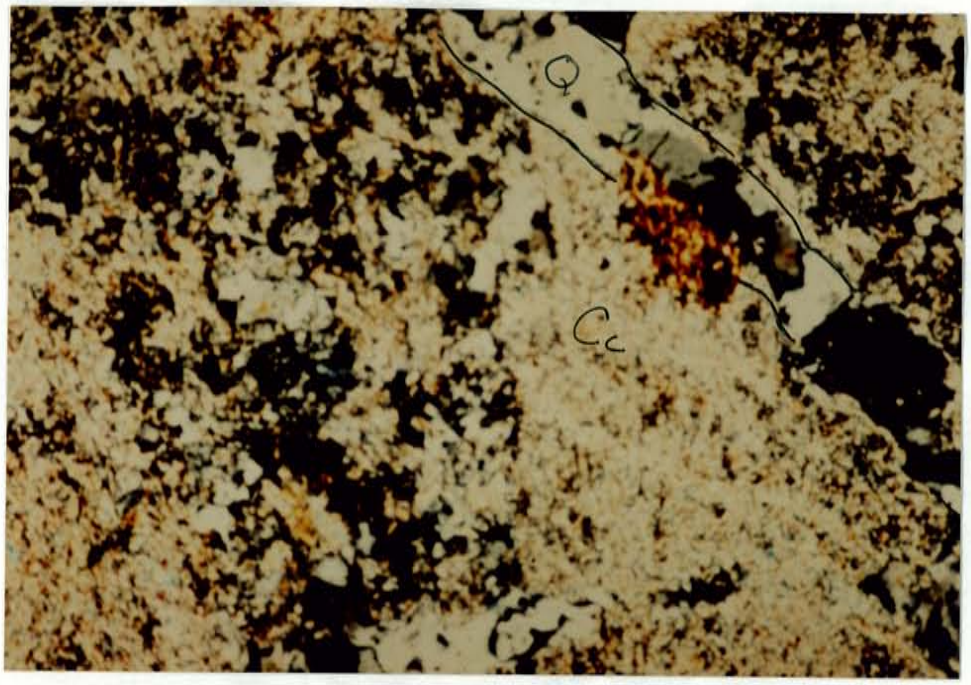

Fig. 18. Transmitted-light photomicrograph of quartz veinlet and completely illitized, chloritized and calcitized plagioclase. Q = Quartz; Cc = Calcite.

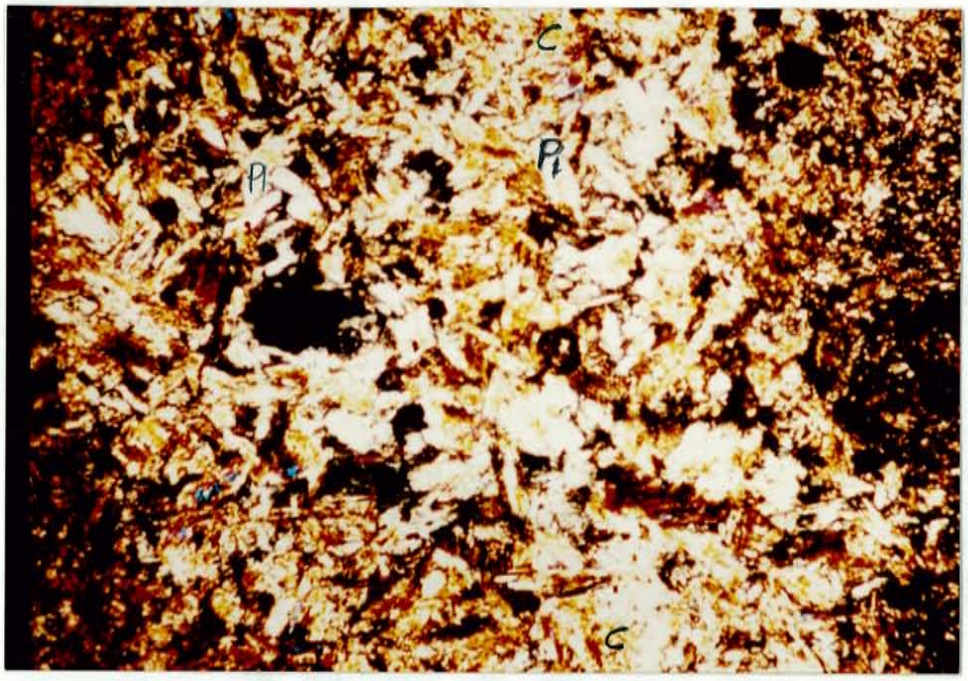

Fig. 19. Transmitted-light photomicrograph of partially altered plagioclase phenocrysts and chloritized biotite. Pl = Plagioclase; C = Chlorite; B = Biotite.

Chlorite-Albite Zone

The zone is defined based on the study of 20 X-ray diffractograms of clay separates, and eight thin sections. Almost all primary minerals have been partially replaced by the assemblages chlorite, albite, K-feldspar, calcite, quartz, and ± epidote, and ± titanite. Plagioclase is partially replaced by albite, chlorite and calcite along cleavages and fractures (Fig. 19). Biotite and hornblende are altered to chlorite (Fig. 19). The groundmass is mostly of chlorite, albite, calcite, and smectites with minor leucoxene and locally minor pyrite. Titanite and rutile may replace illmenite-magnetite.

Spatial Distribution of Alteration Minerals and Zones

The alteration zonation documented above is the same for the four vein types identified in the Virginia subdistrict. Figure 20 illustrates alteration zonation surrounding the veins and the distribution of alteration minerals in the various zones. The alteration style and zonation in the Leitendorf subdistrict is similar to the Virginia area but differs with respect to alteration mineralogy and compositional or structural changes observed in some clay minerals within the zones.

In Nellie Bly, Robert Lee, and Last Chance mines, illite is virtually absent in the alteration zone adjacent the veins. It is replaced by regular (R=3) I/S. Corrensite replaces random C/S as the main C/S mineral in the succeeding outward alteration zones.

The widths of the alteration zones are a function of the vein type and lateral distance from the granodiorite stock. Figure 21 is based on observations made during mapping along the 17 traverses (Appendix I), and is supported by

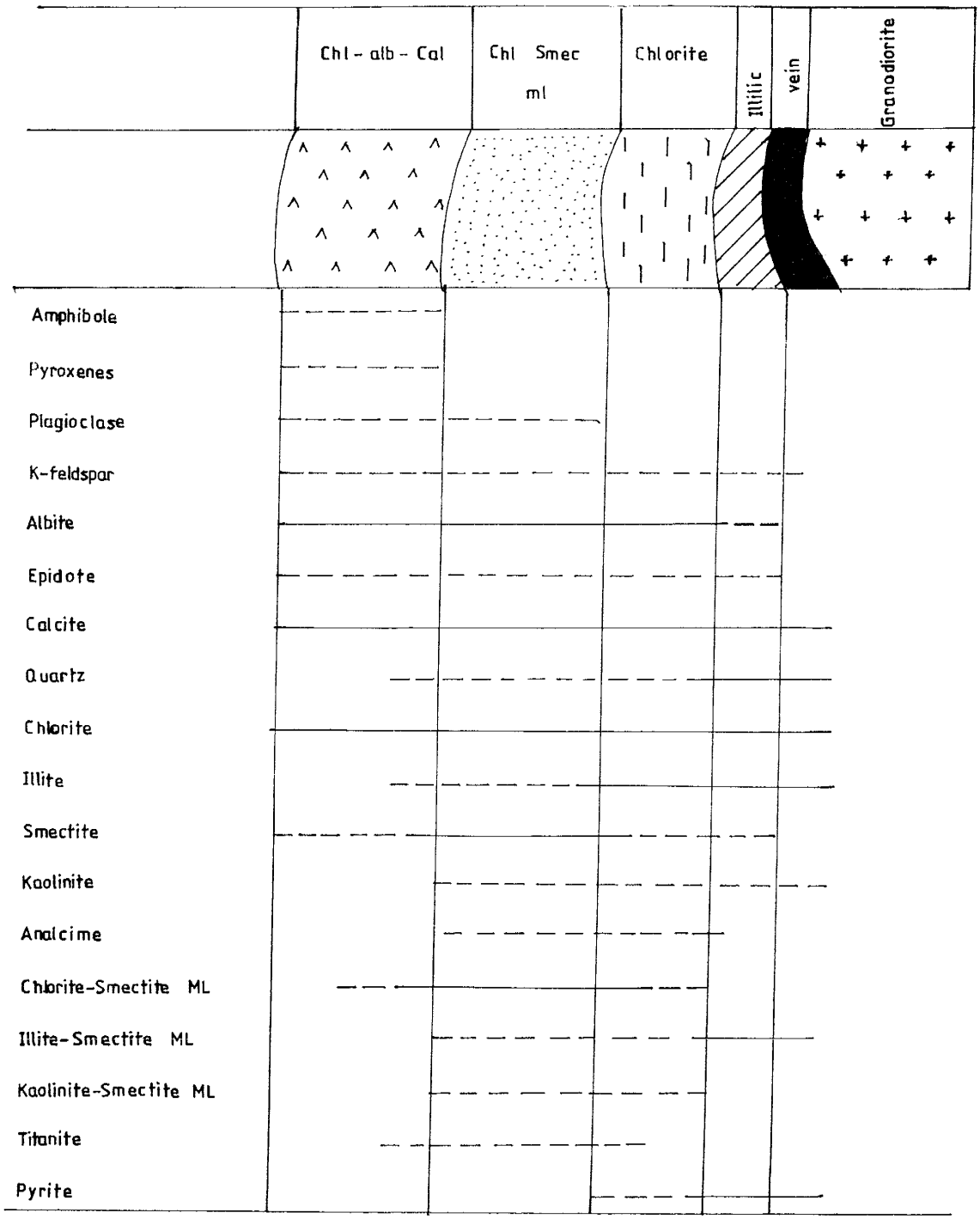

Fig. 20. Idealized alteration zonation associated with mineralized veins in the Lordsburg district and the distribution of alteration minerals in the various alteration zones. Major phases are represented by solid lines. Minor-trace phases are represented by dashed lines.

X-ray diffraction and petrographic studies. It depicts an idealized spatial distribution of alteration zones along a hypothetical continuous vein and it also shows how the widths of the alteration zones correlate with vein types in the district.

Chalcopyrite-rich veins in the 85 and Bonney mines have the widest illitic and chloritic zones. Combined widths of these zones ranges from 0.5 to greater than 50m. Overlapping alteration haloes on numerous veins tend to locally form wide zones of illitic and chloritic alteration, as shown in Figs. 13 and 15. Pyrite-gold veins in the North Atwood mine and galena-sphalerite veins in the Atwood mine have narrower illitic and chloritic zones and a wider C-S zone. The combined widths of illitic and chloritic zones around these veins range from 0.1 to about 20m.

The proportions of illitic polymorphs within the illitic zone surrounding veins varies with vein type. Illite in the salvages of chalcopyrite-rich veins in the 85 and Bonney mines contain mainly $2M_1$ illite, whereas the illite in the selvages of pyrite-gold-rich, and galena-sphalerite-rich veins is mostly 1M illite.1 The proportion of 1M is also observed to increase away from the margins of these veins. The C-S zone also exhibits a marked but gradual change in composition and ordering in the mixed-layer minerals away from the vein margins. A chlorite-rich random C/S yields to a smectite-rich random C-S, and locally corrensite and tosudite.

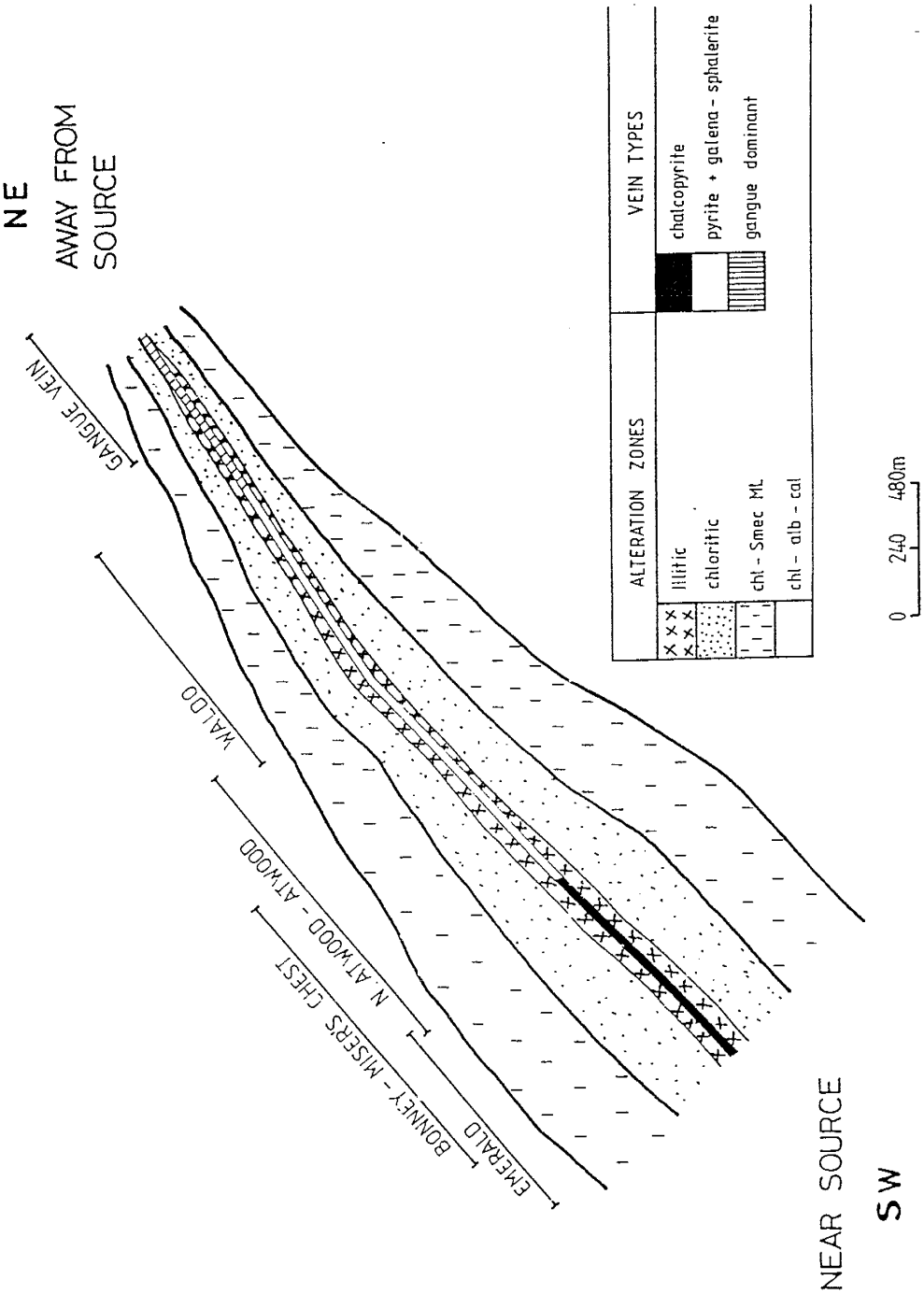

Fig. 21. Generalized schematic correlation between wallrock alteration assemblages and vein types along a hypothetical continuous vein in the Lordsburg district.

Paragenetic Sequence and Formation Temperatures of Alteration Minerals

Petrographic and paragenetic studies of the district suggest the following paragenetic sequence: early illite and calcite followed by chlorite, illite, K-feldspar, and calcite. This was succeeded by the precipitation of chlorite, epidote, K-feldspar, albite, C-S, and I/S, smectite titanite, kaolinite, calcite. This sequence of formation of alteration minerals and quartz veins in the North Atwood, 85 and Bonney mines is summarized in Fig. 22.

Hydrothermally-precipitated discrete illites in active and fossil geothermal systems are known to be stable above temperatures of 220°C (Steiner, 1968; Inoue and Utada, 1983; Horton, 1985). Mica-synthesis experiments have indicated that illiltic polytypes form with increasing temperatures from 1 Md-1M-$2M_1$ (Velde, 1965; Yoder and Eugster, 1955).

Chlorite forms over a wide range of temperatures. Steiner (1968) reported chlorite geing present at temperatures as low as 110°C but stable up to the highest temperature at Wairakei, 270°C. Reyes (1990) reports the occurrence of chlorite in the Phylippines geothermal system over a temperature range of 120°-330°C. Tomasson and Kristmandotirr (1972) and Krismandotirr (1976) recorded chlorite present with epidote above 230°C in basalts in the Icelandic geothermal system.

The temperature range over which chlorite-smectite mixed-layer minerals are predominant in Icelandic geothermal system is 200°-230°C (Palmason, et al., 1970; Kristmandotirr, 1976). corrensite-shlorite-orthoclase are observed between 300°-200°C in active geothermal systems (Steiner,

1968; Muffler and White, 1969). Mixed-layer illite-smectite forms as an alteration product or as newly precipitated phase under relatively low temperature (100°-200°C) petrologic conditions. Illite-smectite in active geothermal systems exhibit systematic variations in composition (i.e. % illite) and structure (i.e. order expressed in terms of Reichweit, R) with respect to temperature (Steiner, 1968; Sumi, 1968; Eslinger and Savin, 1973; Browne, 1978). Authigenic smectite and kaolinite are known to occur in the temperature ranges of 120°-140°C and 140°-180°C, respectively, in geothermal systems (Browne, 1978).

In the North Atwood mine, the occurrence of illite ($1M + 2M_1$) and chlorite as the earliest alteration minerals in veins and wallrock is indicative of formation temperatures greater than 220°C. The presence of minor amounts of smectites, I/S, and kaolinite also indicate formation temperature range of 130°-220°C. The wallrock alteration mineral assemblage thus indicates a temperature range of 130° to >220°C. In the 85 and Bonney mines, similar wallrock alteration mineral assemblages exist, except that $2M_1$ illite polytype is the dominant or only illite polytype present. In geothermal systems, a mineral occurring where temperatures are ** 30°C above its stability range (Reyes, 1990). The alteration mineral geothermometry suggest cooling history in the fluid channet in the vein systems.

In the Nellie-Bly/Robert Lee mines of Leitendorf, the occurrence of regular mixed I/S (R ** 3) expandability ** 10% in place of illite in the wallrock is indicative of formation temperatures in the range of 180°-220°C. It may explain that, early illite that precipitated in the wallrock with chlorite may have

undergone retrogressive alteration to regular mixed-layer I/S due to heating by younger hot spring activities within the vicinity. The areas of hot springs activities in the Lordsburg district is indicated on Fig. 2. This may indicate that mineralization occured in pulses with attendant alteration overprint in the district. Temperature ranges implied by the alteration minerals are indicated in Fig. 22.

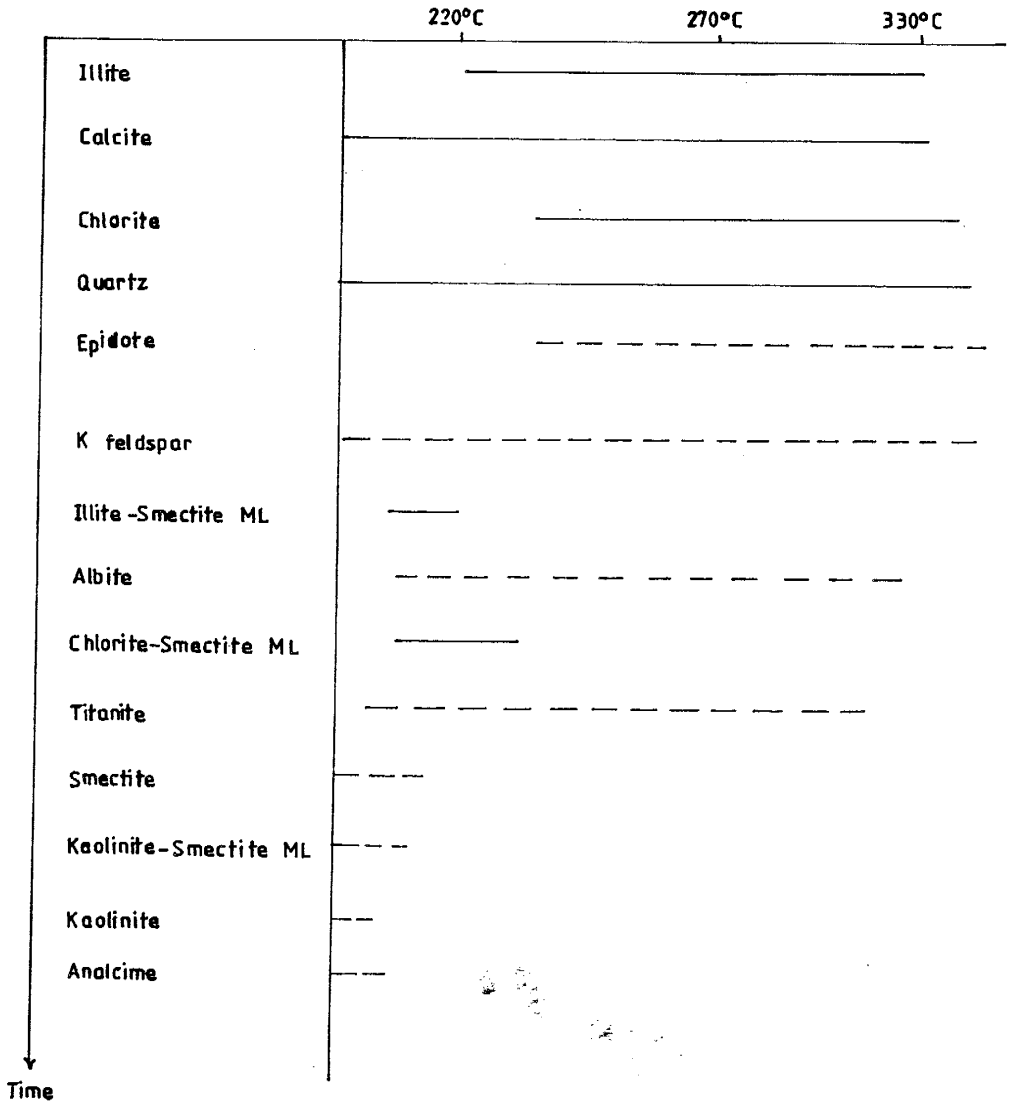

Fig. 22. Paragenesis of alteration minerals and inferred temperatures of formation in the Lordsburg vein system. Major phases are represented by solid lines. Minor-trace phases are represented by dashed lines.

FLUID INCLUSION STUDY

Fluid Inclusion Microthermometry

Method and Procedure

Sampling Methods

Fluid inclusions were examined in 21 samples of quartz, calcite, and fluorite from mineralized veins from mines within the district to document the ranges of fluid composition and temperatures and to investigate fluid evolution during mineralization. No sample of stage 1 material was found suitable for fluid inclusion study. The number of samples and sample types studied at each mine are shown in Appendix IVa.

Analytical Techniques

Doubly polished sections approximately 0.3 mm to 0.6 mm thick were initially examined under a petrographic microscope; areas containing fluid inclusions suitable for freezing and/or heating runs were located. The phases in the inclusions selected for measurement were identified and at lower magnification, their relationship with other inclusions and vein-fill minerals noted. These areas were then separated from the polished section by simply breaking the sample by hand. The samples were then placed on the heating-freezing stage and measurements were made. Some calcite and fluorite samples were simply cleaved and subjected to the same process outlined above.

Fluid inclusion microthermometry was performed on a Linkam TH 600 heating-freezing stage calibrated with de-ionized water, standard CO_2 (-56.6° to 0°C) and potassium dichromate (50° to 400°C). A precision of ± 0.1°C for T á

200°C and ± 1.0°C to T ñ 200°C is ensured. Calibration to 0°C was checked daily by measuring the melting temperature (T_m) of de-ionized water to ensure the repeatability of T_m to ± 0.1°C.

Fluid inclusions in 18 polished plates were examined and measurements were performed on 251 fluid inclusions; 235 homogenization temperatures (T_h) and 106 melting temperatures (T_m) are reported here. All homogenization temperatures were determined at least two times to avoid including data from leaking inclusions. These precision were determined by periodically repeating measurements up to five times per inclusion.

Fluid Inclusion Petrography

Four fluid inclusion types have been recognized in the vein-fill quartz, calcite and fluorite minerals based on their phase ratios at room temperature. These inclusion types, their contained phases at room temperature and homogenization behavior are summarized in Table 5.

Type 1 inclusions are liquid-dominant, two-phase, liquid-vapor inclusions that homogenize into a liquid state. Type 1 inclusions are present in stages 2 and 3 quartz and are the dominant inclusion type in stages 4 and 5 calcite. Inclusion diameters from 5mm to 50mm with are amoeboid to irregular shapes. Type 2 inclusions are single-phase liquid-filled inclusions that are common in samples of all stages and co-exist with all other inclusion types recognized.

Table 5. Summary of fluid inclusion types, their estimated phases at 25°C and homogenization behavior.

Fluid Inclusions	Phases at 25°C			
Type	No.	Dominant	Types	Homogenization behavior
1	2	Liquid	Liquid-vapor	Vapor disappearance
2	1	Liquid	Liquid ± opaque mineral	
3	1	Vapor	Vapor ± opaque mineral	
4	2	Vapor	Liquid + Vapor ± opaque	Liquid disappearance

Type 3 inclusions are single-phase vapor-filled inclusions with no optically resolvable liquid phase. These inclusions are present in all quartz samples studied and all three fluorite samples measured. Sizes are less than 12μm and shapes are variable. Type 3 inclusions occur in clusters on growth planes but are also isolated. These inclusions co-exist with vapor-dominant, two-phase-liquid-vapor inclusions (Fig. 23).

Type 4 inclusions are vapor-rich, two-phase-liquid-vapor inclusions that homogenize to a vapor state. These inclusions have a $\rangle$ 45 vol percent vapor to liquid ratio. Some vapor-rich inclusions co-exist with liquid-rich inclusions in quartz samples of stages 2 and 3 in the 85, Bonney, North Atwood, and Robert Lee/Nellie Bly mines. The sizes of these inclusions range from 2μm to 15μm and average about 10μ. Few of all these inclusions contain opaque mineral particles that do not dissolve on heating.

Primary, pseudosecondary and secondary fluid inclusions were distinguished based upon the criteria proposed by Roedder (1984). Primary inclusions occur as isolated individuals or small groups along growth planes, or in clusters. Pseudosecondary inclusions are recognized by their occurrence along internally intermittent and through-going crystal fractures. Their sizes are generally less than 15μm and shapes are highly variable, from irregular to amoeboid. Secondary inclusions are recognized by their occurrence along fracture planes and they show a wide size variations, from less than 5μm to over 50μm where they occur in groups.

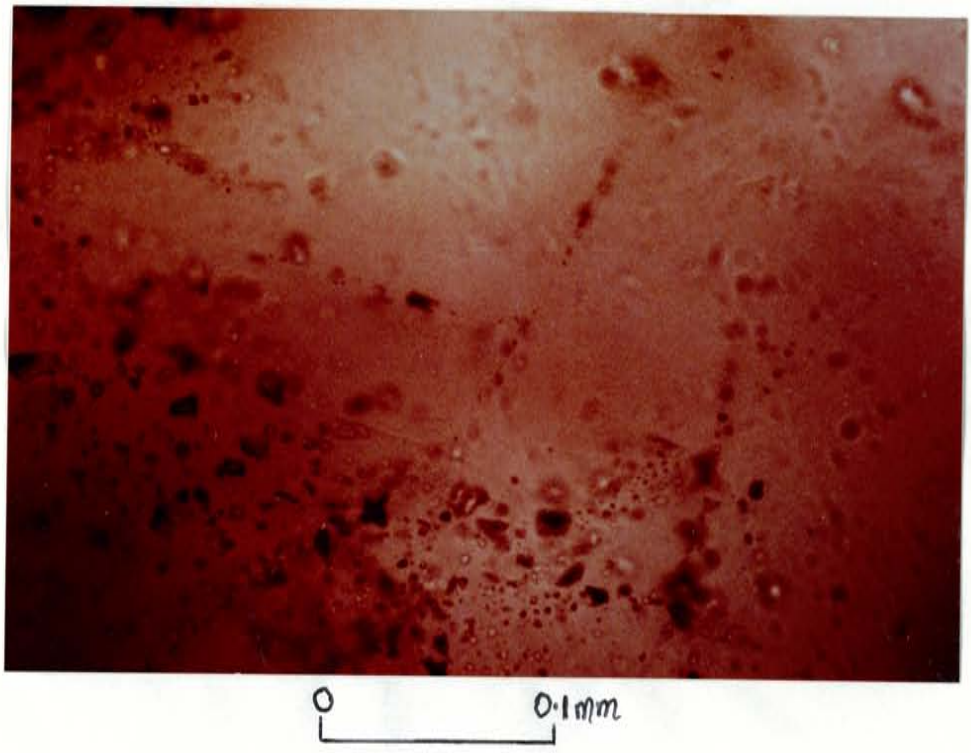

Fig. 23. Transmitted-light photomicrograph of all four types of inclusions. (See text for details.)

Most pseudosecondary and secondary inclusions are represented by the four main types described above.

Microthermometry

Detailed fluid inclusion microthermometric measurements were performed on stages 2 and 3 quartz, stage 2 fluorite, and stages 4 and 5 calcite. Measurements reported were made on primary inclusions and on a few secondary and pseudosecondary inclusions in all samples except stage 2 quartz samples from the Robert Lee/Nellie Bly mines, for which most of the inclusion measurements reported are on pseudosecondary inclusions. Details of all fluid inclusion microthermometry and sampling data are reported in Appendices IVa and IVb. The results of the heating and freezing studies of inclusions for selected major mines in the distinct are presented in Figs. 24 and 25.

Heating Data

Figure 24 shows the frequency diagram of homogenization temperatures of fluid inclusions in vein minerals from the 85, North Atwood, Ruth, Robert Lee/Nellie Bly, and fluorite-calcite mines in the district. Two populations are apparent in the histogram plots of the homogenization temperatures of primary inclusions in stages 2 and 3 minerals from the 85, Bonney, North Atwood and Ruth mines (Fig. 24). A high temperature (240°-~400°C) population and low temperature (120°-230°C) population are represented in the 85 and Bonney mines. In the North Atwood mine, high

temperature (240-270°C) population and low temperature (140°-230°C) temperature (140°-230°C) population are indicated. A single low temperature (140°-230°C) is indicated for the CaF_2-Quartz mine (Fig. 24). A single high temperature (252°-330°C) population is apparent in the plot of the homoganization temperatures of pseudo-secondary inclusions of stage 2 quartz from the Robert Lee/Nellie Bly miens (Fig. 24)

Freezing Data

Figure 25 shows the frequency diagram of salinities estimated from primary fluid inclusions in stages 2 and 3 quartz, stages 4 and 5 calcite, and from pseudosecondary inclusions in stage 2 quartz from 85, Bonney, North Atwood, Ruth, Robert Lee/Nellie Bly, CaF_2-Quartz mines. A single population that ranges from 3.2 to 7 equiv. wt % NaCl is indicated for the district. Salinity range of 3.2 to 7 equiv. wt % NaCl is indicated for 85 and Bonney mines. A range of 3-6 equiv. wt % NaCl is indicated for North Atwood and Ruth mines. Robert Lee/Nellie Bly mines have a range of 3.8 to 5.8 equiv. wt % NaCl, while the CaF_2-Quartz mines have the range 3-6 equiv. wt % NaCl.

Fluid Inclusion Gas Analyses

Sampling and Analyses

The criteria used for selecting samples for fluid inclusion microthermometry was applied here. Almost all samples selected for microthermometry measurements were analyzed for their gas chemistry.

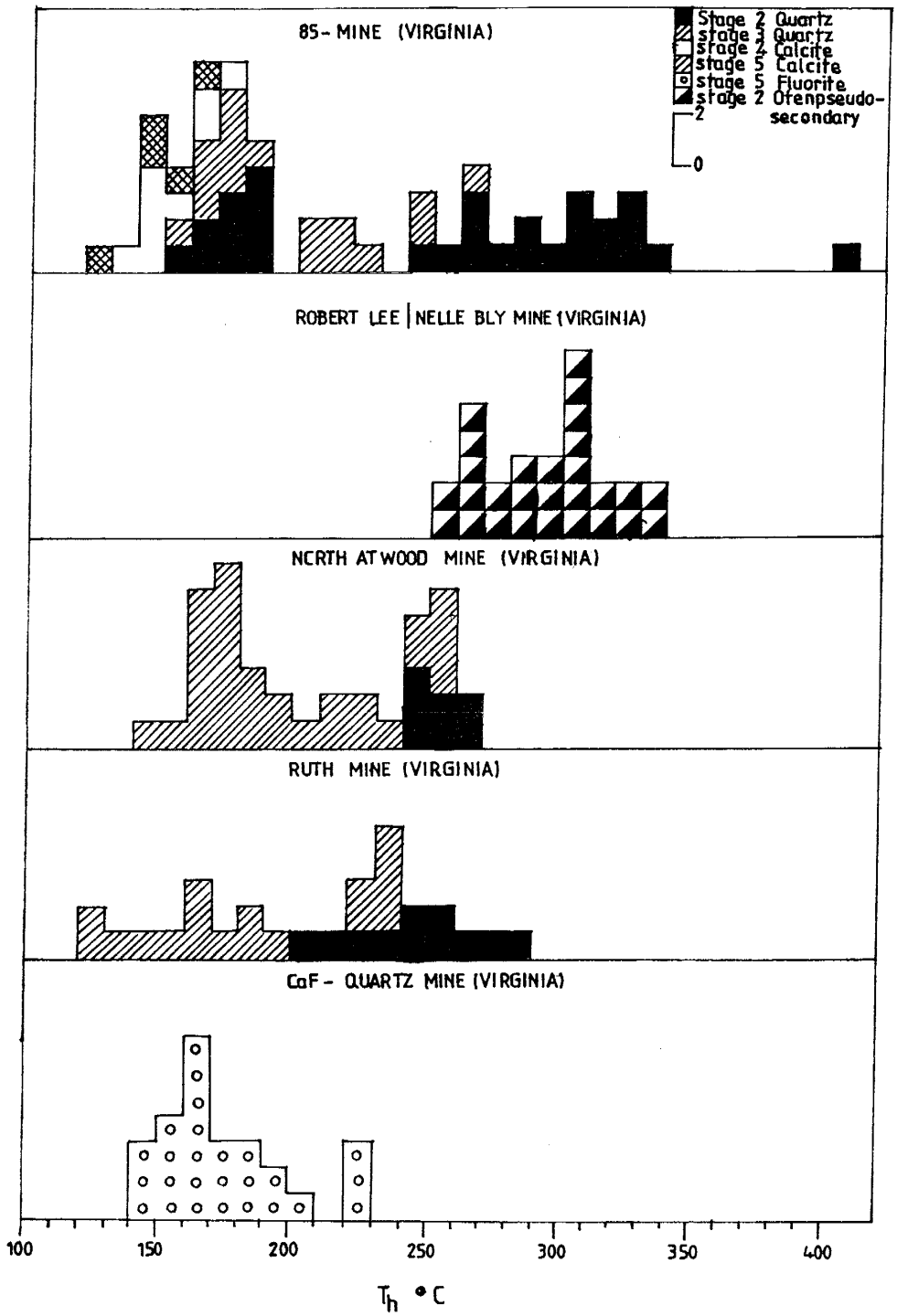

Fig. 24. Histogram of homogenization temperatures of fluid inclusions in vein minerals from 85, Robert Lee/Nellie Bly, North Atwood, Ruth, and Fluorite (CaF_2-Quartz) mines in the Lordsburg district.

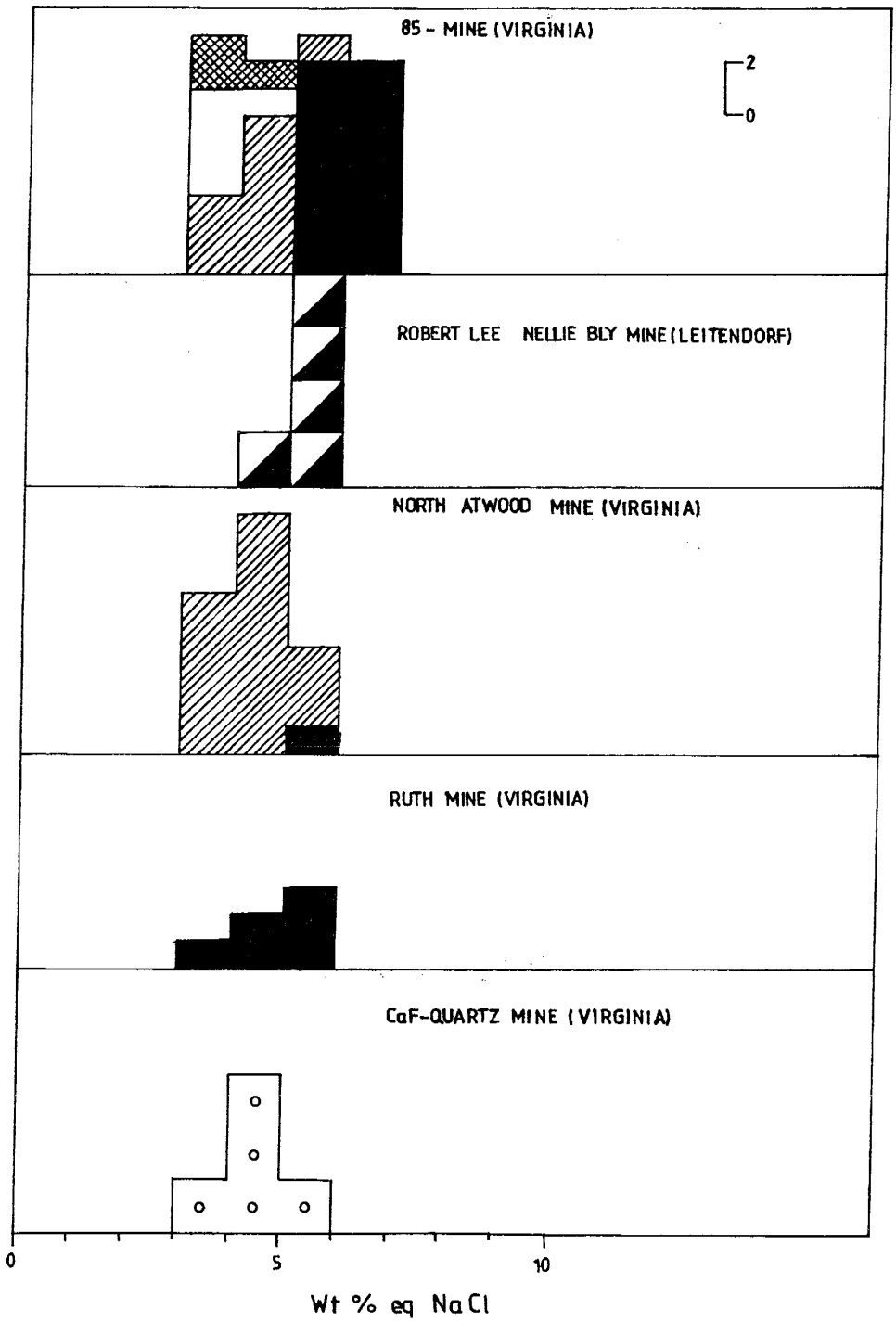

Fig. 25. Histogram of salinities of fluid inclusions in vein minerals from 85, Robert Lee/Nellie Bly, North Atwood, Ruth, and Fluorite (CaF_2-Quartz) mines in the Lordsburg district. Symbols as in Fig. 24.

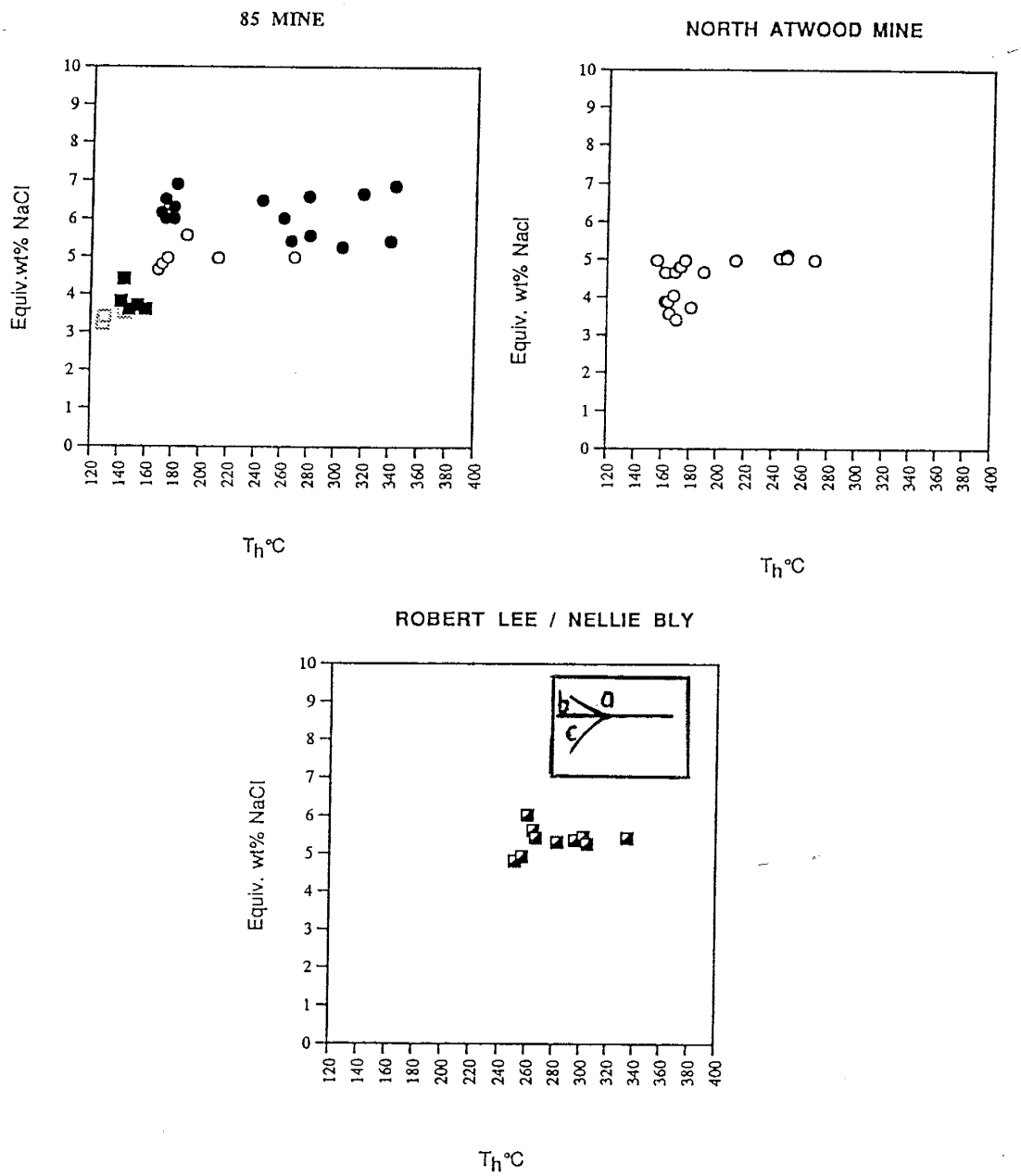

Fig. 26. Plots of homogenization temperature versus salinity for primary and pseudosecondary inclusions in stages 2, 3, 4, 5, and 6 from 85, North Atwood, and Robert Lee/Nellie Bly mines. Solid circles = stage 2 primary inclusions, open circles = stage 3 primary inclusions, solid squares = stage 4 primary inclusions; open squares = stage 5 primary inclusions; half open square = stage 2 pseudosecondary inclusions. Insert: diagram indicates boiling (a), cooling (b), and mixing and dilution (c) trends.

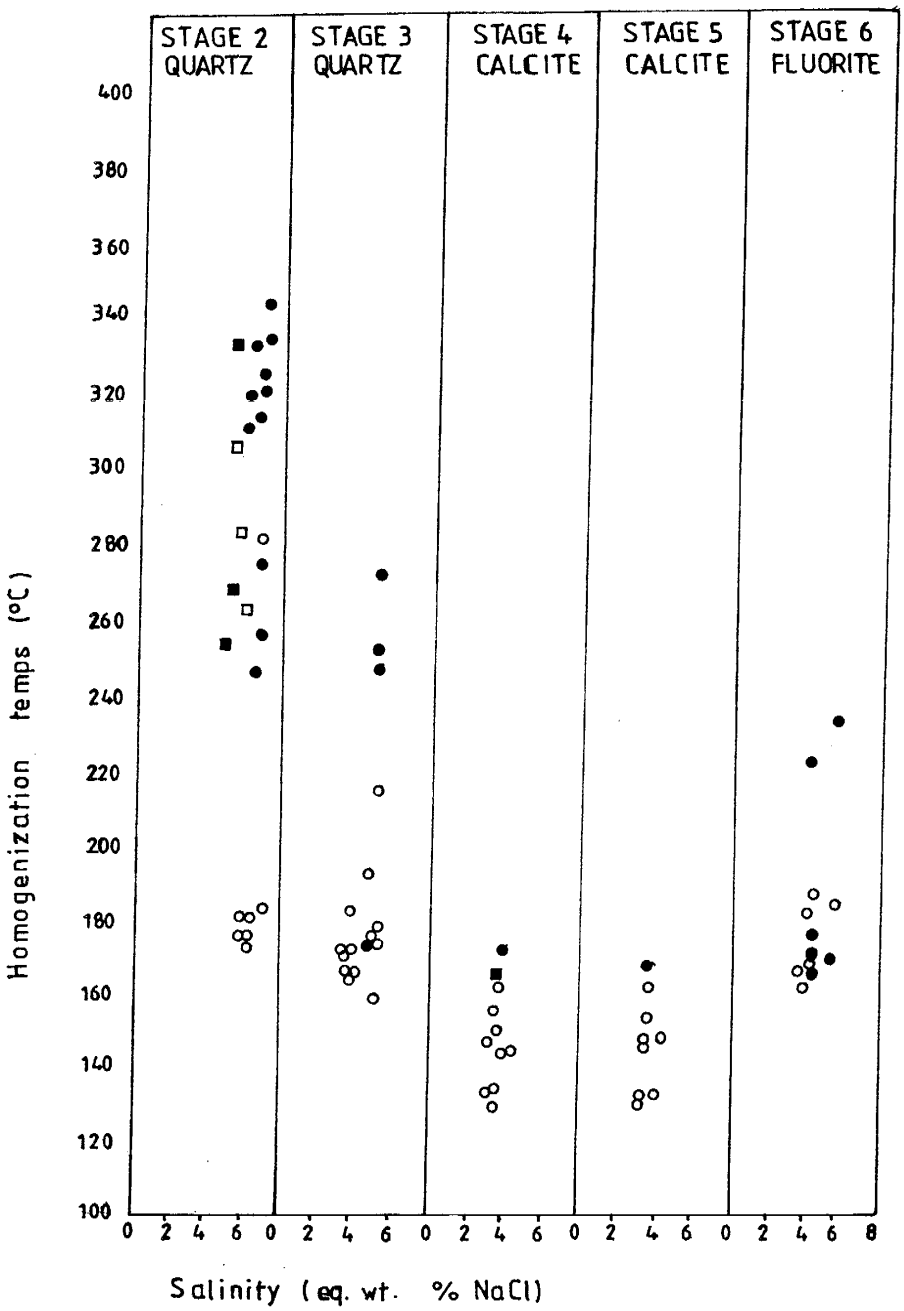

Fig. 27. Salinity versus homogenization temperature for primary and pseudosecondary inclusions from stage 2 quartz, stage 3 quartz, stage 4 calcite, stage 5 calcite, and stage 6 fluorite. Symbols: solid circles = type 4 primary inclusions, open circle = type 1 primary inclusions; solid squares = type 4 pseudosecondary inclusions; open squares = type 1 pseudosecondary inclusions. Note the decline in salinities with homogenization temperatures from stage 2 to 5 and the slight increase in salinities and homogenization temperatures in stage 6.

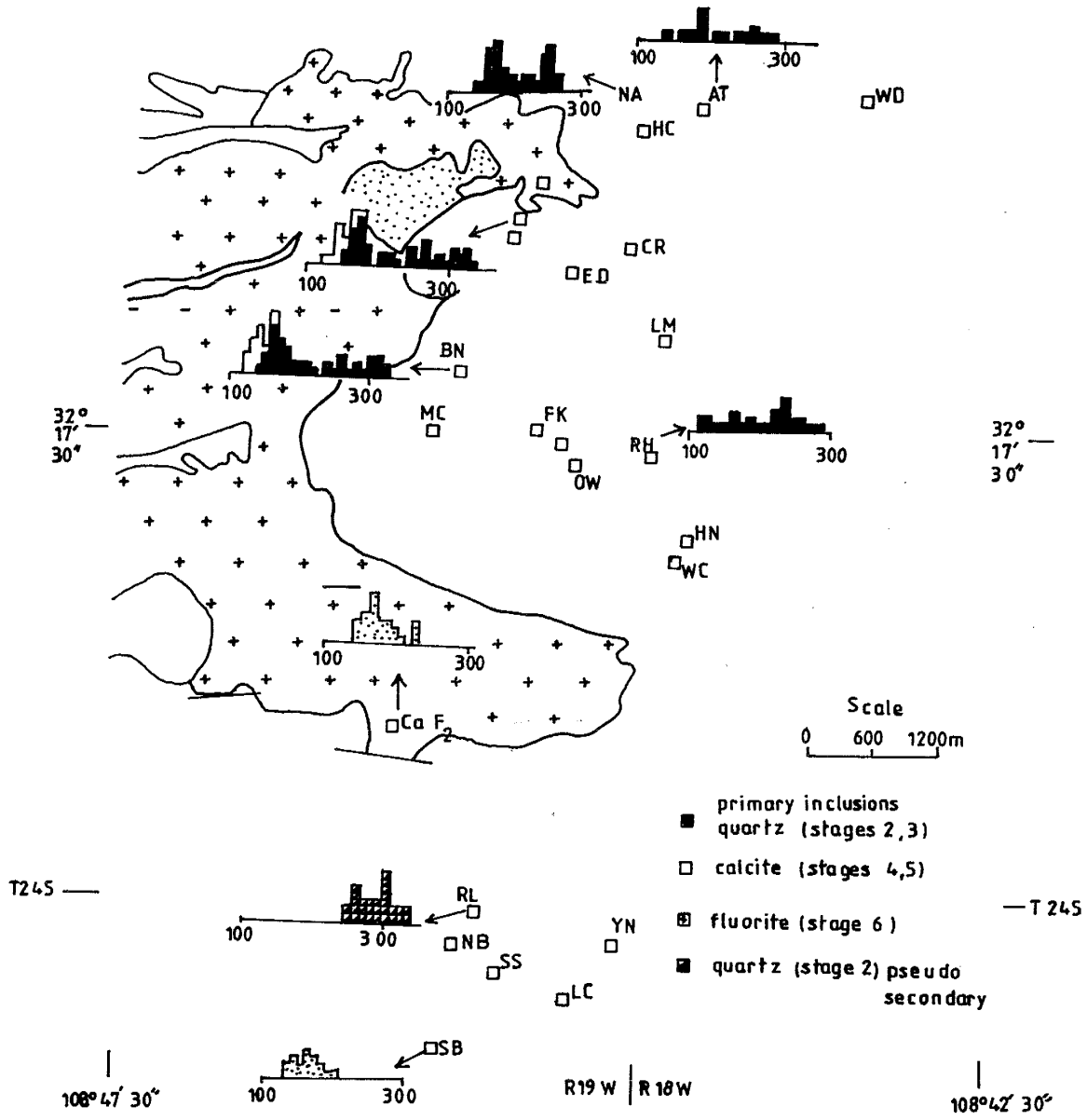

Fig. 28. Temperature zoning in the Lordsburg district. Histograms show ranges of homogenization temperatures of fluid inclusions in vein minerals for selected mines. AT = Atwood mine; BN = Bonney mine; CaF_2 = Fluorite mine; NA = North Atwood mine; RH = Ruth mine; RL = Robert Lee mine; SB = Suzzie mine, and 85 = 85 mine.

Analyses were performed on a total of 18 samples from the district. Seven samples represent four stages of mineralization from 85 and Bonney mines and three represent three stages from Nellie Bly/Robert Lee mines. The remaining eight samples were selected from the North Atwood, Atwood, Ruth, Waldo, and Quartz-fluorite mines. Sample locations are shown in Appendix IVa.

Bulk analyses of fluid inclusion volatiles were carried out on the selected samples using a quadrupole mass spectrometer, as described in Norman and Sawkins (1987) at the New Mexico Institute of Mining and Technology.

Volatile Gas Compositions

The results of gas analyses are shown in Table 6. The water calibration of the system at the time of analysis was not good hence ± 50% on gas/water ratio need to be taken into account. The fluid consists of > 90 mol % H_2O with variable amounts of the other gases. In approximate order of abundance, the principal gases present in the inclusions are CO_2, CO, CH_4, C_nH_n, N_2, H_2S, and SO_2. Variable amounts of H_2, resulting from overheating during decrepitation are also present. Measured concentrations are highly variable, ranging from 84.53 to 94.7 mol % H_2O, 0.226 to 32.0 mol % CO_2, 0 to 1.3 mol % CO, 0.0004 to 1.3 mol % CH_4, 0.005 to 1.35 mol % N_2, and 0.008 to 5.4 mol % H_2S. The C_nH_n includes the various isomers of organic species from C_2 to C_7. Hydrocarbons measured were principally C_3H_6 and C_3H_8.

The concentration of gaseous species in fluid inclusions show a variation with stage of mineralization (Figs. 29 and 30). In the Virginia subdistrict, stages

2, 4, and 5 inclusion fluids have greater amounts of CO_2, C_nH_n, N_2, and total gaseous species than stage 2 (Fig. 29). The amounts of H_2S in the inclusion fluids show a progressive decrease from stage 2 to stage 5 in the two subdistricts (Fig. 29).

Figure 30 shows that H_2S:CO_2 ratios of ore fluids progressively decrease with time in the district. In the Leitendorf subdistrict, CO_2:CH_4 ratios show no obvious variation with stage of mineralization (Fig. 31). Variations in the values of CO_2:H_2S and N_2:CO_2 ratios with stage of mineralization are obvious (Fig. 33). In the Virginia subdistrict, N_2:CO_2 ratio shows no variation while the CO_2:H_2S ratio shows an increase through time (Fig. 31). High values are indicated for the CO_2:CH_4 ratio in stage 3. Values in the later stages are lower (Fig. 31).

The concentration of fluid inclusion gaseous species exhibit obvious variation with the location of vein samples with respect to the granodiorite stock (district center). Data for vein samples from mines along the 85-Waldo mines traverse section are plotted together with a generalized metal zone (Fig. 32). Most obvious is the negative correlation and spatial coincidence between CO_2 and H_2S values, vein types, and lateral distance from the granodiorite stock (district center). The CO_2 levels increase with increasing distance from the stock attaining higher levels in the galena-rich and gangue-dominant veins. The H_2S levels show an verse relationship with distance from the granodiorite stock, reaching lower values in the galena-rich and gangue-dominant veins.

The inclusion gas compositions of the samples from the various stages of the two subdistricts do not exhibit variations or differences that may indicate

Table 6. Composition of fluid inclusion volatiles.

Sample No.	Location	Min	Stage	H_2O	C O_2	CH_4	C_nH_n	H_2	CO	H_2S	SO_2	N_2	A_r	H_e	TG[5]
FA 51	85	Q	2	90.0	2.16	0.121	0.334	0.061	1.06	5.44	0.469	0.160	0.002	0.00002	10.00
FA 193	Robert Lee	Q	3	72.17	24.78	0.980	0.199	0.895	0.895	0.06	0.062	0.534	0.002	0.00005	27.83
FA 208	Bonney	Q	3	99.73	0.226	0.0004	0.009	0.014	0.014	0.006	0.0007	0.006	0.00004	0.00001	0.27
FA 181	Robert Lee	Q	2	99.43	0.260	0.009	0.002	0.00	0.00	0.111	0.006	0.00	0.0006	0.00004	0.57
FA 213	CaF_2 vein, V[1]	F	6	98.61	0.970	0.082	0.093	0.155	0.155	0.007	0.003	0.031	0.00	0.00004	1.39
FA 189	Last Chance	Q	2	97.42	1.166	0.111	0.012	0.980	0.980	0.002	0.0001	0.012	0.00007	0.00	2.58
FA 26	85	Q[2]	2	84.55	10.83	1.298	1.328	0.217	0.217	0.013	0.004	0.438	0.003	0.0002	15.73
FA 211	Ruth	Q	2	98.43	1.463	0.004	0.009	0.037	0.037	0.014	0.002	0.002	0.00003	0.00001	1.57
FA 210	Bonney	C	4	97.50	1.96	0.201	0.023	0.131	0.131	0.0008	0.0001	0.044	0.0007	0.00	2.50
FA 209	Bonney	C	5	95.50	2.91	0.325	0.019	0.881	0.881	0.00	0.0007	0.136	0.0008	0.00	4.50
FA 207	N. Atwood	Q	3	97.99	1.16	0.235	0.028	0.061	0.061	0.298	0.018	0.048	0.0002	0.00	2.01
FA 202	Atwood	Q	2	95.70	2.87	0.119	0.189	0.387	0.387	0.238	0.017	0.025	0.00003	0.00	4.30
FA 30	85	Q	2	97.09	2.52	0.096	0.035	0.058	0.058	0.022	0.010	0.023	0.0001	0.00001	2.91
FA 214	CaF_2-Q Vein, L[3]	F/Q	6	98.53	1.044	0.104	0.125	0.066	0.066	0.001	0.0004	0.037	0.0005	0.00	1.47
FA 171	Robert Lee	C	4	96.01	3.37	0.089	0.023	0.350	0.350	0.006	0.0003	0.033	0.0002	0.00	3.99
FA 212	Waldo	Q	3	67.10	32.04	0.271	0.077	0.258	0.258	0.014	0.092	0.061	0.00	0.00	32.90
FA 206	Bonney	Q	2	98.86	0.958	0.016	0.012	0.005	0.005	0.049	0.0004	0.032	0.0006	0.00004	1.14

Q_1, quartz; c_1 Calcite, F, fluorite
1 V, Virginia subdistrict
2 Q, Barren quartz
3 L, Leitendorf subdistrict
4 C_nH_n is sum of C_2H_4, C_2H_6, C_3H_8, C_4H_{10}, C_6H_6, C_7H_8
5 TG is total gas

mineralization by different ore fluids Fig. 29). One striking similarity is the apparent decrease in H_2S concentrations of the fluid in time and with distance from the granodiorite stock in the subdistrict (Figs. 29 and 30). The CO_2, CH_4, N_2, and C_nH_n concentrations as well as the total gas contents of the ore fluids fall within a similar range of values (Table 6, Fig. 29).

Boiling and Pressure

Figure 27 shows the distribution of the inclusion types and their proportion among the assemblage of inclusions for all the stages. Stage 2 shows a great variation in homogenization temperatures of liquid-rich and vapor-rich inclusions in stage 2 quartz from the 85 and Bonney mines homogenize at the same temperature of ~150° to ~350°C. This indicates that boiling occurred during stage 2 ore deposition over the range of salinity (4.8 to 7.0 equiv. wt % NaCl). Evidence from CH_4-CO_2-H_2S ratios (Fig. 33) and H_2S-CO_2 ratio (Fig. 30) suggests that boiling may have occurred during the early part of stage 2 mineralization. Boiling is not indicated for the subsequent stagesof mineralization. In Fig. 33, the data points plot close to the CH_4 corner. The pattern indicated by the data points may typify loss of vapor from waters initially containing equilibrium amounts of these gases and may indicate early vapor separation process.

Data from the system H_2O-NaCl (Haas, 1971) combined with temperature and salinity data of stage 2 inclusions indicate pressures of $\leq$ 150 bars. Assuming hydrostatic pressure, this corresponds to depth of $\leq$ 1533 m

below piezometric surface. These estimates are based on the assumption that significant amounts of dissolved gases are not present.

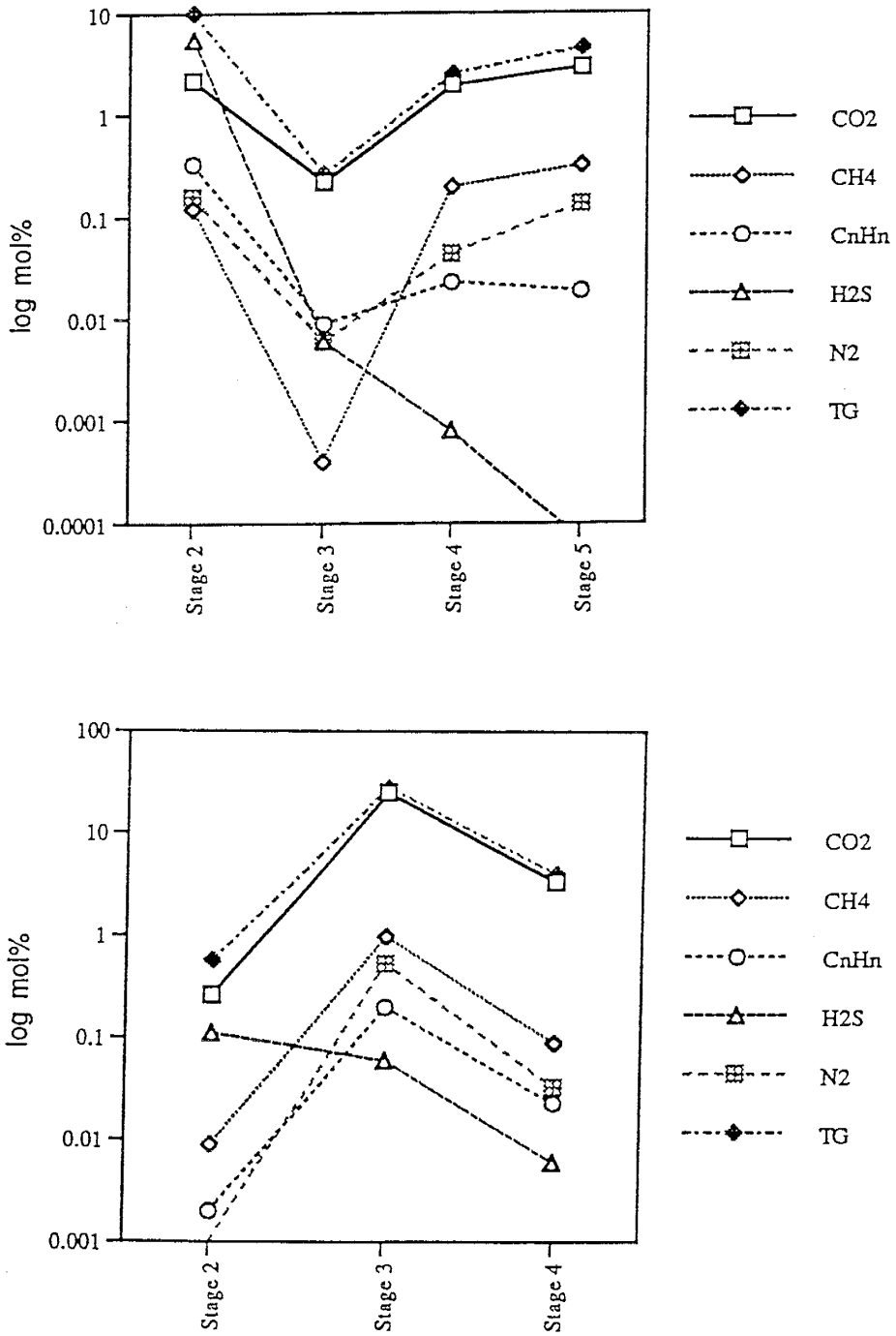

Fig. 29. Variations in fluid inclusion volatiles with stages of mineralization in the Virginia subdistrict-85 mine (above) and the Leitendorf subdistrict-Robert/Lee-Nellie Bly mines (below).

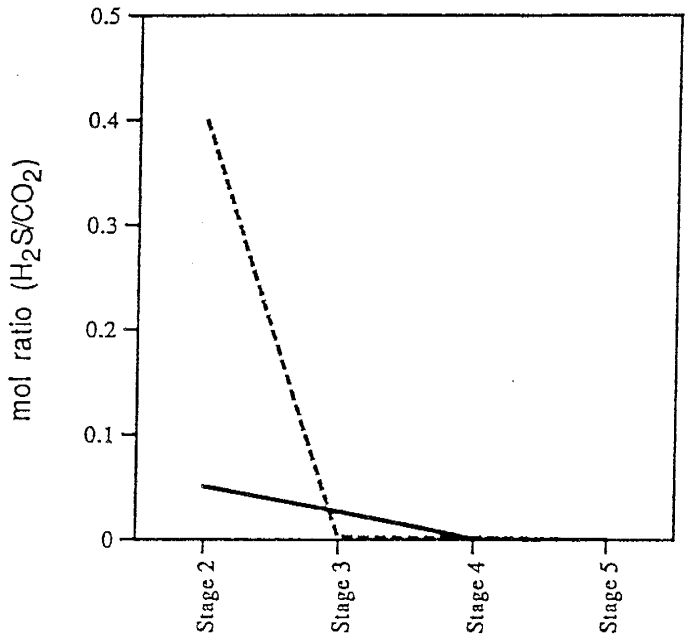

Fig. 30. Plot of H_2S/CO_2 ratios versus stages of mineralization in the Bonney andRobert Lee/Nellie Bly mines. Note the apparent decline in ratios with stages of mineralization. Solid lines = Bonney mine, dashed lines = Robert Lee/Nellie Bly mine.

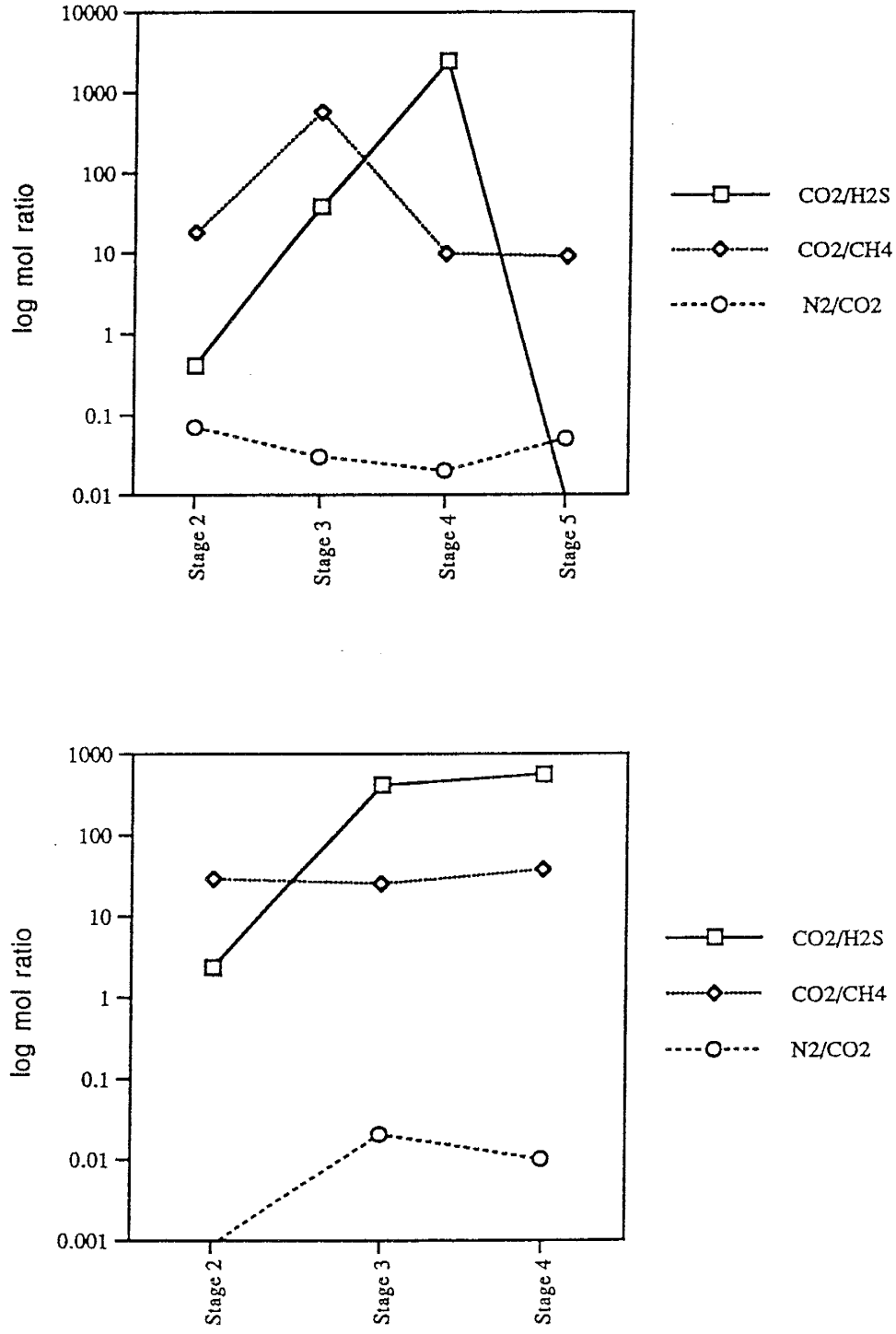

Fig. 31. Plot of log mole ratios (CO_2/H_2S, CO_2/CH_4, N_2/CO_2) versus stage of mineralization in Virginia subdistrict-85 mine (above) and Leitendorf-Robert Lee/Nellie Bly (below).

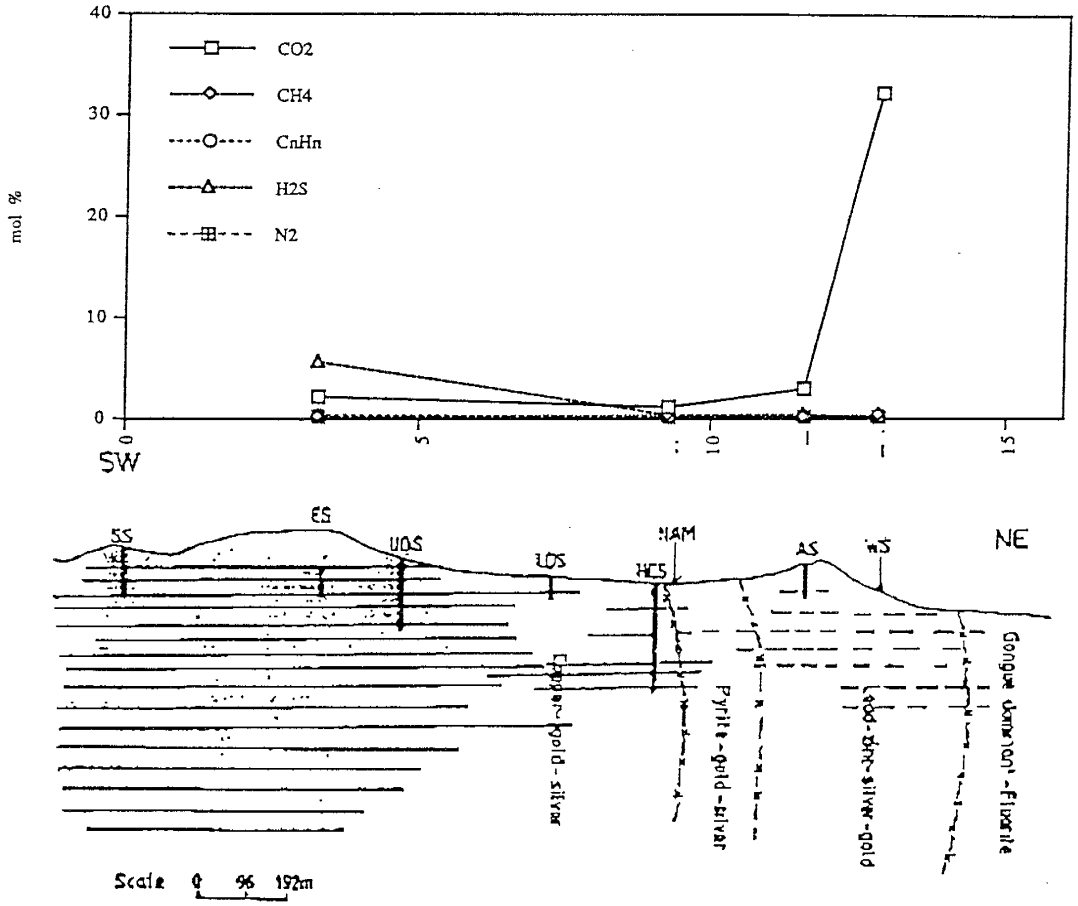

Fig. 32. Variation in fluid inclusion volatiles along the 85-Waldo mine traverse. Mol % CO_2, CH_4, C_nH_n, H_2S, and N_2 along traverse (above). A SW-ME section showing mines along the traverse (below). AS = Atwood Shaft; HCS = Henry Clay Shaft; LDS = Lower Dundee Shaft; NAM = North Atwood Mine; SS = Superior Shaft; UDS = Upper Dundee Shaft; WS = Waldo Shaft; ES = Emerald Shaft.

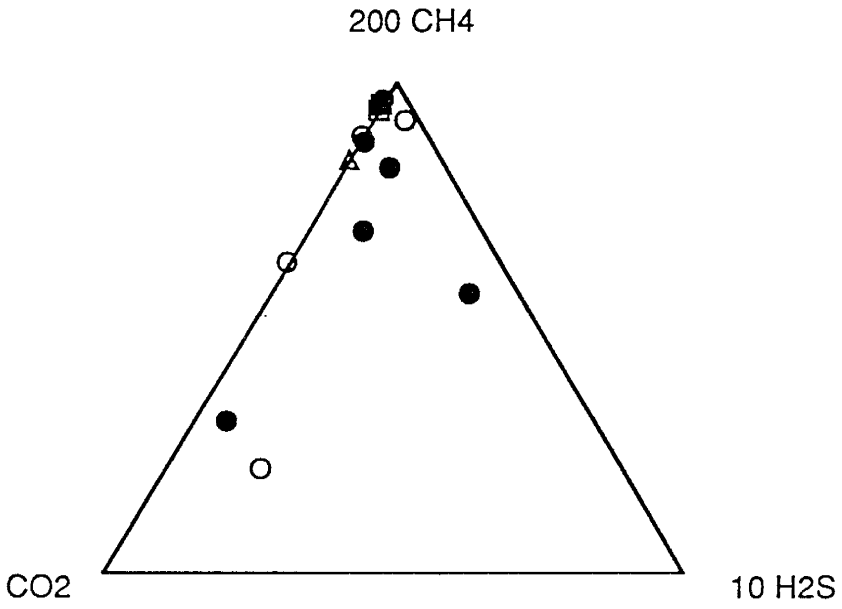

Fig. 33. Ternary plot of relative CH_4, CO_2, and H_2S contents in fluid inclusions from vein minerals in Lordsburg. Data points plot close to the CH_4 corner indicating an early vapor separation (Giggenbach, 1992). Solid circles = stage 2; open circles = stage 3; open triangles = stage 4; solid triangles = stage 5; open square = stage 6.

DISCUSSION

Temperature of Fluid-rock Interaction and Ore deposition

Fluid Inclusion Evidence

Fluid inclusion data in Lordsburg indicate variations in temperature and composition of the hydrothermal fluids during episodes of mineralization. The two populations apparent in the histogram plot of homogenization temperatures (Fig. 24) may be related to specific events during mineralization. The relationship between homogenization temperatures and salinities of the fluid inclusions in the vein minerals of stages 2 to 6 further indicates a complex history of boiling, cooling, mixing, and dilution.

The co-existence of liquid-rich and vapor-rich inclusions that homogenize over the same temperature 240°- >350°C is indicative of boiling (Fig. 23). Boiling during the early part of stage 2 mineralization is indicated by the relationship between T_h and salinity (trend a in Fig. 26). It may be interpreted that, the trend (wide range of T_h over fairly narrow salinity range) reflects boiling of a moderate-temperature, moderately saline hydrothermal fluid. On the other hand, the trend may be an artifact of small data population. Evidence from fluid inclusion gas composition (Figs. 30 and 33) suggest that boiling was one of the processes in ore deposition(Giggenbach, 1992).

Simple cooling coupled with slight dilution by mixing with cooler, less saline fluids occurred during and/or after boiling as indicated by trend b in Fig. 26. Cooling is thus indicated for stage 3 and the later part of stage 2

mineralization. Two-phase liquid - vapor inclusions create a spread in temperature with no change in salinity. However, microscopic evidence indicates that most of the inclusions in trend b are primary inclusions that have not resulted from necking down. Trend c in Fig. 26 shows that fluids ranged from high-temperature, high-salinity end-member towards a lower-temperature, less saline component. This reflects a mixing and dilution trend during calcite deposition in stages 4 and 5. Figure 27 also shows the salinity-homogenization relation for various stages in Lordsburg.

In summary, the wide variations in temperatures of the hydrothermal fluids during ore deposition in the Lordsburg system may have been due to the complex history of boiling, cooling, mixing, and dilution. Economic concentrations of base-and precious-metals occurred mainly during the significant changes in physico-chemical conditions from the period of boiling ($\leq$350°C) to the late period ($\geq$ 128°C) of cooling and dilution. It is difficult to obtain precise estimates of pressure at the time of mineralization. It also appears likely that any pressure correction for true trapping temperatures is negligible compared to the scatter of homogenization data found in each stage of mineralization.

Chemistry of Fluids

pH of Fluids

Petrographic and paragenetic study suggests that an early illite was followed by chlorite + illite and then a later stage chlorite without illite (Figs. 8,

10, and 20). These mineralogical variations indicate a change in fluid pH during ore deposition (Larson, 1984). This observation may be related to boiling during which acid volatiles (e.g. H_2S) are released, thus increasing ore fluid pH, shifting fluid composition from illite to the chlorite stability field. This observation may also reflect mixing and dilution processes during ore deposition.

Hydrolysis and cation exchange equilibria involving the vein-selvage alteration mineral assemblage can be used to constrain stages 1,2 and 3 fluid pH values, provided independent estimates for the activities of one relevant solute species (egK_+,Na_+) are available. The latter were estimated, assuming the similarity in composition of stages 1,2 and 3 fluids, from fluid inclusion measurements on stage 2 and 3 quartz.

The sericite-albite-K-feldspar assemblage in the vein-selvage, represented by the following reactions:

$3KALSi_30_8+2H^+ = KAL_3Si_30_{10}(OH)_2+ 6S_10_2+2K^+$

$3NaALSi_30_8+K_+2H^+ = KAL_3Si_3O_{10}(OH)_2+6SiO_2+3Na_+$

was used to estimate the pH values for the fluid for the temperature range of 300 to 200^0C. The activities of K^+ were estimated using the temperature dependence of Na/K ratios for natural waters combined with salinities of 1.0 molar NaU (from fluid inclusion data) and activity coefficient of K^+ (calculated

with Debye - huckel equation). The calculated pH values for the fluid at the temperature range of 300^0 to 200^0 C are 4.7 - 4.8 to 5.5 to 5.6.

Oxidation and Sulfidation States

A computer program [GASFIX (Norman, unpubl.)] which, utilizes gas compositions and microthermometry data (T_h, salinity), was used to calculate log fO_2 and log fS_2 values for the various stages of mineralization (Tables 7 and 8). Log fO_2 was calculated by means of the reactions $CH_4 + 2O_2 = CO_2 + 2H_2O$ and log fS_2 was calculated from the reaction $2H_2S + O_2 = S_2 + 2H_2O$. The calculated oxygen and sulfur fugacities have ranges of values that agree with the ranges indicated by mineral assemblages. Thus, equilibrium thermodynamics and fluid inclusion data indicate that the ore minerals precipitated mainly over log fS_2 range of -6.4 to -15.6.

The calculated log fS_2 values indicate a decrease in sulfidation state of the hydrothermal fluids in time and in space. The observed outward mineral zoning from cp + py ± bn to gn + sp + py and carbonate-fluorite-gangue reflect the change in space (lateral distance from granodiorite stock). The calculated log $f0_2$ values (-33.8 to -49.9) is a direct result of a decrease in temperature from 350^0C to 150^0C. The significant changes in T, fO_2, fS_2, and pH values of the ore fluids may be explained by the interaction and mixing of high temperature hydrothermal fluids with cooler meteoric waters.

The suite of gases obtained from decrepitated inclusions suggest that the vein-related hydrothermal mineral assemblages in Lordsburg were produced from fluids composed principally of H_2O, CO_2, N_2, organic and sulfur gases. Values obtained for N_2 are indicative of significant magmatic contribution to the hydrothermal system. The sulfur gases (H_2S, SO_2) obtained are in agreement with precipitation of chalcopyrite with minor bornite.

The organic species in the Lordsburg ore fluids may be interpreted to have originated from the underlying Cretaceous-Paleozoic clastic-carbonate sequence. The interaction of the hydrothermal fluid with these formations would explain the copper-rich nature of the mineralization.

Source of Fluids

The salinity values (3-7 equiv. wt % NaCl) of the fluids in primary types 1 and 4 inclusions are consistent with meteoric water dominance. The ternary plot of ratios of N_2, Ar and He gases (Fig. 34) suggest mixing of minor amounts of magmatic fluids with deep circulating meteoric waters (comparison with Fig. 10b of Norman and Musgrave, in press; Giggenbach, 1986). The presence of organic species believed to be from Paleozoic sedimentary beds indicate that deep circulating meteoric waters were probably involved in the deposition of ore in Lordsburg. Thus, the Lordsburg hydrothermal system may have evolved as an extensive deep circulating meteoric system that served as a `condenser' of magmatic volatiles and metals and as a diluent. This may account for the simple picture of salinities observed in Lordsburg.

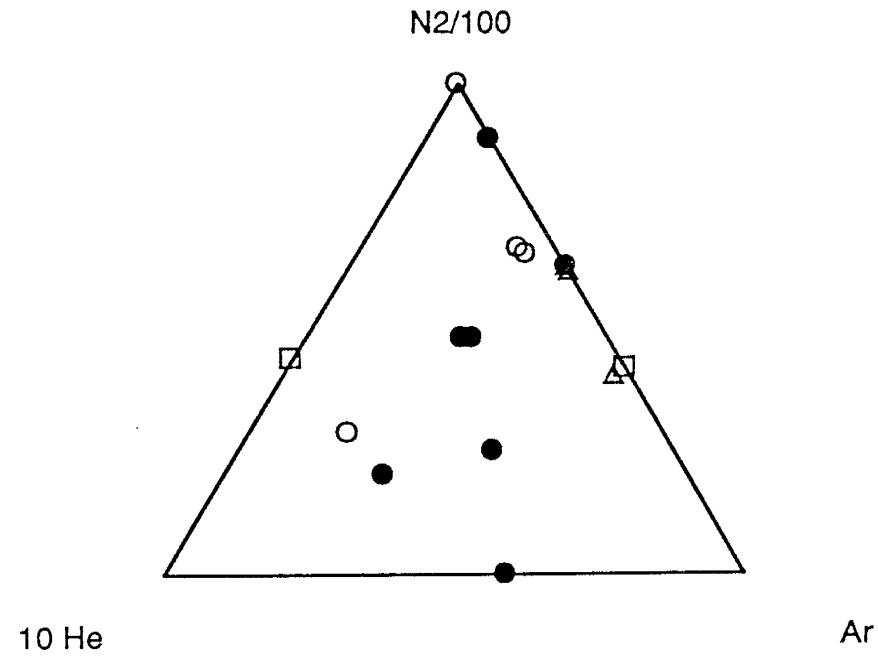

Fig. 34. Ternary plot of relative N_2, He, and Ar contents in fluid inclusions from vein minerals in Lordsburg. Data points plot in area indicating compositions of volatiles mixtures from two sources--magmatic and deep circulating meteoric fluids. Closed circles = stage 2 open circles = stage 3, open triangle = stage 4 closed triangle = stage 5 and open square = stage 6. Data obtained from fluid inclusion gas analysis.

Geochemical Environment of Ore Deposition

The most useful subdivision of ore minerals in the Lordsburg deposit is into a high fS_2 and low fS_2 assemblage. The computed values of log fS_2 of between -6.4 and -15.6 (Table 7) are demonstrated by the ore assemblages of chalcopyrite + bornite ± pyrite (high fS_2 assemblage) and galena + sphalerite + pyrite (lower fS_2 assemblage). Constraints on oxidations states in the district are provided by the presence of hematite (specularite) and barite, and the absence of magnetite, in the district center. The stages 2 and 3 mineral assemblage of pyrite + chalcopyrite ± bornite + sphalerite + hematite + barite in the district center provides an upper limit of oxidation state. This is constrained by the calculated logfO_2 values of -33.8 to -40.0. These equilibrium thermodynamics and fluid inclusion data, combined with the mineral paragenesis, indicate that the ore minerals precipitated mainly over the temperature range of ≤350°-128°C under conditions of -log fS_2 values of 6.4 - 15.6 and -log fO_2 values of 33.8-49.9. These chemical changes responsible for the ore deposition can be defined by using plots of log fS_2 vs, log fO_2 (Fig. 36), and log fS_2 vs_1 T (Fig. 35) and log $f0_2$ vs T (Fig. 37). Figure 36, for convenience, has been constructed for a temperature of 250°C. Figure 37, constructed for pH = 4.5 and $\Sigma S = 10^{-2.5}$ shows the evolutionary path of the Lordsburg system.

The pH values of the mineralizing fluids, calculated to be between 4.7 and 5.6 for stages 2 and 3 mineralization, are well constrained by the common occurrence of sericite (illite) and chlorite in the vein and wallrock.

Table 7. Fluid Inclusion Gases and Derived Gas Fugacities

Sample No.	Sample Location	Paragenetic Stage	Temp of Form Th^{0}C	CO_2(mol %)	CH_4(mol %)	CO (mol %)	H_2S (mol %)	Log fO_2	Log fS_2
FA 26	85 Mine	2	300	10.83	1.298	1.349	0.013	-34.2	-11.9
FA 30	85 Mine	2	300	2.52	0.096	0.141	0.022	-34.0	-11.2
FA 51	85 Mine	2	300	2.16	0.121	1.06	5.44	-34.0	-6.4
FA 171	Robert Lee	4	150	3.37	0.089	0.104	0.006	-48.3	-13.5
FA 181	Robert Lee	2	290	0.260	0.009	0.162	0.111	-34.6	-9.7
FA 189	Last Chance	2	250	1.166	0.111	0.292	0.002	-38.9	-13.8
FA 193	Robert Lee	3	240	24.78	0.980	0.304	0.06	-38.8	-10.8
FA 202	Atwood Mine	2	260	2.87	0.119	0.358	0.238	-34.7	-9.2
FA 206	Bonney	2	300	0.958	0.016	0.069	0.049	-33.8	-10.3
FA 207	N. Atwood	3	250	1.16	0.235	0.152	0.298	-38.2	-9.6
FA 208	Bonney	3	250	0.226	0.004	0.005	0.006	-40.0	-12.2
FA 209	Bonney	5	140	2.91	0.325	0.225	0.00	-48.6	?
FA 210	Bonney	4	150	1.96	0.201	0.140	0.0008	-49.9	-15.6
FA 211	Ruth	2	250	1.463	0.004	0.041	0.014	-37.3	-11.3
FA 212	Waldo	3	250	32.04	0.271	0.088	0.014	-37.6	-11.6
FA 213	CaF_2, Virginia	6	150	0.970	0.082	0.053	0.007	-46.1	-13.4
FA 214	CAF_2, Leitendorf	6	160	1.044	0.104	0.092	0.001	-47.3	-15.0

Table 8. Representative analyses of i
nclusion volatiles and calculated values of the various stages of mineralization in the Bonney mine at Lordsburg.

Analyses (mol %)

Gas Specie	Stage 2	Stage 3	Stage 4	Stage 5
H_2	0.061	0.014	0.349	0.131
H_e	0.0002	0.00001	0.00	0.000
Ar	0.002	0.00004	0.0002	0.0006
N_2	0.160	0.006	0.033	0.045
CO	1.058	0.005	0.104	0.145
CH_4	0.121	0.0004	0.089	0.201
CO_2	2.160	0.226	3.373	1.960
H_2S	5.439	0.006	0.006	0.0008
C_nH_n	0.334	0.009	0.023	0.023
H_2O	90.00	99.73	96.01	97.50
Th° C	300	220	150	140
Sal (eq wt % NaCl)	6.3	4.4	3.8	3.7
Log fO_2	-34.0	-40.0	-48.3	-49.9
Log fS_2	-6.4	-12.2	-12.2	-15.6
Partial Pressure				
CO_2	251.2	16.8	245.2	147.5
CH_4	10.3	0.1	42.38	101.59
H_2S	26.73	0.04	0.05	0.01
H_2O	85.81	23.18	4.76	3.61
H_2	11.06	6.18	252.08	98.26
Total Pressure	374.76	46.3	544.47	350.97

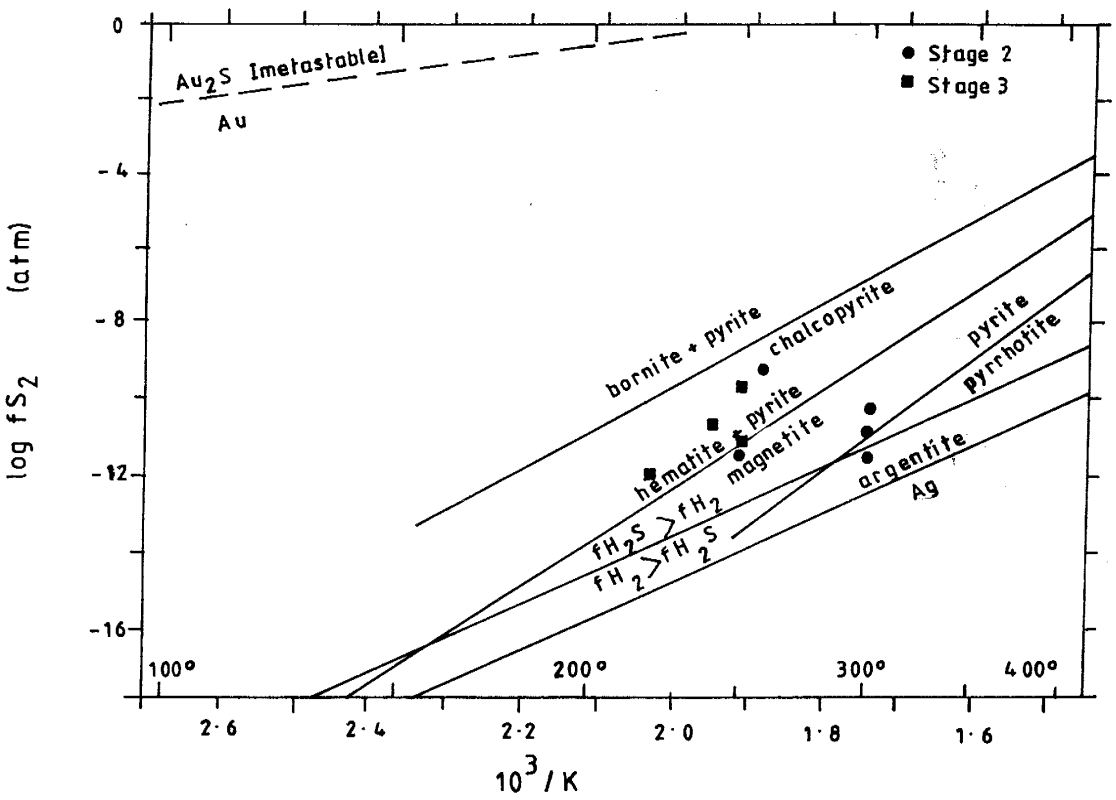

Fig. 35. Plot of temperature versus sulfur fugacities showing possible mineralization conditions for stages 2 and 3 in the Lordsburg district. Plot of logfS_2 versus T showing sulphidation reactions among minerals and values calculated for stages 2 and 3. Values of logfS_2 were calculated using the computer program GASFIX (Norman unpubl) that assumes H_2S-S_2-H_20 equlibria gas analytical data and thermodynamic data from Robie.et al. (1978). Figures inside the lower margin are ^0C.

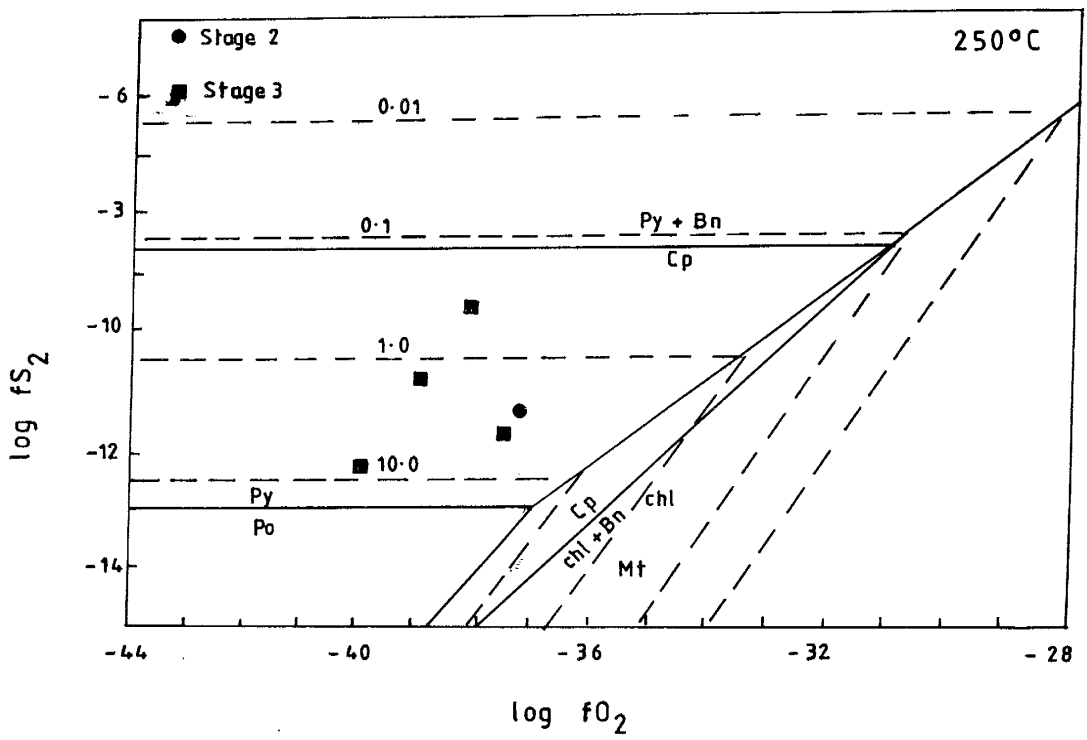

Fig. 36 Plot of log fS_2 versus log fO_2 showing values calculated for stages 2 and 3 samples at 250°C. Values of log fO_2 and log fS_2 were calculated using the computer program GASFIX (Norman, unpubl.) that assumes CH_4-CO_2-H_2O and H_2S-S_2-H_2O equilibria, respectively, gas analytical data and thermodynamic data from Robie, et al. (1978).

Metal Transport and Deposition

The solubility data given by Crerar and Barnes (1976) for chloride complexes was used to construct Fig. 38. The figures shows the relation of copper solubility to log ΣS at several pH values. The diagram indicates that during stages 1 and 2, mineralization at ≤350°C (pH range = 4.7-5.0, log ΣS range = -1.0 to -0), significant amounts of copper (10^3 - 10^2 ppm) could have been dissolved in solution in a weakly acidic, 1 molar NaCl solution. Copper in solution, during the later stages of mineralization (T ≤ 250°C, pH = ≤ 5.6, log ΣS = -4.0. -3.0) Cu concentration could have been about 10^1-10^{-0} ppm. Thus, copper concentration of >10^2 ppm could have been dissolved and transported by chloride complex in the initial ore fluids.

Copper bisulfide complexes becomes significant in weakly basic or near-neutral solutions, at higher total sulfur activities and at lower temperatures. However, available data on the solubilities of copper sulfides (Crerar and Barnes, 1976) indicate that the solubility of copper sulfide complexes would have been negligible in the ore fluids. It therefore implies that the sulfides were not effective transporting ligands of Cu in the ore fluids at Lordsburg.

Bisulfide complexing is important in gold solubilization and transport at relatively moderate temperatures (Seward, 1974; Romberger, 1986). Sufficient gold and iron may have been transported as solvated species in the presence of sufficient dissolved reduced sulfur ($aH_2S \geq 10^{-3}$) to account for the copper-

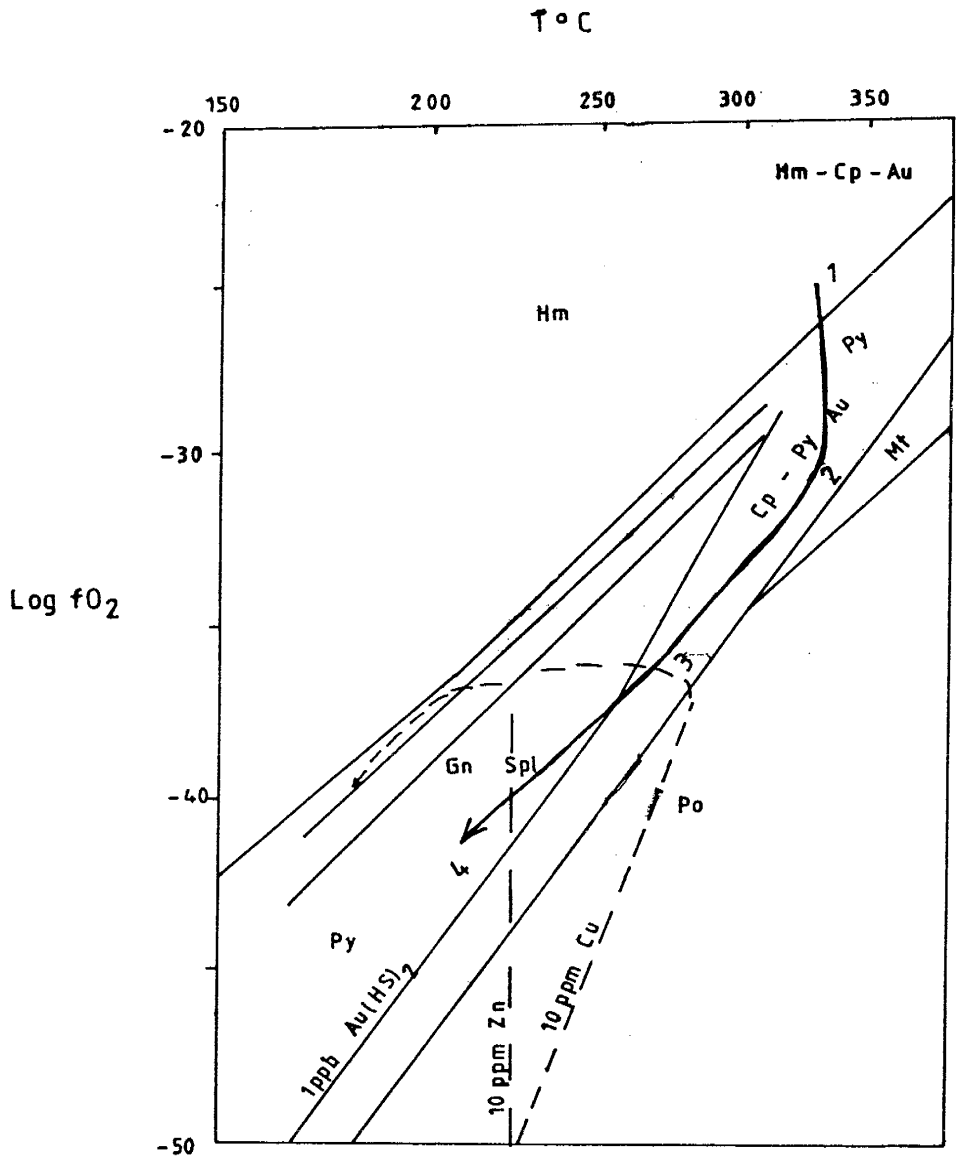

Fig. 37. Temperature - Log fO_2 diagram showing depositional fields for the various vein ore types in Lordsburg. The arrow indicates the probable path of ore fluids away from the district center (see text for details). pH = 4.5, a $\Sigma S = 10^{-2.5}$. Modified after Huston and Large (1989).

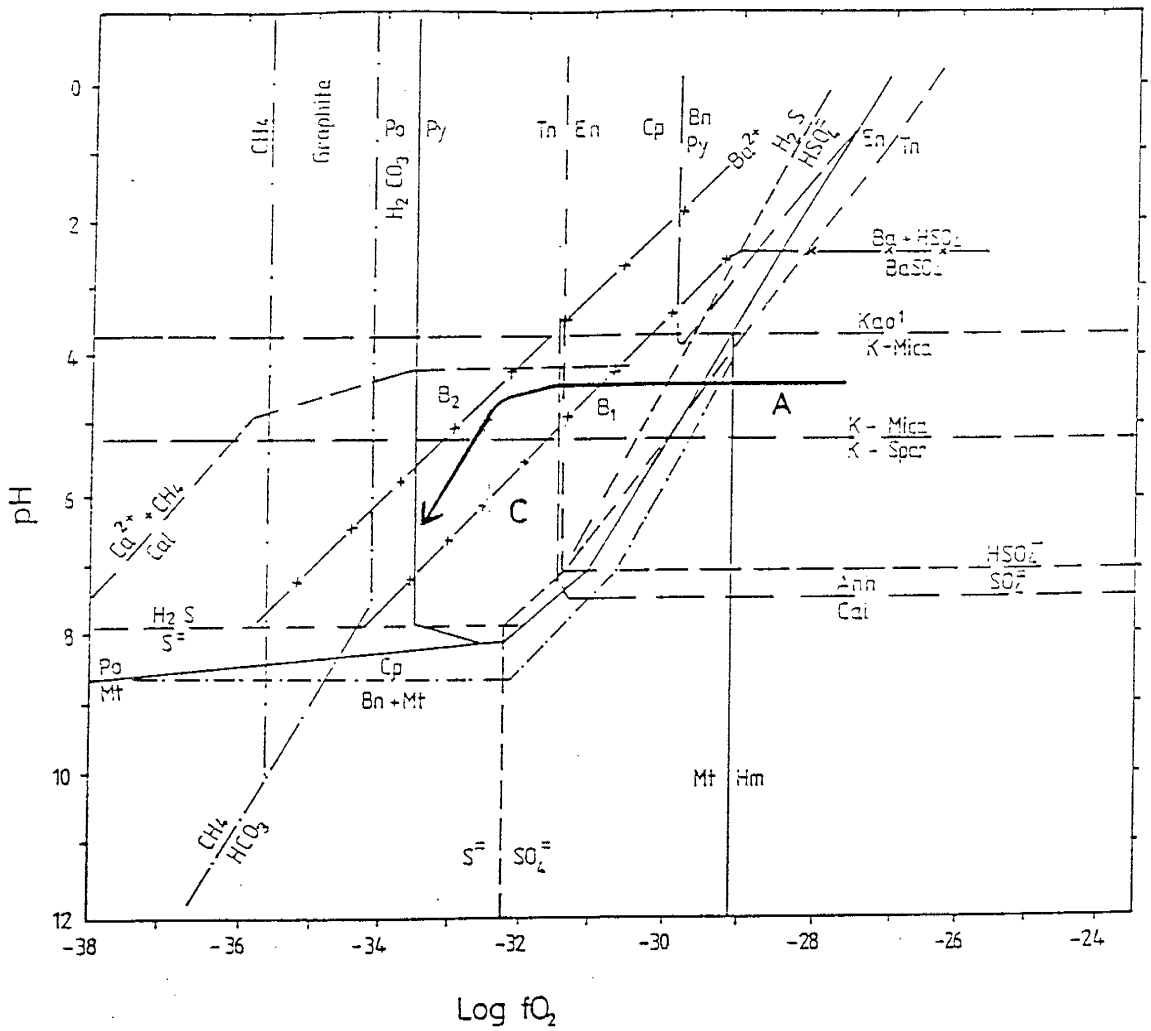

Fig. 38. pH-Log fO_2 diagram at 300°C showing the stability fields of mineral assemblages. The arrow indicates the proposed path of ore fluids from the fluid channel into the wallrock. Log Σ S = - 1.5, ΣK^+ = 0.1m, $\Sigma Ba^{2+} \geq 10^{-2}$ m, Σ C = 0.1 m, Ca^{2+} = 0.1m.

iron sulfide-gold ore deposition. The geochemical conditions outlined above (Crerar and Barnes, 1976) suggest that a minimum gold concentration of 10 ppb could be dissolved and transported by a bisulfide complex in the initial ore solution.

Copper deposition in the Lordsburg system was probably the result of a progressively decreasing temperature due to boiling and mixing (see interpretation of fluid inclusion data) and of changes in chemical conditions (fO_2, fS_2, pH). These resulted in the decrease in solubility of copper chloride complexes. The main precipitation temperature range of the copper sulfides in the Lordsburg system (128° - $\leq$ 350°C), indicate that cooling was a prominent factor in the copper mineralization. Gold was precipitated after the depletion of reduced S in these ore fluids through boiling and sulfidation.

Changes in Ore Fluids with Time

The ore structures in the mines at Lordsburg display similarities in mineralogy, temperature and pressure, and fluid composition. In detail, however, the paragenetic mineral assemblages, fluid compositions, and temperatures of formation in each mine (area) and/or of each vein are different. This may indicate that the evolution of hydrothermal fluids in the Lordsburg system varied in time and space with respect to the granodioritic magmatism. The brecciation and fracturing events that separate the stages of mineralization, and the crosscutting relationships indicate that mineralization occurred in various pulses.

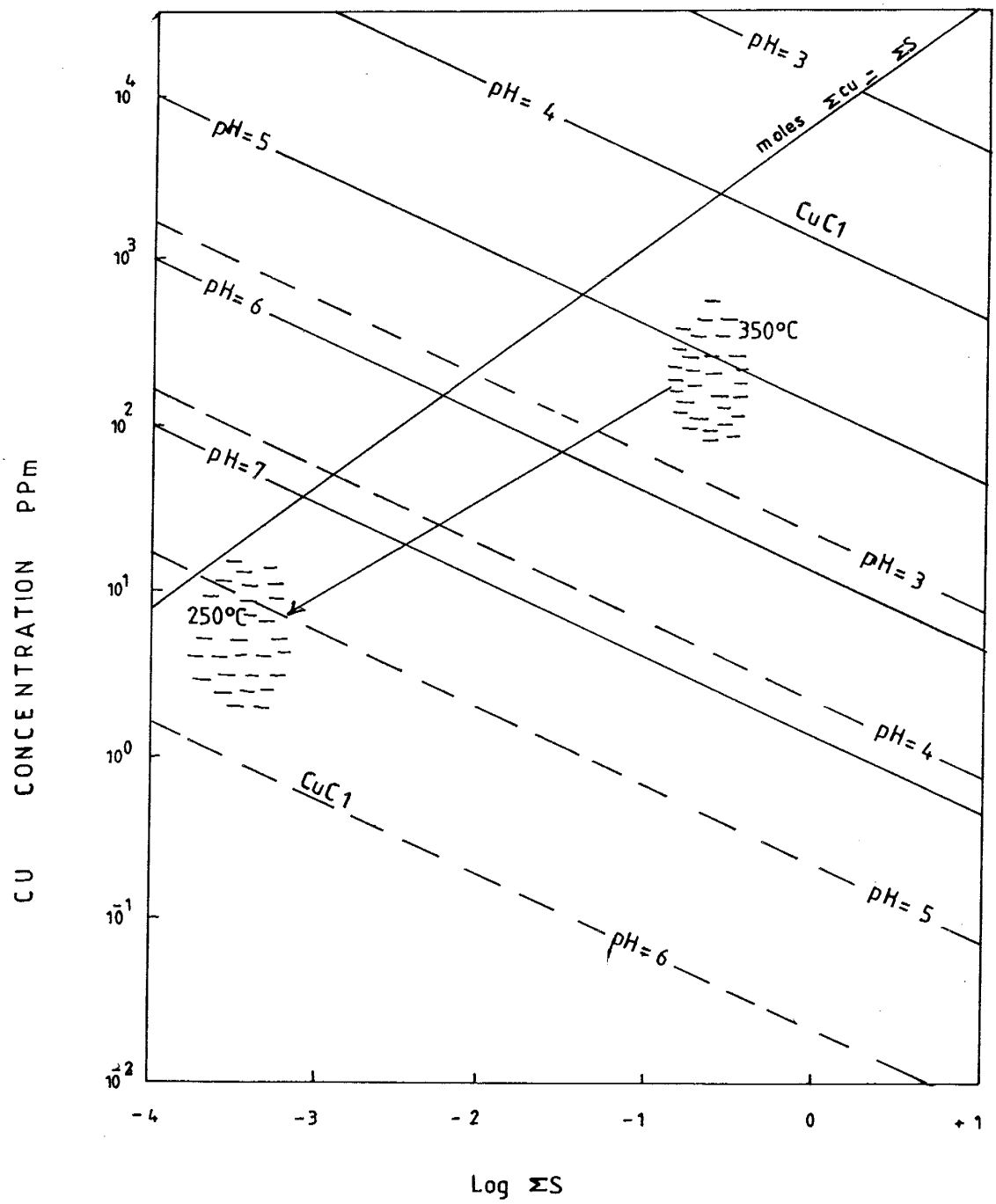

Fig. 39. Concentration of cuprous complex (CuCl) in solution at equilibrium with chalcopyrite + pyrite ± bornite as a function of total sulfur concentration and pH. Solid lines = pH at 350°C and Cl^- activity of 0.5;dashed lines = pH at 250°C and log Cl^-. Modified from Crerar and Barnes (1976).

Center of Mineralizing System

Temperatures of formation and vein mineral zoning patterns are asymmetrical about the exposed Lordsburg granodiorite stock (Figs. 4, 12, and 28). The mineral zonation and the calculated fS_2 and fO_2 values point to decreasing sulfidation and oxidation states away from the granodiorite stock. A lateral fluid movement and cooling outward from the granodiorite stock is implied by the decreasing homogenization temperatures and salinities.

The changes observed in temperatures of formation, fluid composition, and mineralogy are not only the results of different stages of mineralization but are also reflections of lateral changes that occur with increasing distance from the granodiorite stock. The changes may be a function of dilution concomitant with cooling of ore-stage fluid as it circulated away from the granodiorite stock.

Vertical flow is indicated in the 85 mine by the vertical distribution of galena and sphalerite. Galena and sphalerite were observed to increase upwards from the 2000 ft-level to the surface (Lasky, 1938). The amounts of galena and sphalerite are also observed to increase outward from the 85 mine, attaining a peak in the Waldo and Ruth mines in the Virginia subdistrict. These observations suggest that centers of mineralizing fluids are close to the granodiorite stock-andesite contact (85 mine in the Virginia subdistrict and Robert Lee-Nellie Bly mines in the Leitendorf subdistrict).

Type of Deposit

The zonation of alteration and mineralization coupled with the observed changes in T, fS_2, fO_2, and pH in Lordsburg are typical of certain zoned base-metal lode deposits such as Butte, Montana (Meyer et al., 1968; Brimhall, 1979), Julcani, Peru (Peterson et al., 1977; Mosier et al., 1986), Quiruvilca, Peru (Bartos, 1987), Central City, Colorado (Sims and Barton, 1962; Rice et al., 1985) and Cerro de Pasco, Peru (Petersen, 1970; Einaudi, 1977). These base-metal lode veins exhibit zoning from a high-sulfur, Cu-rich core (Chalcopyrite-pyrite or bornite-pyrite) to an outermost Pb ± Zn± Ag zone (galena-sphalerite-carbonate). Alteration, zoned from vein margins is from sericitic(quartz-pyrite-sericite) or advanced argillic (kaolinite + pyrite + alunite) through intermediate argillic (smecitites + quartz + calcite + pyrite) alteration to an outer propylitic alteration (Einaudi, 1977, 1982; Bartos, 1989). Temperatures of formation range from >350°C to <200°C for most of these deposit types. Most of the deposits are associated with mineralizing intrusives and may or may not be spatially associated with porphyry copper systems. Lordsburg exhibits most of these key features associated with these base-metal lodes.

Lordsburg also has several characteristics that are similar to certain epithermal polymetallic veins such as Filandia, Peru (Kamilli and Ohmoto, 1977), Lake City, Colorado (Slack, 1980), Sunnyside, Colorado (Casadevall and Ohmoto, 1977), and Mayflower, Utah (Nash, 1973). Similarities are noted in fluid inclusion data: homogenization temperatures (~140°-330°C); salinities

(0-13 equiv. wt % NaCl); depths of formation (~500-1500 m); evidence of aqueous phase boiling; meteoric water dominance. Lordsburg differs from these deposit types in terms of alteration and mineralization styles. The base-metal content of epithermal typically often increases with depth, commonly reaching ≥ 5% (Buchanan, 1981) and may reach up to 20% as at (Parral, Chihuahua, Mexico (Buchanan, 1981). Gold and silver contents decrease with depth. This vertical changes in metals content and zonation were not observed in Lordsburg. Mine records indicate either consistent metal values or steady increase in Cu, Au, and Ag with depth in the 85 mine.

The Lordsburg deposit shows features of both epithermal and mesothermal vein deposits. Lordsburg is most similar to base-metal lode vein type deposits in such details as mineral zonation and spatial relationships to an intrusive. The ore textures, alteration, and ore mineralogy fit the base-metal lode deposits better than epithermal deposits. However, episodic mineralization and lateral flow of ore solutions as observed in Lordsburg are common in certain epithermal deposits.

A Model for Lordsburg

The model proposed for the genesis of Lordsburg based on evidence from the district and from other well-documented cases is as follows:

1. A magmatic hydrothermal system was initiated by the intrusion of granodiorite stock, porphyry and aplite dikes into an andesitic stratovolcano complex, an environment typical of the tops of porphyry copper systems (Sillitoe, 1973).

2. The intrusive complex evolved magmatic discharges of volatiles (CO_2, SO_2, H_2S, HCl, HF, etc.) and metals (Henley and McNabb, 1978; Giggenbach, 1987; Gerlach, 1979, 1981) which rose through permeable channels created by regional faulting, encountered and mixed with an extensive deep circulating meteoric water system.

3. The magmatic volatiles and metals were condensed by the convective meteoric water into a gaseous, metalliferous, low-moderate salinity and moderately high temperature hydrothermal system with high sulfidation and oxidation states and moderate hydrogen ion activities.

4. Focussed ascent of these modified hydrothermal fluids along faults and fractures occurred in episodes. Deposition of metals and gangue minerals in response to chemical changes in fluid accompanied phase separation, cooling, mixing, and dilution processes.

5. In the area close to or immediately above the intrusion rapid deposition of sulfide phases with the development of illitic (sericitic) alteration that are characteristic of the chemical state of the fluid occurred. Deposition of sulfide phases at decreasing sulfidation and oxidation states and increasing pH in time and space then commenced.

6. The fluctuations in the chemical states of the ore fluid leading to changes in ore and alteration mineral assemblages were due to the waning of the volatile discharges from the parent magma and an increase in the degree of water-rock interaction and/or increase in meteoric diluent.

SUMMARY AND CONCLUSIONS

1. The mineralization of the polymetallic silica-sulfide vein deposits of Lordsburg occurred in six stages. The stages are separated in time by fracturing and brecciation. Stage 2 is the main stage of ore mineralization in the district. A district zonation from Cu-Au to Pb-Zn exists.

2. Vein mineralization is accompanied by illitic, intermediate argillic and propylitic alteration that are zoned from the vein in the order: illitic, chloritic, chlorite-smectite mixed-layer and chlorite-albite-calcite.

3. Fluid inclusion data and alteration mineralology suggest that the veins formed from fluids of 3 to 7 equiv. wt % NaCl at temperatures that decrease through time and laterally from to $\leq$350°C to 128°C. Stages 2 and 3 represent boiling, cooling, mixing, and dilution in the mineralizing system. Fluid inclusion data from the carbonate dominant late stages of mineralization reflect much cooler (down to 128°C), more dilute (down to 3.2 equiv. wt % NaCl) hydrothermal fluids.

4. Equilibrium thermodynamic interpretation indicates that the base-metals in the Lordsburg system were transported as a chloride complexes. Gold was probably transported as a chloride complex in initial fluids (pH = 4.7-5.0, T $\geq$ 250°C) and as bisulfide complexes at lower temperature (< 250°C). A temperature decrease of ore fluids from about 350° to about 128°C due to boiling, mixing, and dilution with meteoric waters destabilized the chloride complexes to precipitate the base-metals and

gold. Gold precipitation from bisulfide complex may have been controlled dominantly by the depletion of reduced S from solution through precipitation of sulfides and boiling.

5. A hydrothermal system with meteoric water dominance but with significant magmatic component is indicated by the ternary plot of non-reactive fluid inclusion gases (N_2, Ar, He). A deep circulating meteoric water system is implied by the presence of significant amount of organic species in fluid inclusions believed to be sourced from the Paleozoic clastic-carbonate sequence and suggested by the ternary diagram.

6. The vein deposits display similarities in mineralogy, temperature and pressure, fluid composition, and age of mineralization. In detail, however, the paragenetic mineral assemblages, fluid compositions, and temperatures of formation of each vein and/or each mine are different. This suggests that the evolution of hydrothermal fluids in the Lordsburg system varied in time and space with respect to granodioritic magmatism.

7. Metals and volatiles in the Lordsburg system may be considered to have been infused directly into the hydrothermal system via magmatic plumes or fluids with minor contributions from the underlying Paleozoic sediments. Alternatively, the metals and sulfur may be considered to have been remobilized from earlier stages of magmatic-hydrothermal mineralization and from the underlying Paleozoic sediments.

REFERENCES

Bartos, P. J., 1987, Quiruvilca, Peru: Mineral zoning and timing of wallrock alteration relative to Cu-Pb-Zn-Ag vein-fill deposition: Econ. Geol., v. 82, p 1431-1452.

Bartos, P. J., 1989, Prograde and retrograde base metal lode deposits and their relationship to underlying porphyry copper deposits: Econ. Geol., v. 84, p 1671-1683.

Belt, C.B., 1960, Intrusion and ore deposition in New Mexico: Econ. Geol., v. 55, p 1144-1271.

Bodner, R. J., 1992, Revised equation and table for freezing-point depression of H_2O-salt fluid inclusion: PACROFI IV abstract. Vol.

Brimhall, G.H., Jr., 1979, Lithologic determination of mass transfer mechanisms of multiple-stage porphyry copper mineralization at Butte, Montana: Vein formation by hypogene leaching and enrichment of potassium-silicate protore: Econ. Geol., v. 74, p 556-589.

Browne P.B.L., 1978, Hydrothermal alteration in active geothermal fields. Ann. Rev. Earth Planet. Science 6, p 229-250.

Buchanan, L. J., 1981, Precious metal deposits associated with volcanic environments in the Southwest: Geol. Soc. Arizonal Digest, V. 14, p. 237-262.

Casadevall T and Ohmoto H., 1977, Sunnyside mine, Eureka Mining District, San Juan County, Colorado. Geochemistry of gold and base metal ore deposition in a volcanic environment. Econ. Geol. 72, p 1285-1320.

Clark, K.F., 1962, Hypogene zoning in the Lordsburg mining district, Hidalgo County, New Mexico: Master's thesis, Univ. New Mexico, p 136.

_____, 1964, Hypogene zoning in the Lordsburg mining district, Hidalgo County, New Mexico (abs.) in New Mex. Geol. Soc. Guidebook of the Ruidoso County: 15th Field Conf., 1964, p 186-187.

_____, 1970, Zoning paragenesis, temperature formation in the Lordsburg District: New Mexico Geological Society Guidebook, 21st Field Conference, p 107-113.

Crerar, D. A. and Barnes, A. L., 1976, Ore solution chemistry V. Solubilities of chalcopyrite and chalcocite assemblages in hydrothermal solution at 200° to 350°C: Econ. Geol., v. 71, p.. 772-794.

Darton, N.H., 1933, Guidebook of the Western United States, pt. F, The Southern Pacific Lines, New Orleans of Los Angeles: U.S. Geol. Survey Bull. 845, p 304.

Davis, G.H., 1979, Laramide folding and faulting in southeastern Arizona: American Journ. Sci., v. 279, p 543-569.

Einaudi, M.T., 1977, Environment of ore deposition at Cerro de Pasco, Peru: Econ. Geol., v. 72, p 873-924.

Einaudi, M.T., 1982, Description of skarns associated with porphyry copper plutons, southwestern North America, in Titley, S.R., ed., Advances in geology of the porphyry copper deposits, southwestern North America: Tucson, Univ. Arizona Press, p 139-184.

Elston, W.E., 1965,, Mining districts of Hidalgo County, New Mexico in New Mex. Geol. Soc. Guidebook of southwestern New Mexico II: 16th Field Conf., 1965, p 210-214.

Elston, W.E, Erb, E.E., and Deal, E.G., 1979, Tertiary geology of Hidalgo County, New Mexico: Guide to metals, industrial minerals, petroleum and geothermal resources: New Mexico Geology, v. 1, p 1-6.

Eslinger, E.V. and Savin S., 1973, Mineralogy and oxygen isotope geochemistry
of hydrothermally altered rocks of the Ohaaki-Broadlands, New Zealand geothermal area. Am. J. Sci. 273, p 240-267.

Flege, R.F., 1959, Geology of the Lordsburg quadrangle, Hidalgo County, New Mexico: New Mexico Bureau of Mines and Mineral Resources, Bulletin 62, p 36.

Giggenbach, W.F., 1986, The use of gas chemistry in delineating the origin of fluids discharged over the Taupo volcanic zone: Proc. Symp V. Intern. Volcanol. Congr., Auckland, New Zealand, p 47-50.

Giggenbach, W.F., 1987, Redox processes governing the chemistry of fumarolic gas discharges from White Island, New Zealand: Appl. Geochem., v. 2, p 145-161.

Gillerman E., 1958 Geology of the Central Peloncillo Mountains, Hidalgo County, New Mexico, and Cochise County, Arizona: New Mexico Bur. Mines and Min. Res. Bull. 57, p 152.

Gerlach, T.M., 1979, Evaluation and restoration of the 1970 volcanic gas analyses from Mount Etna, Sicily: J. Volcanol. Geotherm. Res., v. 6, p. 165-178.

_____, 1981, Restoration of new volcanic gas analyses from basalts of the Afar region: further evidence of CO_2 degassing trends: J. Volcanol. Geotherm. Res. v. 10, p. 83-91.

Haas, J.L., Jr., 1971, The effect of salinity on the maximum thermal gradient of a hydrothermal system at hydrostatic pressure: Econ. Geol., v. 66, p 940-946.

Henley, R.W. and McNabb, A., 1978, Magmatic vapor plumes and ground-water interaction in porphyry copper emplacement: Econ. Geol., v. 73, p. 1-20.

Hill, J.D., 1924, The Mining districts of southwestern New Mexico: Master's thesis, Univ. Colo., p 134 (unpublished).

Horton, D.G., 1985, Mixed-layer illite-smectite as a paleotemperature indicator in the Amethyst Vein System, Creede District, Colorado, U.S.A. Contri. Mineral. Petrol. 91, p 171-179.

Huntington, M.G., 1947, Atwood copper group, Lordsburg District, Hidalgo County, New Mexico: U.S. Bureau of Mines Report of Investigations 4029, p 9.

Huston D.L. and Large R.R., 1989, A chemical model for the concentration of gold in volcanogenic massive sulfide deposits: Ore Geology Rev. v. 4, p 171-200.

Inoue A. and Utada M., 1983, Further investigations of a conversion series of dioctahedral mica/smectites in the Shinzan hydrothermal alteration area, Northeast Japan. Clay and Clay Minerals 31, p 401-412.

Jones, F.A., 1904, New Mexico mines and minerals: Santa Fe, World's Fair ed., p 349.

_____, 1907, The Lordsburg mining region, New Mexico: Eng. Mining Journal, v. 84, p 444-445.

Kamilli, R.J. and Ohmoto, H., 1977, Paragenesis, zoning, fluid inclusion and isotopic studies of the Filandia vein, Colqui district, Central Peru: Econ. Geol. v. 72, p 950-982.

Kristmandotirr H., 1976, Types of clay minerals in hydrothermally altered basaltic rocks, Reykjanes, Iceland. Jokull 26, p 30-39.

Lacy, W.C., 1959, Structure and ore deposits of the east Sierrita area: Ariz. Geol. Soc. Guidebook II, Southeastern Arizona, p 184-192.

Larson, P.B., 1984, Geochemistry of the alteration pipe at the Bruce Cu-Zn volcanogenic massive sulfide deposit, Arizona: Econ. Geol., v. 79, p 1880-1896.

Lasky, S.G., 1938, Geology and ore deposits of the Lordsburg mining district, Hidalgo County, New Mexico: U.S. Geological Survey, Bulletin 885, p 62.

Lindgren, W., Graton, L.C., and Gordon, C.H., 1910, The ore deposits of New Mexico: U.S. Geological Survey, Professional Paper 68, p 332-335.

Meyer, C., Shea, E.P., Goddard, C.C., Jr., and Staff, 1968, Ore deposits at Butte, Montana, in Ridge, J.D. ed., Ore deposits of the United States, 1933-1967 (Graton-Sales vol): New York, Am. Inst. Mining Metall. Petroleum Engineers, v. 2, p 1373-1416.

Moore, D.M. and Reynolds R.C., Jr., 1989, X-ray Diffraction and the Identification and Analysis of Clay Minerals. Oxford Univ. Press, New York, p 241-269.

Mosier, D.L., Menzie, W.D. and Kleinhampl, F.J., 1986, Geologic and grade-tonnage information on Tertiary epithermal precious and base-metal deposits associated with volcanic rocks: U.S. Geol. Survey Bull, 1666, p 39.

Muffler, L.J.P. and White D.E., 1969, Active metamorphism of Upper Cenozoic sediments in the Salton Sea geothermal fields and the Salton trough, Southeastern California. Geol. Soc. Am. Bulletin 80, p 157-182.

Nash, J.T., 1973, Geochemical studies in the Park City district, Utah: I: Ore fluids in the Mayflower mine: Econ. Geol., v. 68, p. 34-51.

Norman, D.I. and Sawkins, F., 1987, Analysis of volatiles in fluid inclusions by mass spectrometry: Chem. Geol., v. 61, p 1-10.

Norman, D.I. and Musgrave, J.A., 1993, N_2-Ar-Helium compositions in fluid inclusions: Indicators of fluid source: in press.

Palmason, G. Arnorsson, S., Fridleifsson, I.B., Kristmandotirr, H, Saemundsson, K., Stefansoon, V., Steingrimsson, B., and Tomasson,

J., 1979, The Iceland Crust: Evidence from drillhole data on structure and processes, in Talwani, M., Harrison, C.G., and hayes, D.E., eds., Deep drilling results in the Atlantic Ocean Crust, Maurice Ewing Series, v. 2: Washington Am. Geophys. Union, p 230-238.

Petersen, U., Noble, D.C., Arenas, M.J., and Goodell, P.C., 1977, Geology of the Julcani mining district, Peru: Econ. Geol., v. 72, p 931-949.

Reyes A.G., 1990, Petrology of Philippine geothermal systems and the application of alteration mineralogy of their assessment. J. Vocanol. Geotherm. Research 43, p 279-309.

Rice, C.M., Harmon, R.S., and Shepherd, T.J., 1985, Central City, Colorado: The upper part of an alkaline porphyry molybdenum system: Econ. Geol., v. 80, p 1769-1796.

Richter, D.H. and Lawrence, V.A., 1983, Mineral deposit map of the Silver City 1°x2° quadrangle, New Mexico and Arizona: U.S. Geological Survey, Misc. Investigations Series Map I-1310-B, scale 1:250,000.

Richter D.H., Sharp W.N., Watts K.C., Raines, G.L., Houser B.B., and Klein, D.P, 1983, Mineral resource assessment of the Silver City 1°x2° quadrangle, New Mexico-Arizona: U.S. Geological Survey, Open-File Report 83-924,,p 77.

Robie, R A., Hemingway, B. S., and Fisher, J., 1978. Thermodynamic properties of minerals and related subtances at 298.95K and at higher temperatures: U.S. Geol. Surv. Bull. 1452, 456 p.

Roedder, E., 1984, Fluid inclusions: Rev. Mineralogy, v. 12, p 646.

Romberger, S.B., 1986, Mechanisms of deposition of gold in low temperature hydrothermal systems [abs.]: Journ. Geochem. Explor., v. 25, p 237.

Schmitt, H.A., 1966, The porphyry copper deposits in their regional setting, in Titley, S.R., and Hicks, C.L. eds., Geology of the porphyry copper deposits, southwestern North America: Tuscon, Univ. Ariz. Press, p 17-33.

Seward T.M., 1984, The transport and deposition of gold in hydrothermal system, in Foster R.W., ed., Gold '82: Rotterdam, Balkema, p 165-181.

Sillitoe, R.H., 1973, The tops and bottoms of porphyry copper deposits: Econ. Geol., v. 68, p 799-814.

Sims, P. K. and Barton, P.B., Jr., 1962, Hypogene zoning and ore genesis, Central City district, Colorado: Geol. Soc. America Spec. vol. D, p 373-395.

Slack, J.F., 1980, Multistage vein ores of the Lake City district, Western San Juan Mountains, Colorado: Econ. Geol. v. 75, p. 963-991.

Steiner A., 1968, Clay minerals in hydrothermally altered rocks at Wairakei, New Zealand. Clay and Clay Minerals 16, p 193-213.

Storms, W.R., 1949, Mining methods and costs at the Atwood copper mine, Lordsburg mining district, Hidalgo County, New Mexico: U.S. Bur. Mines Inf. Cir. 7502, p 11.

Sumi K., 1968, Hydrothermal rock alteration of the Matsukcawa geothermal area, Northeast Japan. Geol. Sur. Japan Rep 225.

Thorman, C.H., 1978, Geologic map of the Coyote Peak and Brockman quadrangles, Hidalgo and Grant Counties, New Mexico: U.S. Geol. Surv. map MF-924.

Thorman, C.H. and Drewes, H., 1978, Geological map of the Gary and Lordsburg quadrangles, Hidalgo County, New Mexico: U.S. Geological Survey, Misc. Investigation series Map I-1151, scale 1:24,000.

Tommasson J. and Kristmandotirr H., 1972, High temperature alteration minerals and thermal brines, Reykjanes, Iceland.

Turner, G.L., 1962, The Deming axis southeastern Arizona, New Mexico, and Trans-Pecos Texas in New Mex. Geol. Soc. Guidebook to Mogollon Rim Region: 13th Field Conf., 1962, p 59-71.

Velde B., 1965, Phengite micas: Synthesis, stability and natural occurrence. Am. J. Sci. 263, p 886-913.

Wells, J.L., 1909, Mines of the Lordsburg district, New Mexico: Eng. Mining Journal, v. 87, p 890.

Wilkins, J., Jr., 1984, The distribution of gold- and silver-bearing deposits in the Basin and Range province, Western United States: Arizona Geol. Surv. Digest, v. 15, p. 1-27.

Yoder H.S. and Eugster H.P., 1955, Synthesis and natural nuscuvites. Geochimica et Cosmoschimica Acta 8, p 225-280.

Youtz, R.B., 1931, Mining methods at the Eigthy-Five mine, Calumet and Arizona Mining Co., Valedon, N. Mex.: U.S. Bur. Mines Inf. Circ. 6413, p 26.

Zeller, R.A., Jr., Stratigraphy of the Big Hatchet Mountains area, New Mexico: New Mexico Bur. Mines and Min. Res. Mem. 16, p 128.

APPENDIX I
SAMPLING TRAVERSE - ALTERATION STUDY

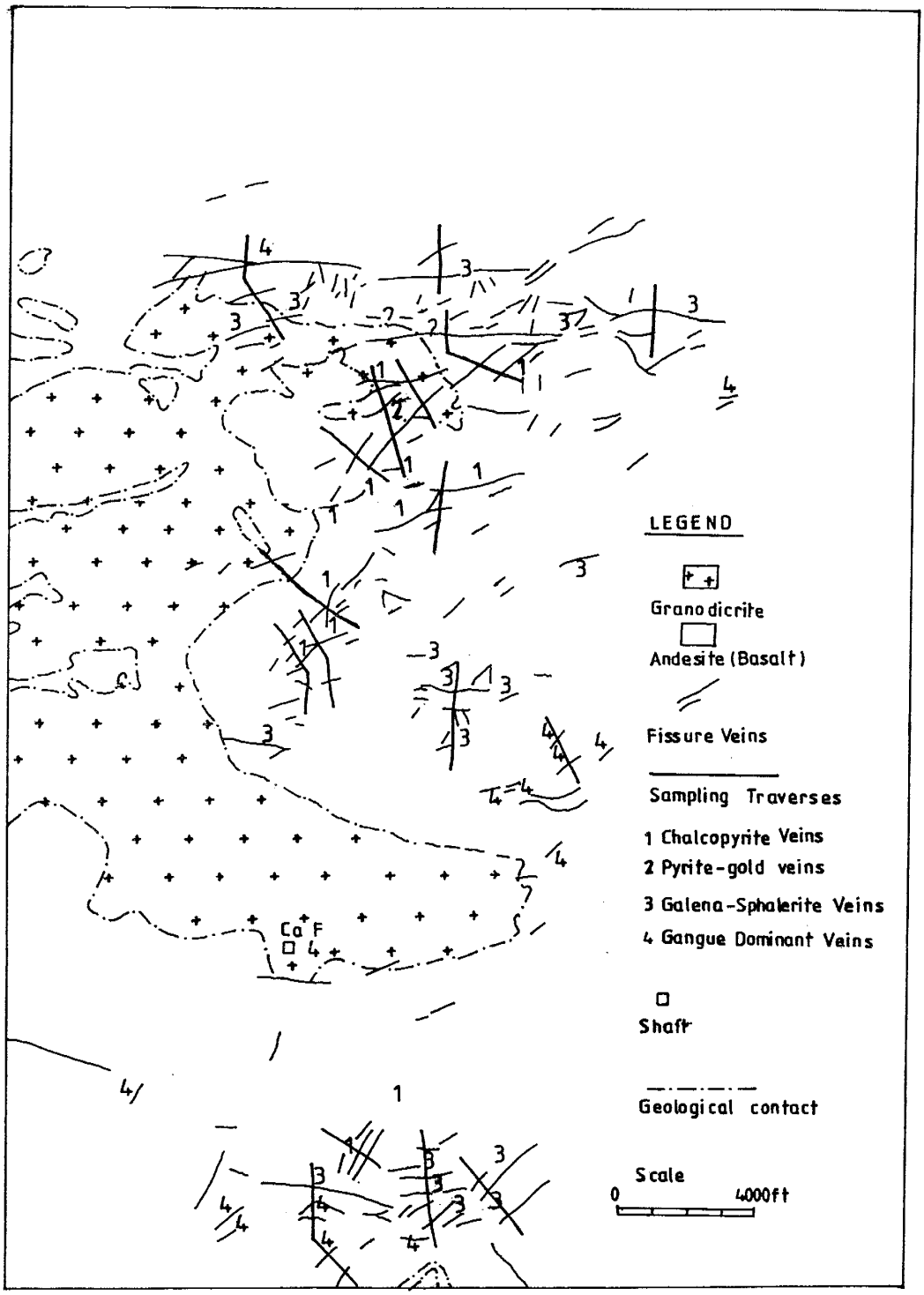

APPENDIX II

X-ray patterns of oriented ≤2 micron fractions of selected samples from the Lordsburg district. All d-spacings are in A. Sample locations are indicated in Appendix I III. A - air-dried pattern, B - glycolated pattern, C - heated to 375°C pattern, D - heated to 550°C pattern.

FA 31 illite (I), kaolinite (K), smectite (S), K-feldspar (Kfs), quartz (Q).

FA 38 Mg-chlorite (C), smectite (S), chlorite-smectite (C-S,) illite (I), albite (Ab), K-feldspar (Kfs), calcite (Cc).

FA 80 smectite (S), chlorite (C), illite (I), albite (Ab), calcite (Cc), K-feldspar (Kfs), quartz (Q).

FA 91 chlorite (C), smectite (S), illilte (I), albite (Ab), calcite (Cc), K-feldspan (Kfs).

FA 185 illlite (I), Corrensite (Cr), Chlorite(C), albite(Ab), K-feldspar(Kfs) Calcite (Ce), epidote (Ep).

FA 113 chlorite (C), K-feldspar (Kfs), calcite (Cc), illite(I)

FA 123[B] smectite (S), illite (I), chlorite (C), albite (Ab), calcite (Cc), quartz (Q).

FA 169[c] chlorite (C), illite/smectite (R3 I/S), kaolinite (K), calcite (Cc), quartz (Q).

FA 184 corrensite (Cr), chlorite (C), illite/smectite (R3 I/S), albite (Ab), K-feldspar (Kfs), calcite (Cc), epidote (Ep)

FA 196[A] tosudite (Ts), chlorite (C), albite (Ab), calcite (Cc), K-feldspar (Kfs), analcime (Anc).

APPENDIX II (cont.)

X-ray patterns of randomly oriented, air-dried, < 2 micron size fractions of FA 15, FA 20, FA 74, and FA 96^{B}. All d-spacings are in A. Polytypes of illite are indicated.

FA 15 $2M_1$ illite ($2M_1I$), 1M illite (1MI), illite (I), quartz (Q).

FA 20 1 M illite (1MI), $2M_1$ illite ($2M_1I$), illite (I), quartz (Q).

FA 74 $2M_1$, illite ($2M_1I$), illite (I), quartz (Q).

FA 96^{B} $2M_1$ illite ($2M_1I$), 1M illite (1MI), illite (I), quartz (Q).

APPENDIX II (CONT.)

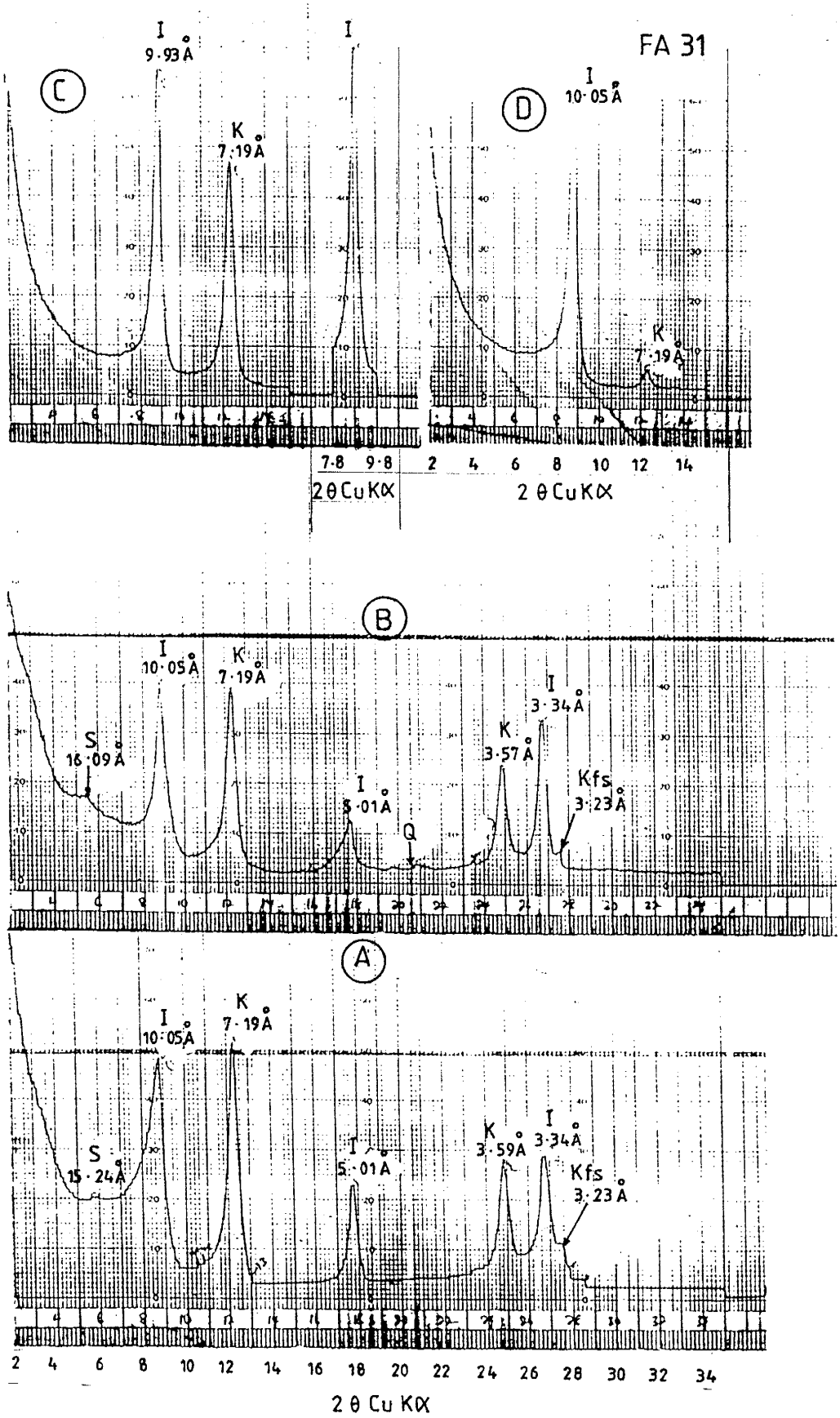

APPENDIX II (CONT.)

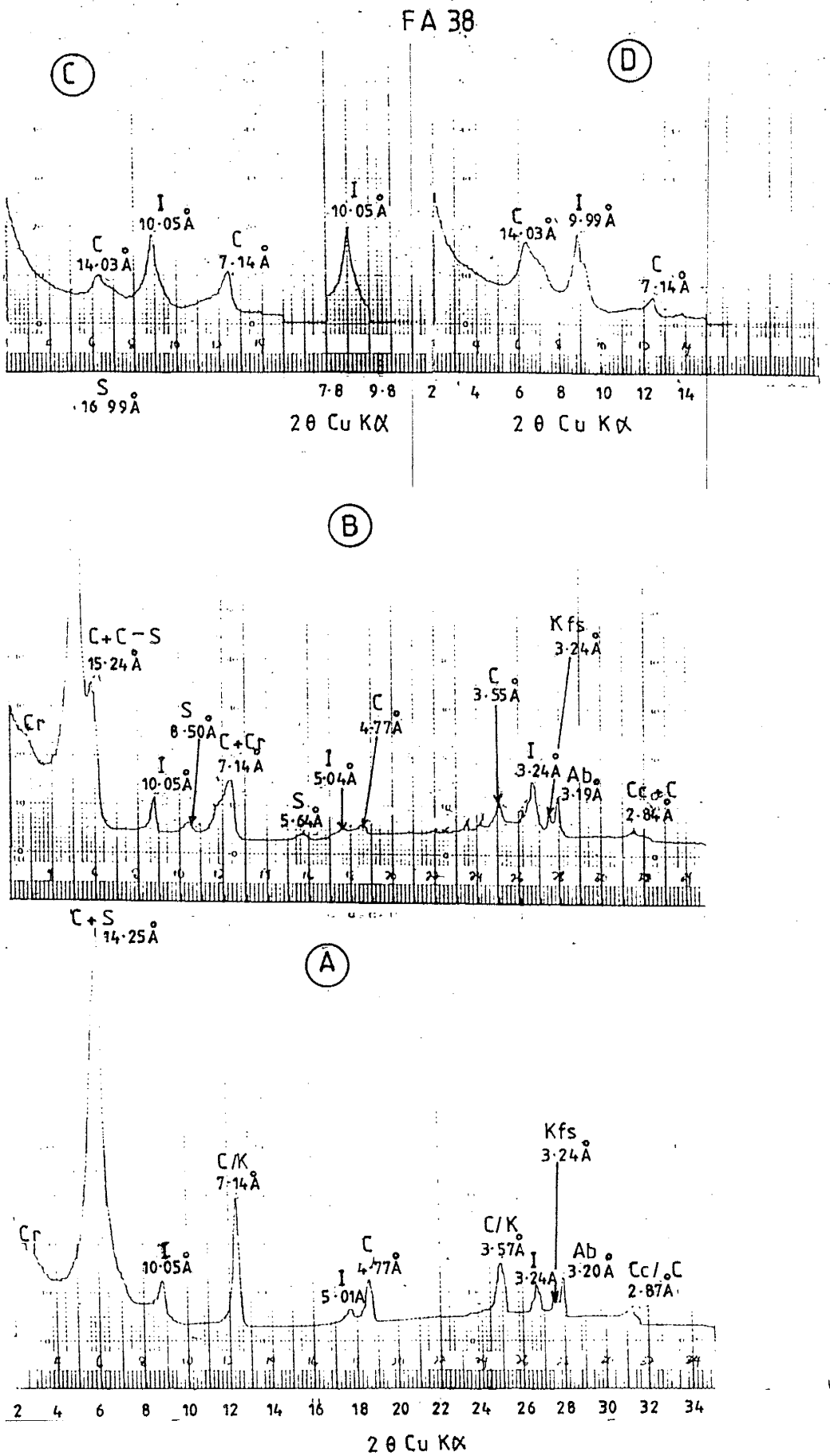

APPENDIX II (CONT.)

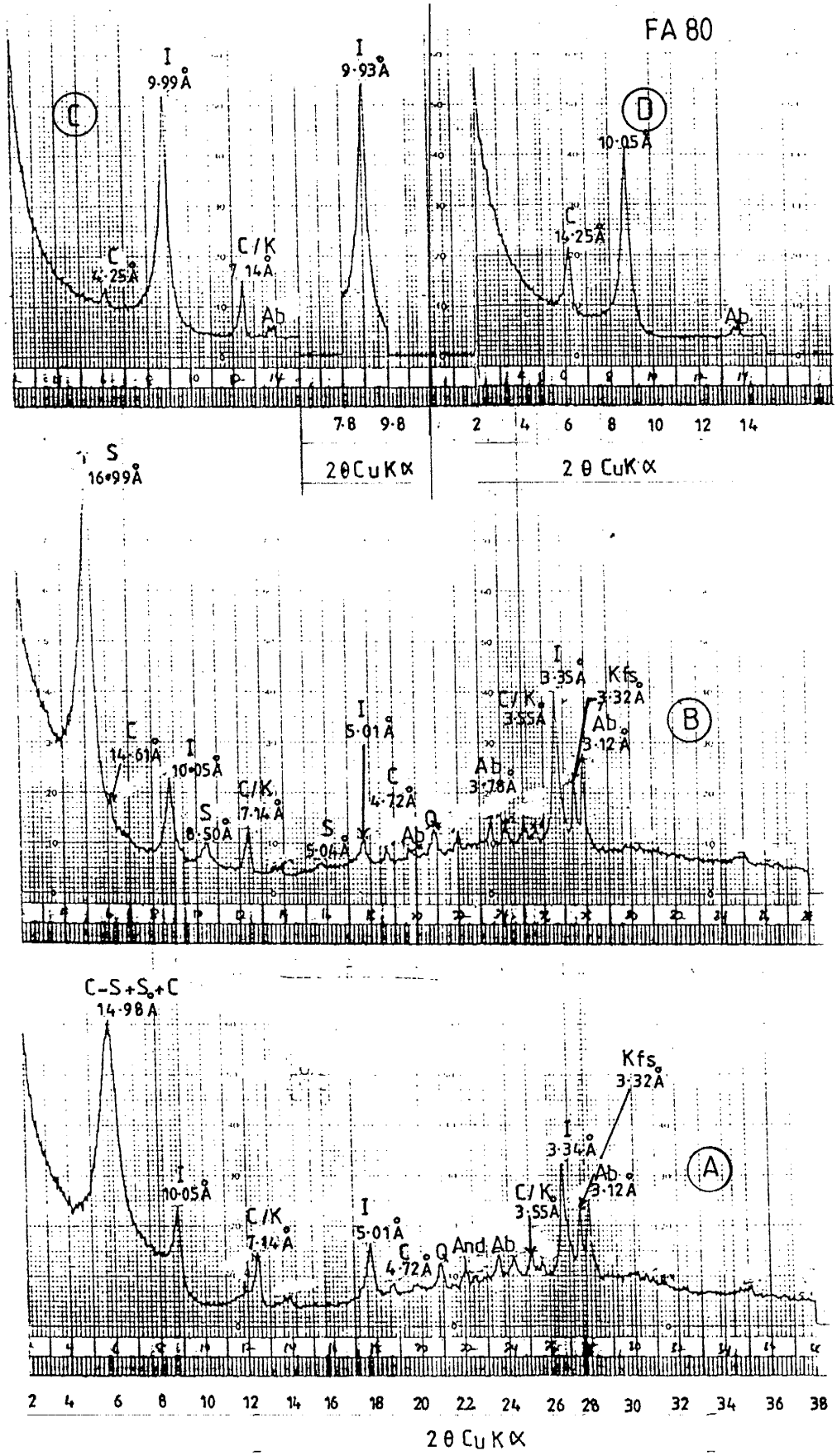

APPENDIX II (CONT.)

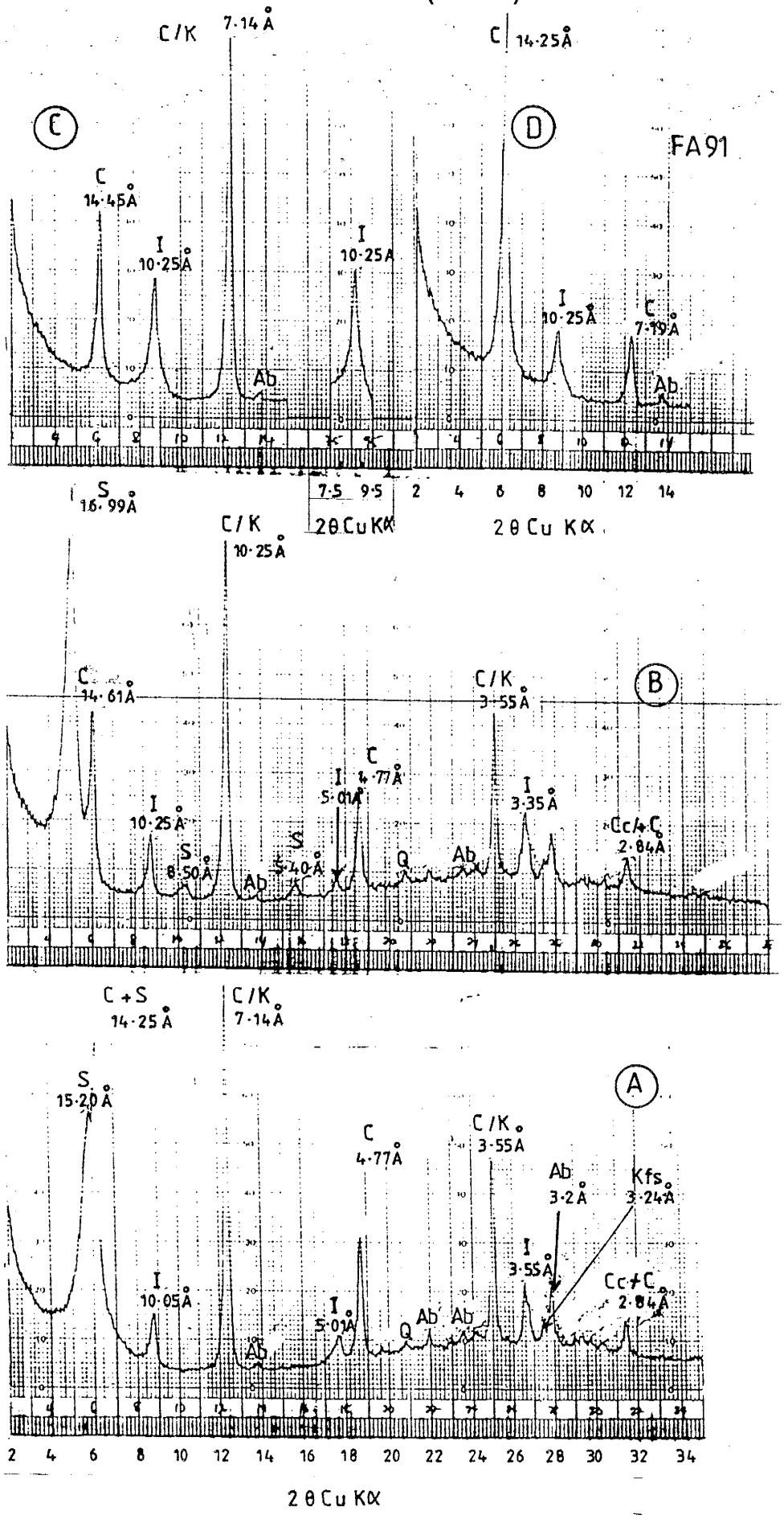

APPENDIX II (CONT.)

FA 185

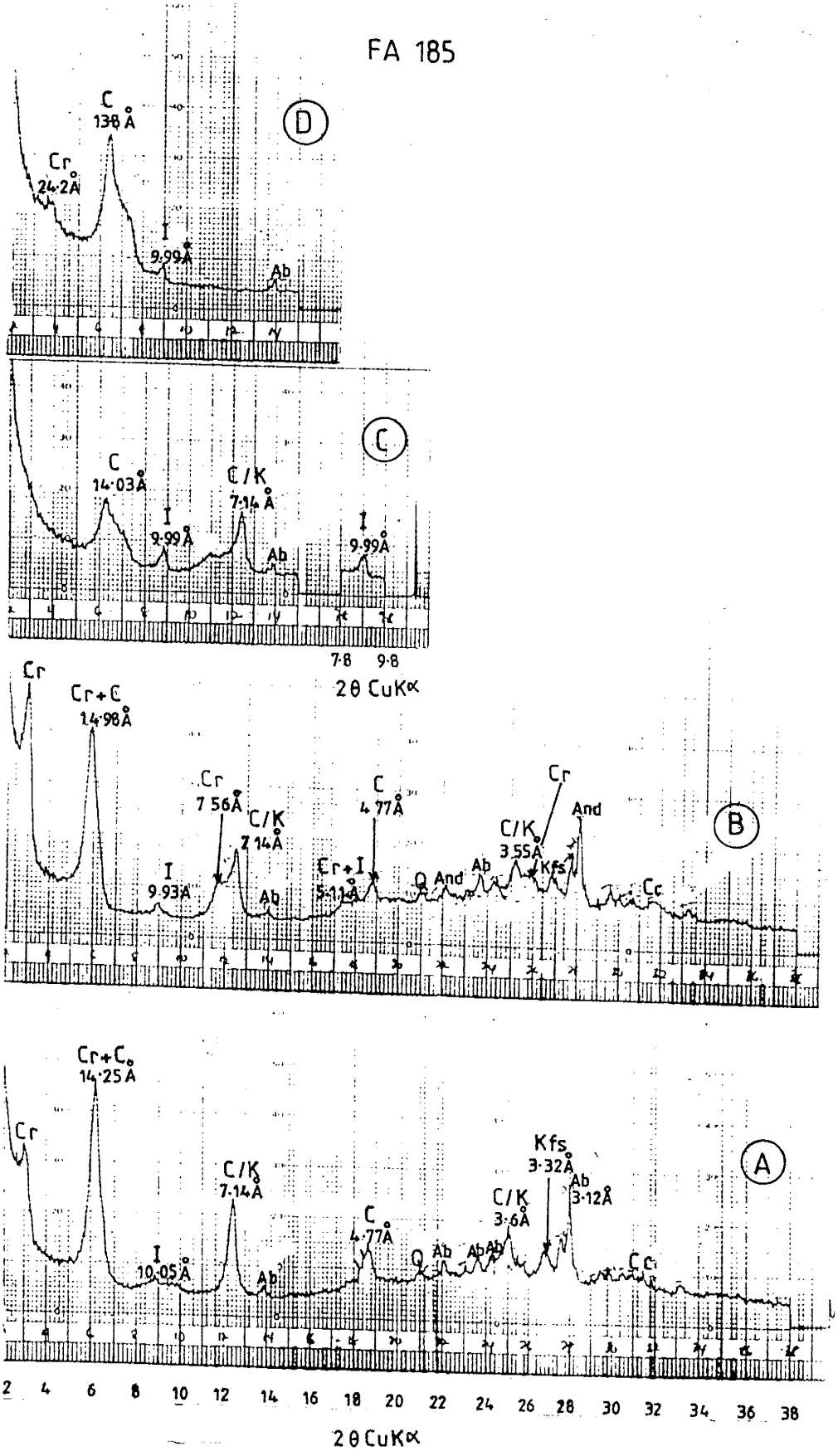

APPENDIX II (CONT.)

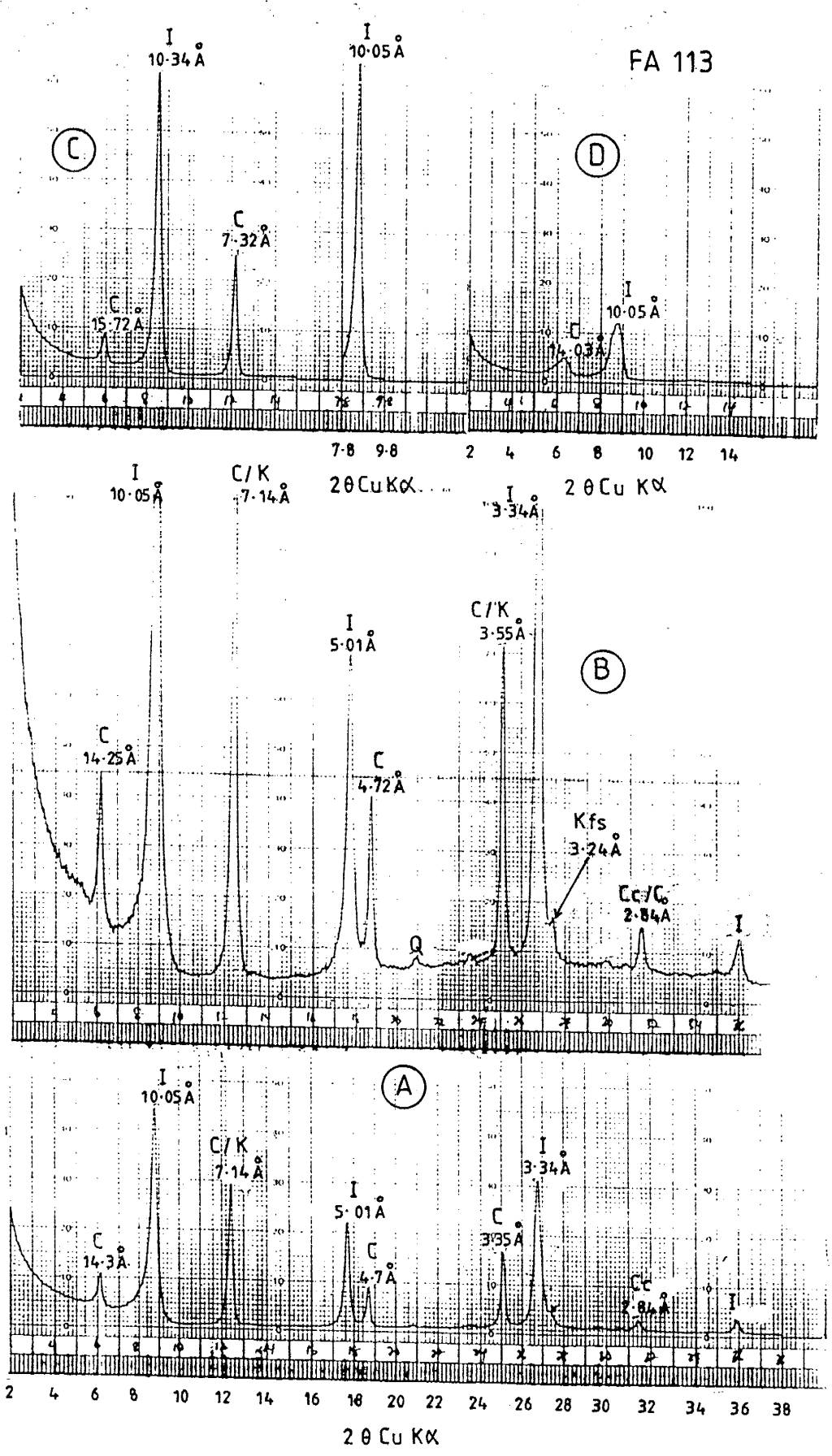

APPENDIX II (CONT.)

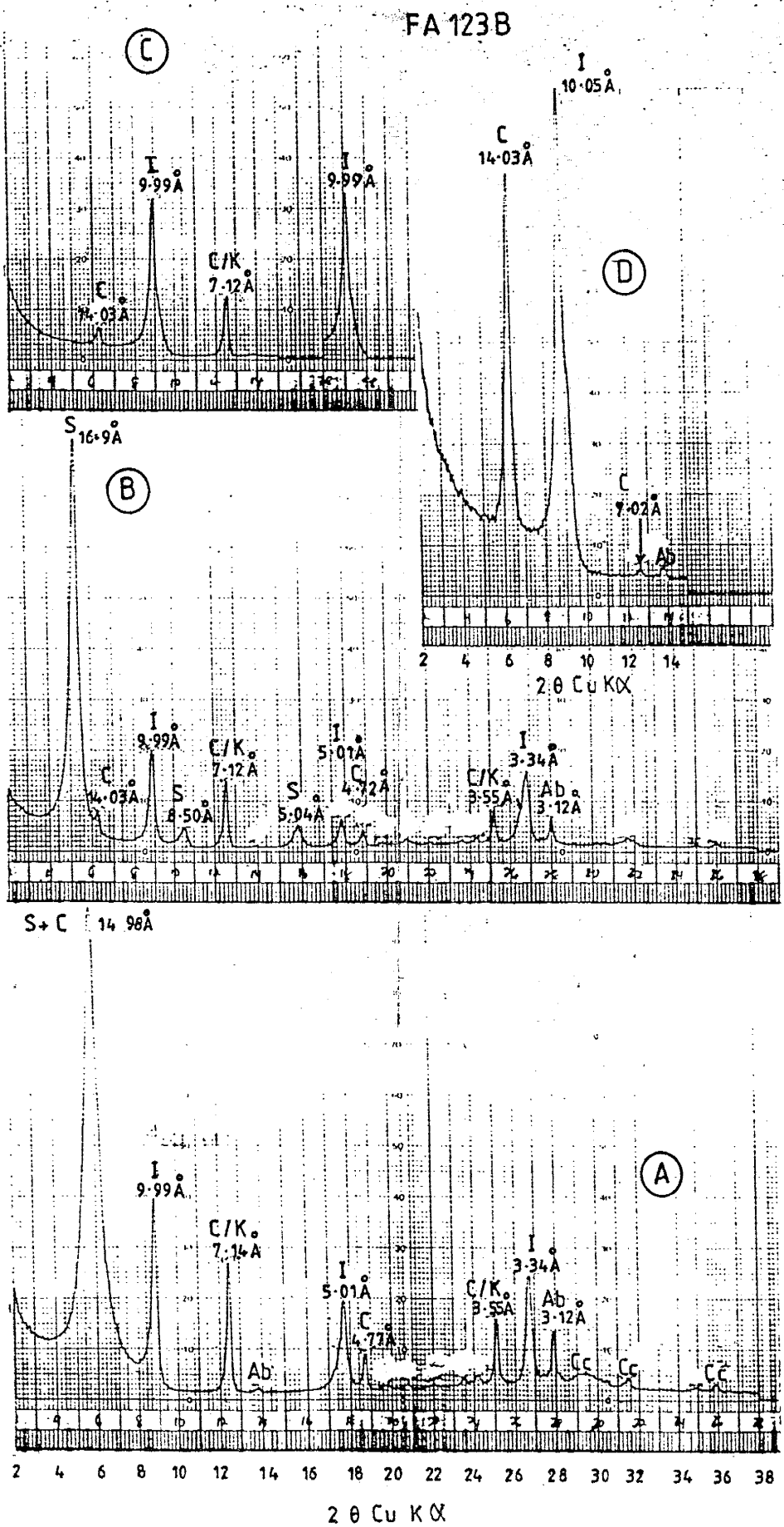

APPENDIX II (CONT.)

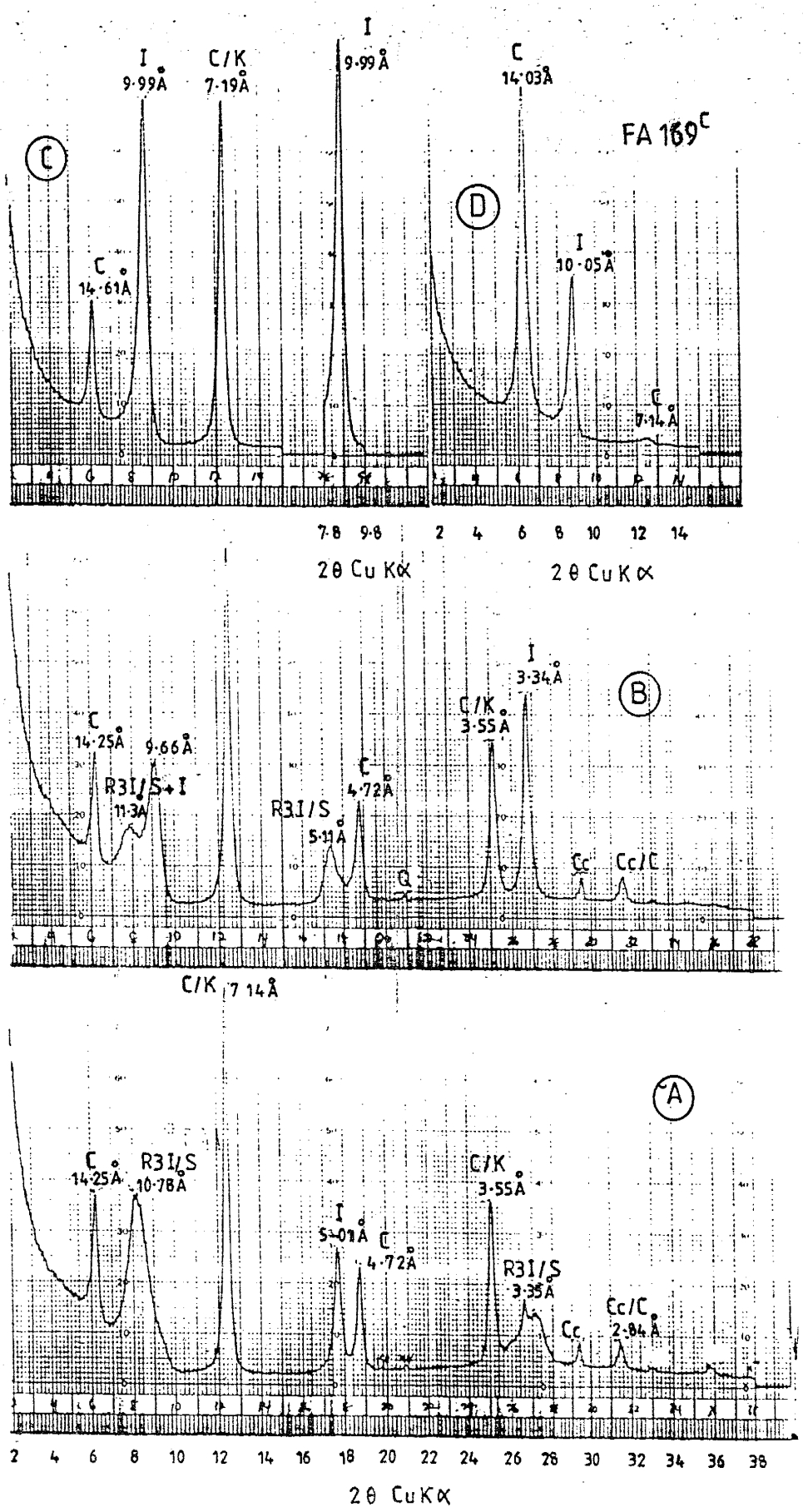

APPENDIX II (CONT.)

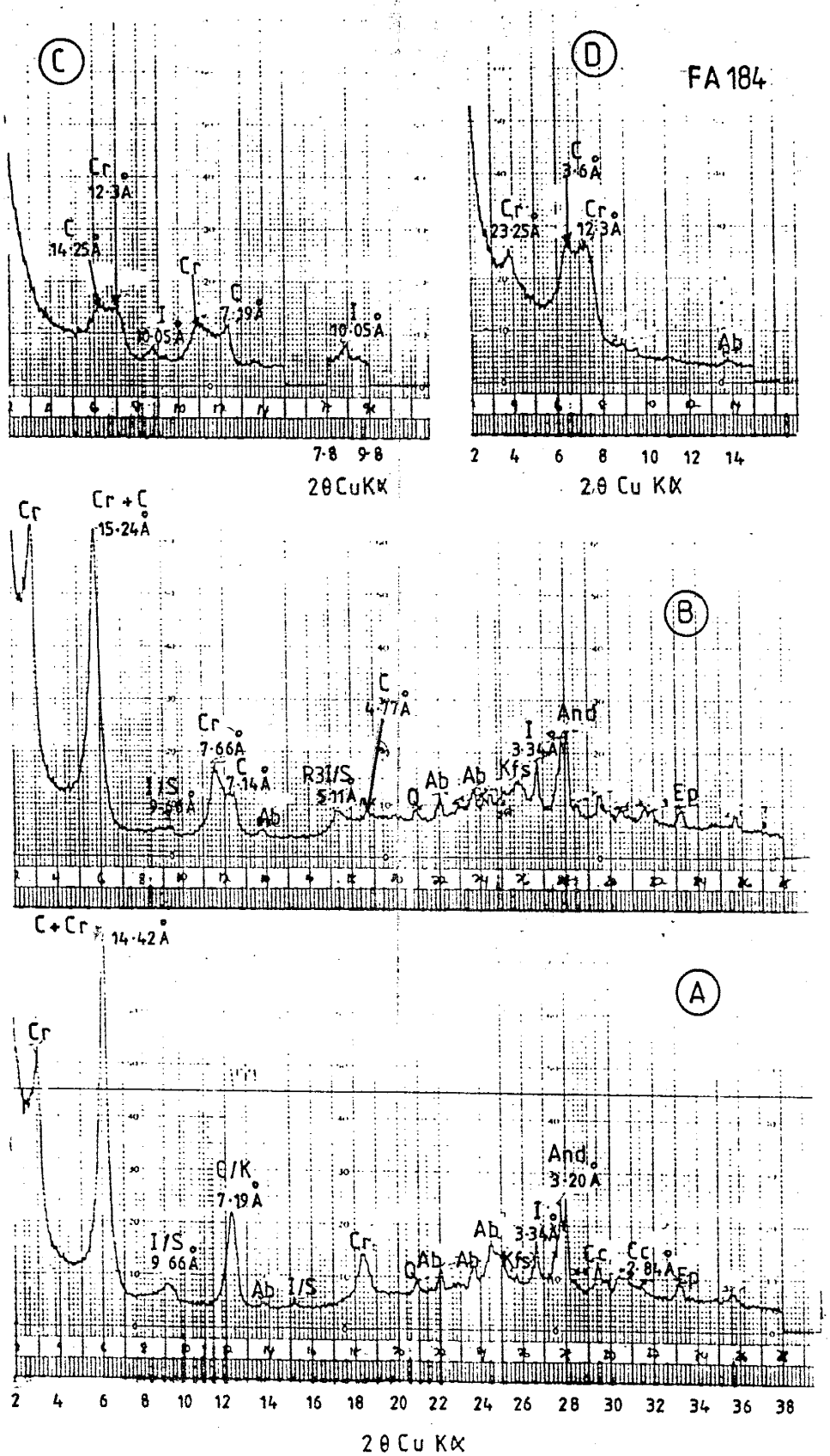

APPENDIX II (CONT.)

FA 196A

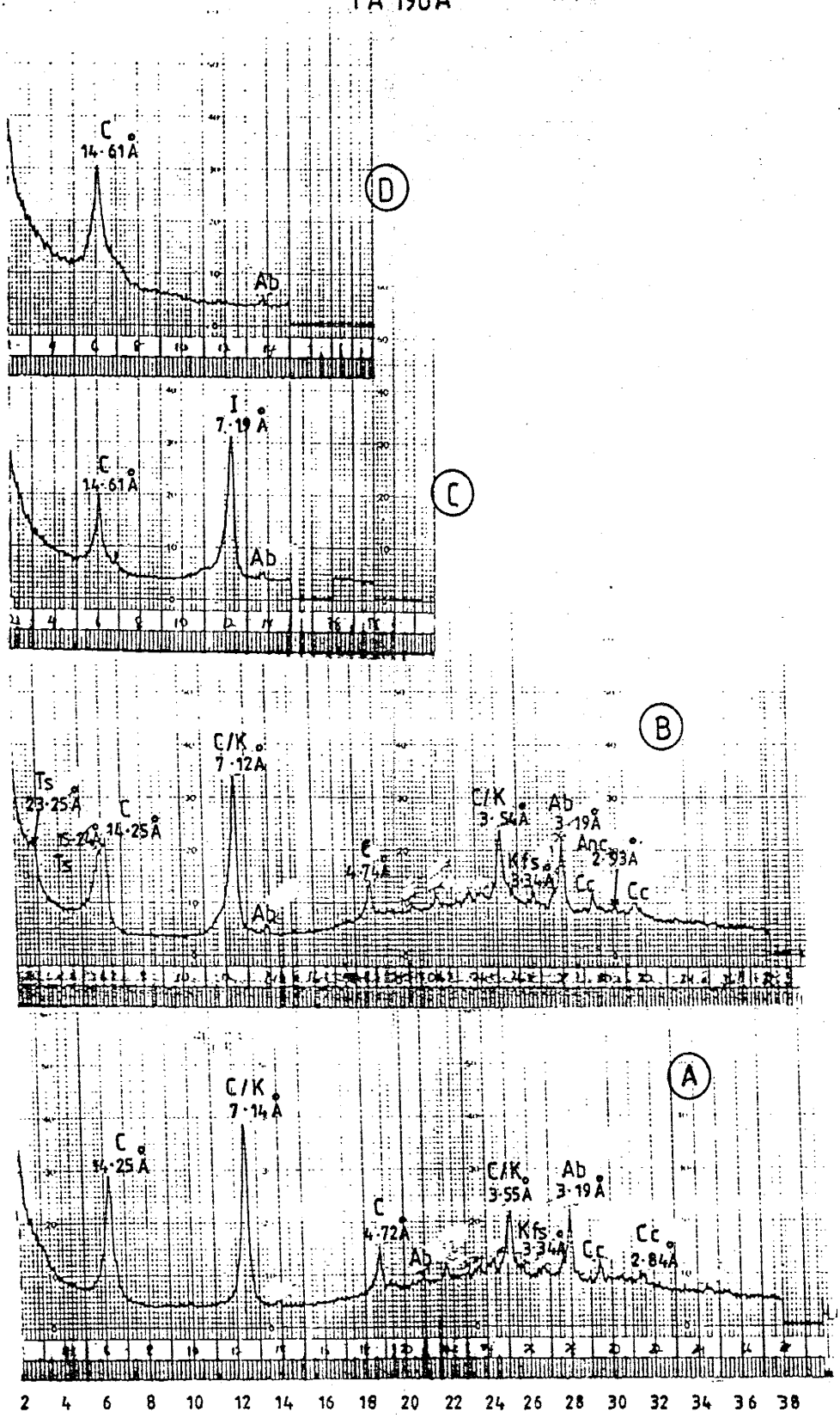

APPENDIX II (CONT.)

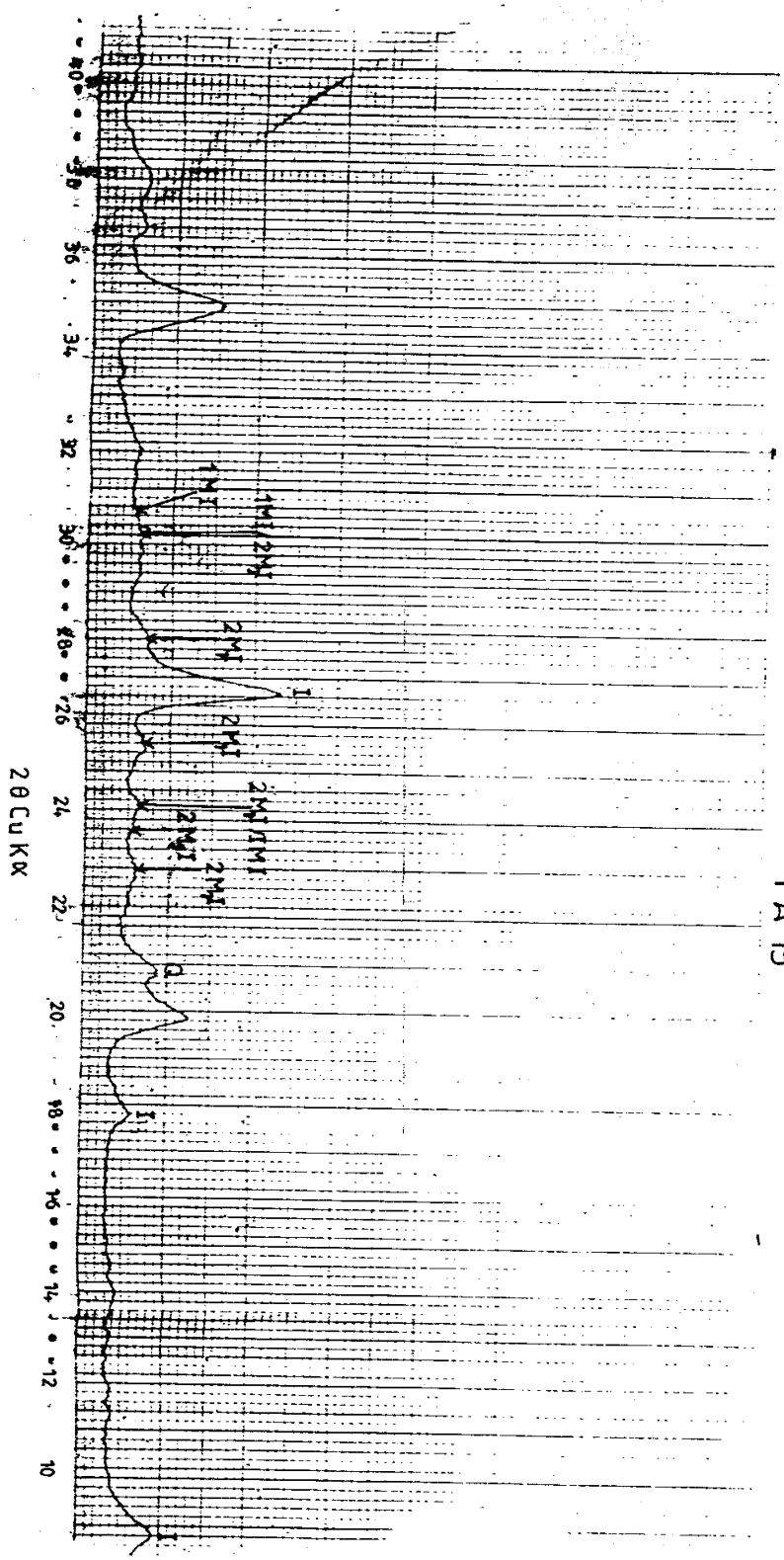

FA 15

APPENDIX II (CONT.)

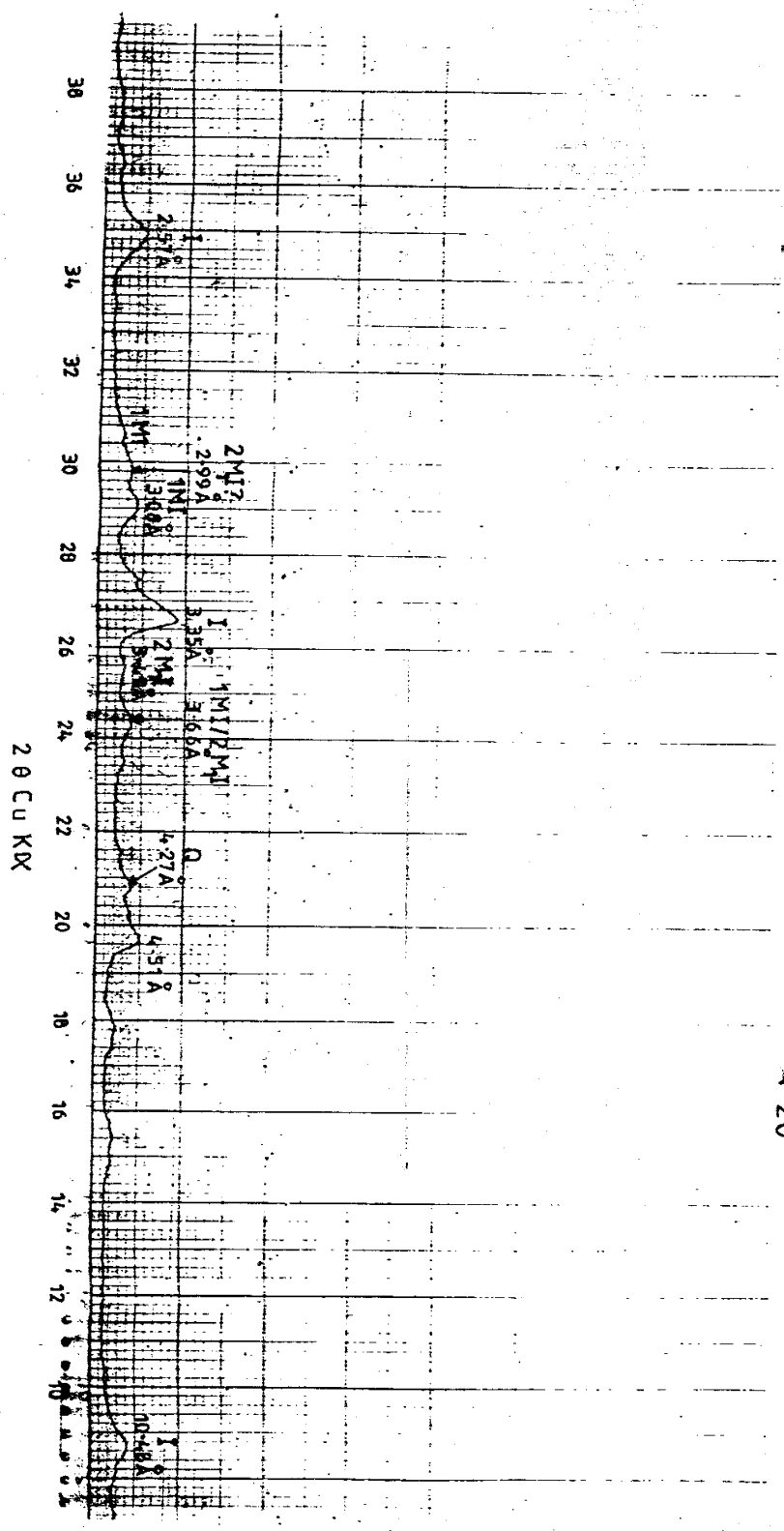

APPENDIX II (CONT.)

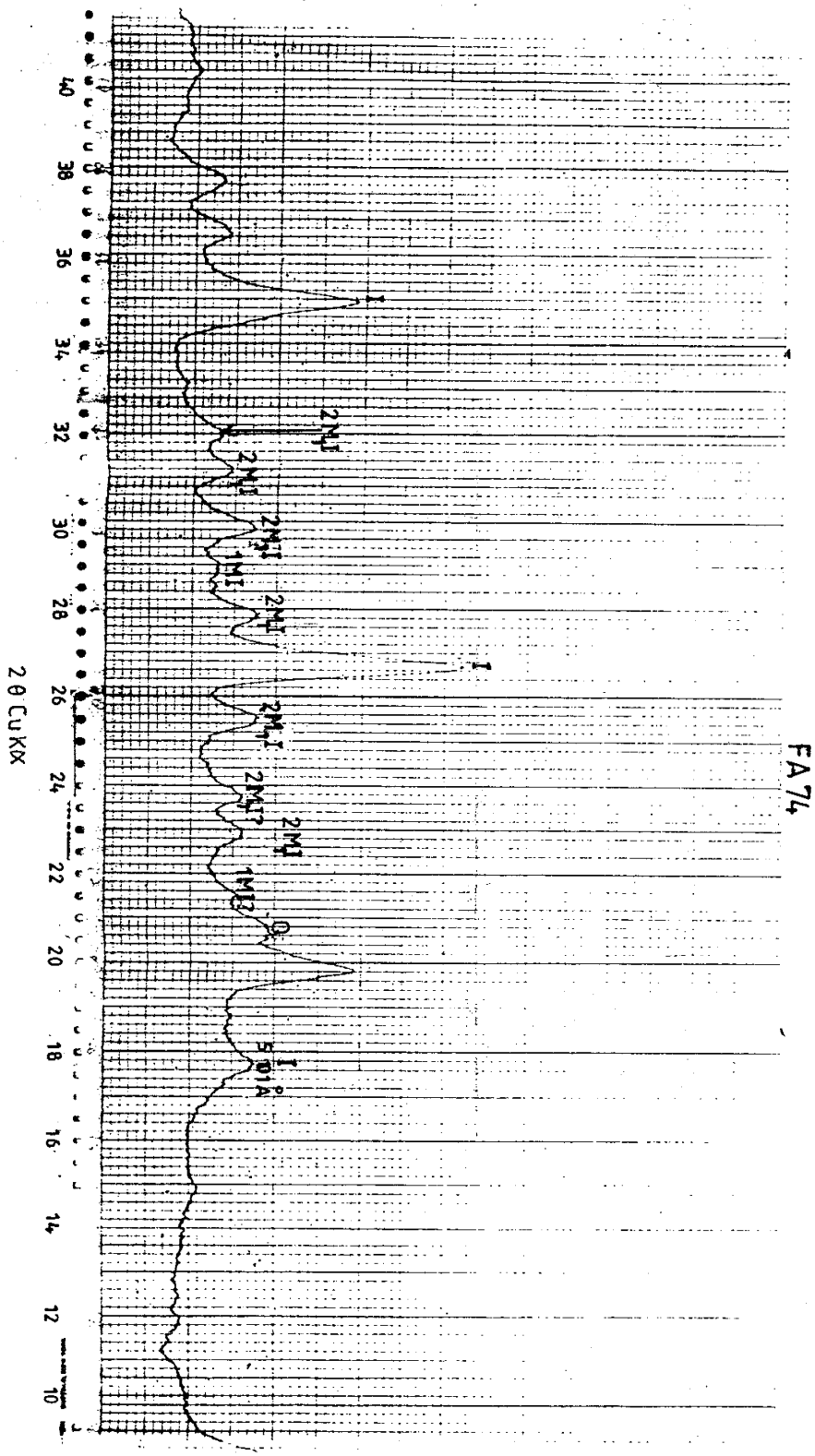

Appendix III.		PETROGRAPHIC AND X-RAY DATA			
Sample #	Location	Visual Description (Hand Specimen)	Thin Section Alteration Mineralogy	Bulk Mineralogy (XRD)	Alteration Clay Mineralogy (XRD)
FA 1	NA Vein System	Quartz Vein	ND		I
FA 3	NA Vein System	Silicified andesite	I, C, Cc, Ep		I, Cg
FA 4	NA Vein System	Quartz Vein	ND		$2M_1$ I
FA 5	NA Vein System	Altered andesite	T, C, Cc		I, C(Di + Tri), K
FA 6	NA Vein System	Silicified andesite	ND		K/S
FA 7	NA Vein System	Quartz Vein	ND		I, C(Di) S
FA 9	NA Vein System	Bleached grey andesite	C, Cc, I, K	Cc	I, C(Di)
FA 10	NA Vein System	Altered Andesite	Cc, C, I	Cc	I, Cg
FA 11	NA Vein System	Quartz vein	ND		T, S, K
FA 12	NA Vein System	Altered andesite	ND		I, ROC/S (80% C=Di + Tri)
FA 13	NA Vein System	Quartz seamed andesite	C, I		I, C(Tri), ROC/S (80% C)
FA 15	NA Vein System	Quartz vein	ND		1($2M_1$ + 1M), S
FA 16	NA Vein System	Dark grey andesite	I, C, Cc		I, C
FA 20	NA Vein System	Pale grey andesite	ND		I(1M + $2M_1$)
FA 22	Oakley Ridge OC	Red-brown andesite	I, C, Cc		I, C
FA-GH-1	NA-DGH1 10-19.5'	Pale green andesite	ND		R-3 I/S, ROC/S (85% C)

Appendix III. (cont.)		PETROGRAPHIC AND X-RAY DATA			
Sample #	Location	Visual Description (Hand Specimen)	Thin Section Iteration Mineralogy	Bulk Mineralogy (XRD)	Alteration Clay Mineralogy (XRD)
FA-GH-1	NA-DGH1 104-114'	Calcite seamed andesite	I, C, Cc, Ab, Kfs	Cc, AB, Kfs, Q	I, C, S, K
FA-GH-1	NA-DGH1 218-227'	Dark silicified andesite	C, I, Ab, Cc	Ab, Cc, An, Bc	C, ROC/S (95% S), I, Cr
FA-GH-1	NA-DGH1 274-283'	Dark green andesite	ND	Cc, Ep	C, ROC/S (95% S), I
FA-GH-1	NA-DGH1 326-330'	Dark green andesite	ND	Ab, Kfs, Ep	Cr, S, C, I
FA-GH-1	NA-DGH1 381-386'	Pale green andesite	C, I, Cc, Ab, Kfs,	Cc, Ab, Kfs	C,S, I
FA-GH-1	NA-DGH1 469-471'	Silicified andesite	ND	Cc	C, I, K
FA-GH-1	NA-DGH1 486'	Pale green altered andesite	ND	Ab, Ep	I, C(Di)
FA-GH-1	NA-DGH1 531-542'	Silicified andesite	I, C, Cc, Ab, Kfs, Ep	Ab, Kfs, Cc	I, C(Di), S, K
FA-GH-1	NA-DGH1 161'	Pale green andesite	I, C, Ab, Cc	Ab, Q, Cc	I, C, S(Na), K
FA-GH-1	NA-DGH1 48.5-59.9'	Pale green andesite	C, Ab, Cc, Kfs	Ab, Q, Cc, Kfs,	C, S
FA-GH-1	NA-DGH1 424-433'	Green Altered andesite	ND	Kfs, Cc, Q	I, C
FA-GH-2	NS DGH2 125'	Green Altered andesite	ND	Cc, Ab, Kfs	S, C, I
FA-GH-2	NS DGH2 201'	Pale green altered andesite	C, I, Cc, Ab, Kfs	Cc, Ab, Kfs	S, C, I
FA-GH-2	NS DGH2 300'	Pale green altered andesite	C, I, Ab, Cc	Ab, Cc	S, C, I
FA-GH-2	NS DGH2 360'	Silicified andesite	ND	Q	I, C, S
FA-GH-2	NA-DGH2 459'	Pale green silicified andesite	C, I, Ab, Cc, Ep	Ab, Cc, Q, An	Ts, C, I

Appendix III. (cont.)		PETROGRAPHIC AND X-RAY DATA			
Sample #	Location	Visual Description (Hand Specimen)	Thin Section Alteration Mineralogy	Bulk Mineralogy (XRD)	Alteration Clay Mineralogy (XRD)
FA-GH-3	NA-DGH3 288'	Pale green granodiorite	C, I, Ab, Kfs	Ab, Kfs, An	C(Di), ROC/S (80% S), I
FA-GH-3	NA-DGH3 353'	Pale green granodiorite	ND		T, C(Di), ROC/S (80% S)
FA 17	Emerald Vein (85-Hill)	Silcified andesite	ND		I, Cg(Di)
FA 31	Emerald Vein (85-Hill)	Pale Altered granodiorite	ND	Kfs, An, Bc, Q	I, K, S, I/S (10% S)
FA 32	Emerald Vein (85-Hill)	Pale green granodiorite	I, C, K, Ab, Kfs, Cc	Ab, Kfs, Cc	I, S, C, K
FA 33	Emerald Vein (85-Hill)	Pale green granodiorite	C, I, Ab, Kfs, Ep, Ap	Ab, Bc, Kfs, Ep, Ap	Cr, ROC/S (80% S), I
FA 36	Emerald Vein (85-Hill)	Pale green granodiorite	I, C, Cc, Kfs	Kfs, Cc	I, C(Di + Tri), K
FA 38	Emerald Vein (85-Hill)	Pale green granodiorite	ND	Ab, Kfs, Cc	C (Mg-rich), S, ROC/S (80% C), I, Cr
FA 40	Emerald Vein (85-Hill)	Pink-green granodiorite	C, I, Ab, Kfs, Cc, Pl	Ab, Kfs, Cc, Q	ROC/S (90% S), C, I
FA 47	Emerald Vein (85-Hill)	Leached granodiorite	ND	Ab, Cc	I, C
FA 53	Emerald Vein (85-Hill)	Bleached andesite	I, Cc	Q	I
FA 55	Emerald Vein (85-Hill)	Silicified andesite	ND	Ab, Au	ROC/S (80% S), C, I
FA 60	Emerald Vein (85-Hill)	Dark green andesite	I, C, Ab, Cc, Ep	Ab, Cc, MnC	I, C, ROC/S (90% S)
FA 64	Emerald Vein (85-Hill)	Slightly altered granodiorite	ND	Ab, Kfs, Cc, MnC, An	ROC/S (60% S), S, C, I
FA 69	Emerald Vein (85-Hill)	Slightly altered granodiorite	C, Ab, Kfs, Cc	Ab, Kfs, Cc	C, ROC/S (80% S), R3 1/S, S

Appendix III. (cont.)		PETROGRAPHIC AND X-RAY DATA			
Sample #	Location	Visual Description (Hand Specimen)	Thin Section Alteration Mineralogy	Bulk Mineralogy (XRD)	Alteration Clay Mineralogy (XRD)
FA 71	Emerald Vein (85-Hill)	Slightly altered granodiorite	ND	Kfs, Ab, An, Cc, MnC	S, ROC/S (95% S) I/S (10% S), K
FA 73	Emerald Vein (85-Hill)	Slightly altered granodiorite	ND	Ab, Kfs, An, Q	ROC/S (95% S), C, I
FA 74	Emerald Vein (85-Hill)	Silicified granodiorite	I, Ab, Cc	Ab, Cc	I($2M_1$)
FA 75	Emerald Vein (85-Hill)	Slightly altered granodiorite	ND	Ab, Kfs, An, Q	I, S(Na), ROC/S (95% S)
FA 80	Emerald Vein (85-Hill)	Pinkish granodiorite	C, I, Ab	Ab, Kfs, An, Q	S, C(Di + TRi), I, K, ROC/S (95% S)
FA 123[A]	South Emerald Vein	Altered hybrid andesite	ND	Ab, Cc, An	C, S, I, ROC/S (95% S), K
FA 123[B]	South Emerald Vein	Altered granodiorite	I, C, Ab, Cc	Ab, Au, Cc, Q	S, I, C
FA 127[A]	South Emerald Vein	Pale green andesite	ND	Ab, Cc, An	C, S, I, K, ROC/S (90% S)
FA 127[C]	South Emerald Vein	Pale green andesite	C, Ab, Kfs, Cc	Ab, Kfs, An	C, ROC/S (80% S), R3 1/S,S
FA 88	Miser's Chest Vein System	Altered andesite	ND	Ab, Kfs, Cc	I, C(Tri, ROC/S (95% C)
FA 89	Miser's Chest Vein System	Silicified andesite	ND		I, C
FA 91	Miser's Chest Vein System	Argilized andesite	C, I, Ab, Kfs, Cc	Ab, Kfs, Cc, An	C(Tri), S, I
FA 92	Miser's Chest Vein System	Argilized andesite	C, I, Ab, Cc	Ab, Kfs, Cc	ROC/S (90% S), C, I

Appendix III. (cont.)		PETROGRAPHIC AND X-RAY DATA			
Sample #	Location	Visual Description (Hand Specimen)	Thin Section Alteration Mineralogy	Bulk Mineralogy (XRD)	Alteration Clay Mineralogy (XRD)
FA 93	Miser's Chest Vein System	Silicified andesite	ND	Kfs, Cc, An, Ab, Amp	C, ROC/S (80% S), I, K
FA 94	Miser's Chest Vein System	Argilized andesite	C, Ab, C	Ab, Kfs, An, Cc, Px	C, ROC/S (70% S), K
FA 96[A]	Miser's Chest Vein System	Silicified andesite	ND	Cc	C(Tri), I, K
FA 96[B]	Miser's Chest Vein System	Bleached andesite	I, Cc		(I($2M_1$ + $1M_1$)
FA 97	Miser's Chest Vein System	Silicified andesite	ND	Ab, Kfs, Bc, Cc, Amp	C, I
FA 99	Miser's Chest Vein System	Argilized andesite	C, I, Ab, Cc	Ab, Cc, MnC, Bc, Amp	C, Cr, I, K
FA 103[B]	Bonney Vein System	Silicified andesite	ND	AB, An, Cc, Q	S, C(Tri), I
FA 104	Bonney Vein System	Dark green andesite	C, Ab	Amp, Bc, Ab	C
FA 106	Bonney Vein System	Argilized andesite	ND	Ab, Kfs, An, Cc, Q, Amp	C, Cr, I, K
FA 110	Bonney Vein System	Dark green andesite	ND	Ab, Cc, Bc, An, Amp	Cr, C, I
FA 113	Bonney Vein System	Quartz seamed andesite	C, Cc, Kfs, EP	Cc, Kfs	C(Di + Tri)
FA 115	Bonney Vein System	Dark green andesite	ND	Ab, Kfs, Cc, Bc, MnC, Amp, Ap	C(Tri), I
FA 118	Bonney Vein System	Mineralized andesite	I, C, Cc, EpO	An, Ep	1($2M_1$ + 1M), C
FA 119	Bonney Vein System	Mineralized andesite	ND	An, Ep	I($2M_1$) + C(Di)
FA 120	Bonney Vein System	Mineralized andesite	ND	Cc	1($2M_1$) C(Di)
FA 169	Leitendorf, RL-NB	Pale green andesite	C, Cc, Py	Cc, Q	C(Tr), R≥3 I/S, K

Appendix III. (cont.)		PETROGRAPHIC AND X-RAY DATA			
Sample #	Location	Visual Description (Hand Specimen)	Thin Section Alteration Mineralogy	Bulk Mineralogy (XRD)	Alteration Clay Mineralogy (XRD)
FA 169[C]	Leitendorf, RL-NB	Dark green andesite	C, Cc, Py	Cc	C(Tri+Di), R≥3 I/S, K
FA 169[D]	Leitendorf, RL-NB	Dark green andesite	ND	Cc	C, R=3 I/S, K
FA 170	Leitendorf, RL-NB	Dark green andesite	ND	Kfs, Cc	C(Di), R=3 I/S, K
FA 172[D]	Leitendorf, RL-NB	Pyritic rhyolite	C, I, Cc, Kfs, Py	Cc, Kfs	C, I
FA 182	Leitendorf, RL-NB	Pyritic rhyolite	ND	Ab, Kfs, Cc, EP, An	C, Cr
FA 183	Leitendorf, RL-NB	Dark andesite	C, Ab, Cc, Kfs	Ab, Kfs, Cc, Ep	Cr, C(Tri), R=3 I/S
FA 184	Leitendorf, RL-NB	Dark andesite	ND	Ab, Kfs, An, Cc, MnC, Ep	Cr, C, R=3 I/S
FA 185	Leitendorf, RL-NB	Hematite andesite	C, I, Ab, Cc	Ab, Kfs, Cc, Ep	Cr, C(Tri), I
FA 190[A]	Leitendorf, RL-NB	Quartz latite	Ab, Cc, Kfs	Ab, Kfs, Q, Cc	R≥I I/S, ROC/S (90% S), C, K
FA 190[B]	West of NB-RL	Hematite andesite	C	Ab, Cc, Ep, An	C, R=3 I/S, K
FA 191	West of NB-RL	Pyrite-chlorite-andesite	C, Cc	Q	C
FA 194	West of NB-RL	Grey rhyolite	ND	Ab, Kfs, An, Q	---
FA 196[A]	CaF_2-Qtz-Cal Veins	Dark green andesite	ND	Ab, Cc, An, Kfs, Anc	C, Ts
FA 197	CaF_2-Qtz-Cal Veins	Hematitic granodiorite	C, Ab, Kfs	Ab, Kfs, Anc	Cr, K/S (35% S), S
FA 196[B]	Northeast of RL-NB	Pyritic quartz latite	ND	Ab, Kfs, An, Anc	Cr, K/S (35% S), S
FA 199[B]	South of RL-NB	Drak grey granodiorite	ND	Ab, An, Anc	Cr, K, R=1 I/S
FA 205	SA Vein	Pale green andesite	C, Cc, Ab	Ab, Cc, Pl	Ts, S, C(Tri)

Mineral Abbreviations:

I	- Illite
C	- Chlorite
K	- Kaolinite
S	- Smectite
Cg	- Swelling chlorite
Cr	- Corrensite
I/S	- Illite-smectite mixed layer
ROC/S	- random chlorite-smectite mixed-layer
Ts	- Tosndite
K/S	- Kaolinite-smectite mixed-layer
S(Na)	- Sodium smectite
Cc	- Calcite
Ab	- Albite
Kfs	- K-feldspar
An	- Andesine
Ep	- Epidote
Bc	- Baryto calcite
Q	- Quartz
Ap	- Apatite
MnC	- Manganoan calcite
Amp	- Amphibole
Px	- Pyroxene
Anc	- Analcime
Pl	- Phlogopite

Other Abbreviations:

R	-	Reichweite
1M, 2M	-	Ilite polytypes
Di	-	Dioctahedral
Tri	-	Trioctahedral
NA	-	North Atwood Area
EV	-	Emerald Vein
BV	-	Bonney Vein
MCV	-	Miser's Chest Vein
RL-NB	-	Robert Lee-Nellie Bly
LC	-	Last Chance
ND	-	Not determined
DGH	-	Diamond Drillhole
SA	-	South Atwood

APPENDIX IV a
SAMPLE LOCATION - FLUID INCLUSION STUDY

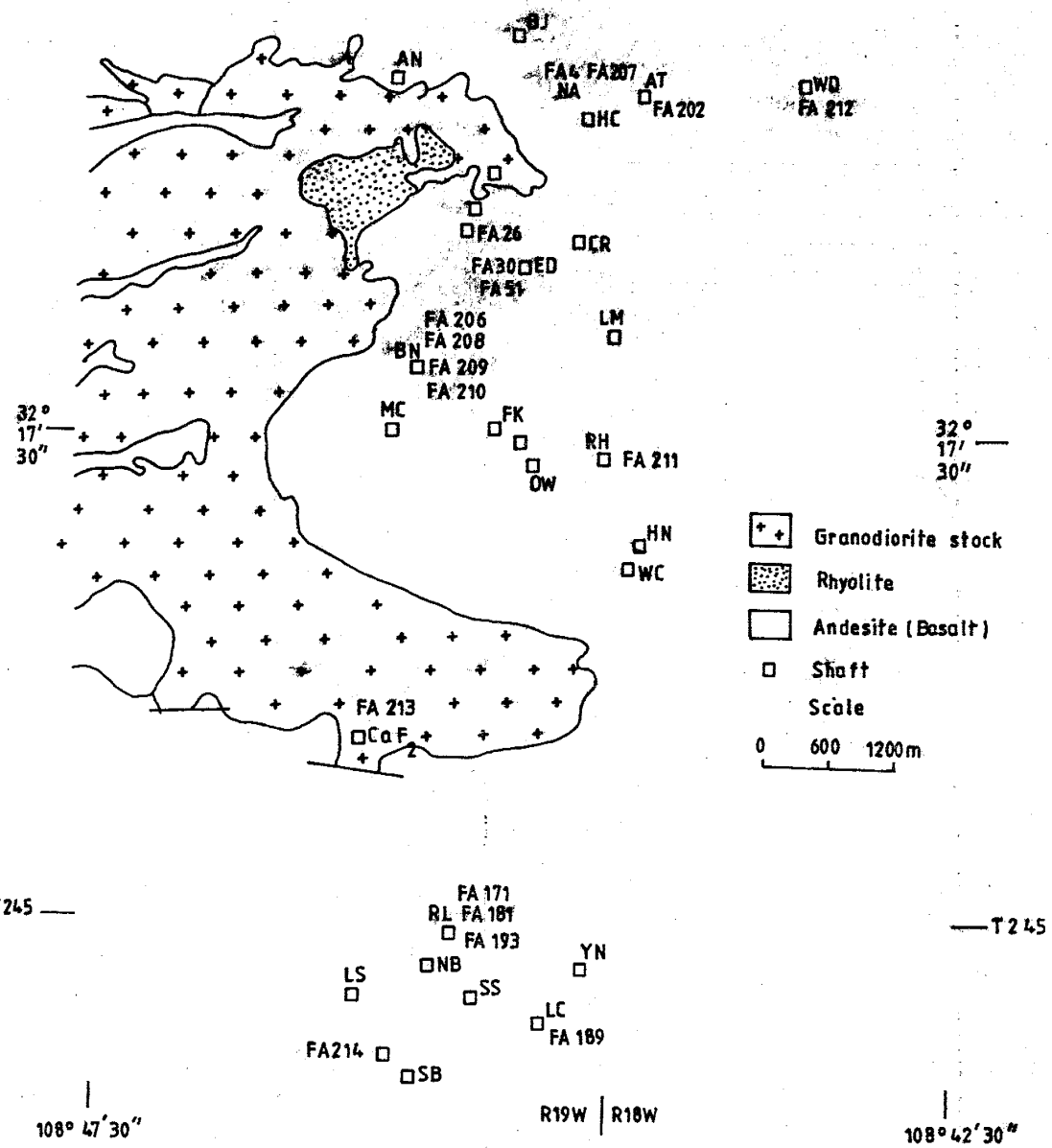

APPENDIX IV b
FLUID INCLUSION MICROTHERMOMETRIC DATA

85 - MINE

SAMPLE NO.	STAGE	MINERAL	Th	SALINITY
FA 26	2	Quartz	321	6.7
			283	5.6
			264	6.1
			183	6.0
			180	6.0
FA 30	2	Quartz	343	5.4
			305	5.3
			271	5.5
			183	6.4
			180	6.5
			176	6.2
FA 51	2	Quartz	346	6.9
			282	6.6
			250	6.5
			189	6.9
FA 15	3	Quartz	270	5.0
			220	5.0
			190	5.6
			180	5.0
			176	4.8
			172	4.6
FA 22	4	Calcite	160	3.6
			156	3.7
			150	3.6
			146	4.4
			144	3.8
FA 65	5	Calcite	146	3.5
			132	3.4
			132	3.2

BONNEY MINE

FA 206	2	Quartz	340	6.6
			329	6.2
			325	5.7
			316	
			312	
			309	5.4
			307	5.6
			304	
			302	5.4
			297	
			296 (2)	
			281 (2)	
			280	5.7
			271 (2)	
			261 (2)	(2)
			260 (2)	
			253	
			251	

FA 208	3	Quartz	237 (2)	
			235	
			233	5.2
			231	5.0
			228 (2)	
			221	
			194	
			186	
			182	6.1
			176	4.9
			168	
			163	
			156	
			147	
			138	
			130 (2)	
FA 210	4	Calcite	174	4.7
			168	
			166	
			154	
			147 (2)	
FA 209	5	Calcite	174	4.7
			163	
			162	
			154	
			157	3.8
			146	
			144	
			138	

NORTH ATWOOD MINE

FA 207	3	Quartz	270	5.0
			251	5.1
			246	5.1
			214	5.0
			190	4.6
			185	3.7
			180	5.0
			176	4.7
			170	4.6
			170	3.4
			168	4.1
			165	4.7
			165	3.8
			165	3.5
			160	3.6
			158	5.0
FA 4	2	Quartz	250	5.2
			162	3.8

ATWOOD MINE

FA 202			289	
			278	4.6
			267 (2)	
			263 (2)	5.1
			254	5.4
			246 (2)	
			220 (2)	
			209	
			188 (3)	
			186 (2)	
			184	
			177	
			168 (2)	
			148	

WALDO MINE

FA 212	2	Quartz	252	
			250	
			247	
			236 (2)	
			235	4.2
			221 (2)	4.4
			206 (2)	3.4
			187 (2)	
			177 (3)	
			164	
			162 (2)	
			150 (2)	

RUTH MINE

FA 211	2	Quartz	290	5.5
			276	
			265	5.2
			260	4.8
			252	5.3
			245	4.4
			236	
			230	
			217	
			208	3.6
			196	
			190	
			184	
			172	
			168	
			165	
			162	
			158	
			146	
			137	
			130	
			124	

FLUORITE MINE (VIRGINIA)

FA 213	6	FLUORITE	186	
			185	
			182	4.8
			177	
			176 (2)	4.5
			164	4.4
			168 (2)	5.6
			165 (2)	
			162	4.6
			161	
			155	
			156 (2)	4.6
			152	
			148	
			146	3.4
			142	3.8
			190	4.8
			192	
			210	
			223	
			215	
			230	5.8

ROBERT LEE MINE

FA 171	2 (PS)	Quartz	335	5.4
			332	
			327	
			316	
			309	
			307	
			305	5.2
			303	
			302	5.4
			296	5.3
			281	5.2
			268	5.4
			265	5.6
			260	6.1
			256	4.9
			250	4.7
FA 181	2 (PS)	Quartz	323	
			318	
			305	
			301	
			295	
			283	
			262	
FA 193	3 (PS)	Quartz	297	
			288	
			274	
			272	
			261	

LAST CHANCE MINE

FA 189	2	Quartz	261 (2)	5.1
			258 (2)	5.2
			223 (3)	4.4
			208	4.2
			206	
			204 (2)	
			202	
			199	
			197	

FLUORITE MINE (LEITENDORF)

FA 214	6	Fluorite	201	5.2
			192	
			181	
			173	
			171	
			167	4.3
			164	
			163	
			161	
			156	
			152	3.7
			145	
			143	
			141	
			138	
			136	3.4

Abbreviations:

PS - Pseudo-secondary

This document is accepted on behalf of the faculty of the Institute by the following committee:

David A. Noon

Adviser

Christopher R. Caldwell

William X. Chavez, Jr. 6 December, 1995

Larry L. Campbell 12/6/95

Date

I release this document to New Mexico Institute of Mining and Technology.